Scuola di Chimica Bioinorganica - Roma 12-15 Febbraio 2019

Divisioni di Chimica dei Sistemi Biologici e di Chimica Inorganica della Società Chimica Italiana

X-ray spectroscopy methods in Bioinorganic Chemistry

Prof. Stefano Mangani
Dipartimento di Biotecnologia, Chimica e Farmacia
Università di Siena
e-mail: stefano.mangani@unisi.it

X-ray Absorption Spectroscopy

Lecture outline:

- Overview of XAS Spectroscopy and its uses
  - Synchrotron sources
- Theory (a little)
- Experiment
- Information content
- Data Analysis examples
  BioXAS examples from literature

lecture slides and learning material available

X-ray Absorption Spectroscopy

The electromagnetic spectrum

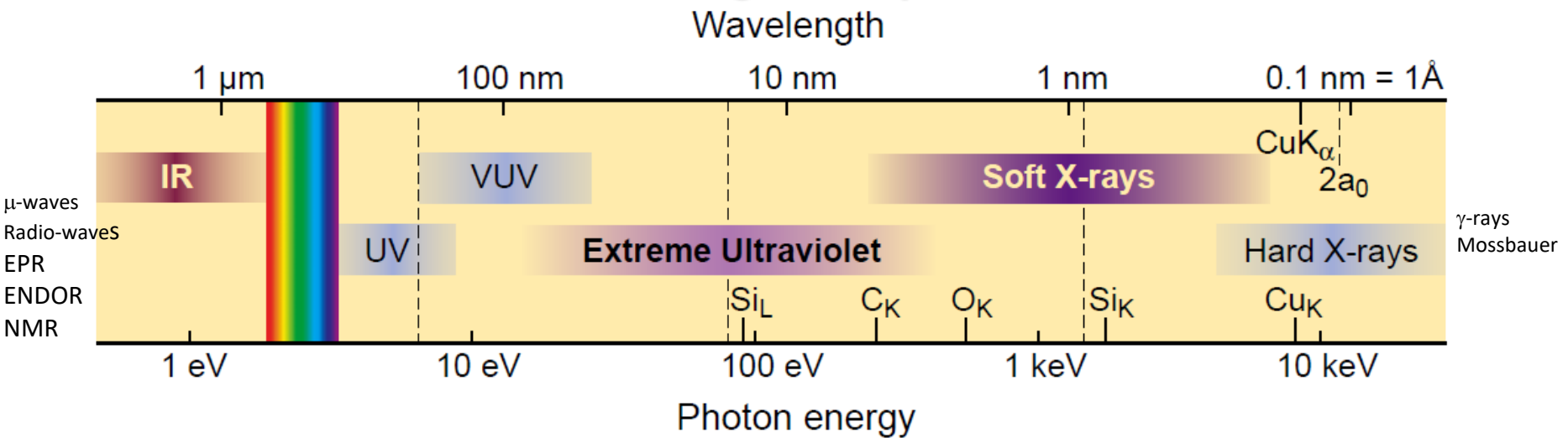

X-rays are high energy photons: Energy from about 200 eV (soft) to 120 keV (hard)

wavelength λ: from 100 Å to 0.1 Å

E is usually expressed in electron volts (eV) or kilo eV (keV) where 1 eV = 1.610^{-19} J.

E.g.: blue light has E = 3 eV

$$E = \frac{hc}{\lambda} \qquad E(eV) = \frac{1.24 \cdot 10^4}{\lambda(in\ \text{Å})}$$

For X-ray spectroscopy we need tunable, intense, X-ray sources

Modern synchrotrons & XFELS

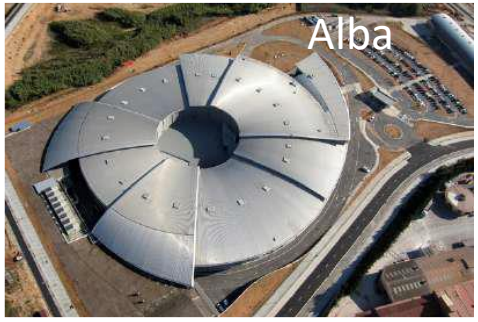

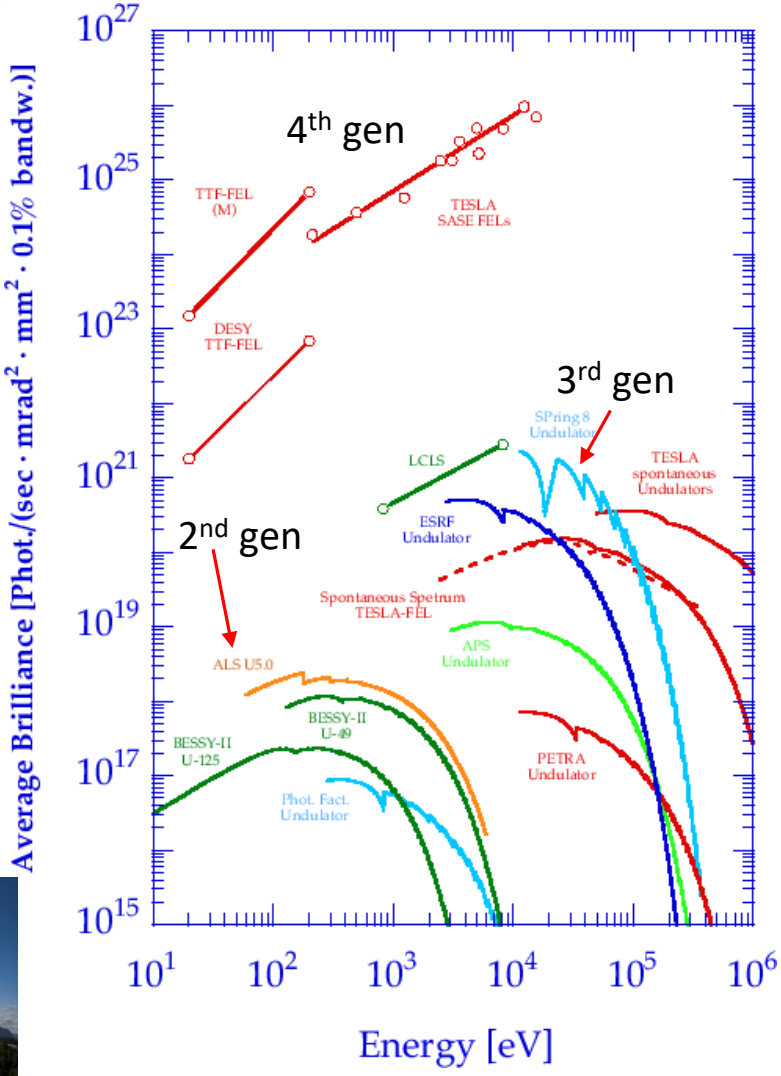

Synchrotron radiation

When charged particles, moving at RELATIVISTIC speeds (v ≈ c), are forced to change the direction of their motion (acceleration), under the effect of magnetic fields, in circular particle accelerators, like synchrotrons, the radiation produced is called *Synchrotron Radiation*.

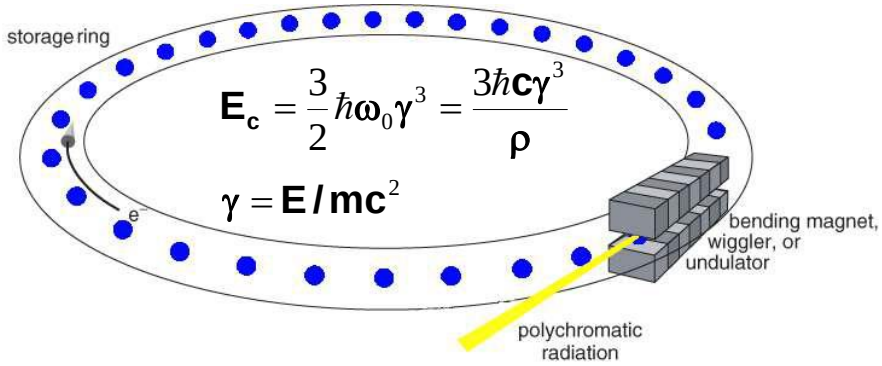

ω_0 = angular frequency in classical approximation
ρ = radius of instantaneous curvature of electron trajectory
E_c: critical photon energy
E (or E_e) = electron beam energy

Brightness = Flux of photons of freq. ω emitted from unit source area into unit solid angle.
Flux/S·Ω
Brilliance = brightness/mm²
Spectral brightness ($\Delta\omega/\omega$) = $\frac{photons}{s \cdot mrad^2 \cdot mm^2 \cdot 0.1\%BW}$

Synchrotron radiation is characterized by:

- Continuum source from IR to γ-rays
- High brightness and high intensity, many orders of magnitude more than with X-rays produced in conventional X-ray tubes
- High brilliance, exceeding other natural and artificial light sources by many orders of magnitude:
  3rd generation sources typically have a brilliance larger than 10^{18} photons/s/mm²/mrad²/0.1%BW, where 0.1%BW denotes a bandwidth $10^{-3}\omega$ centered around the frequency ω.
- High collimation, i.e. small angular divergence of the beam.
- Low emittance, i.e. the product of source cross section and solid angle of emission is small
- Widely tunable in energy/wavelength by monochromatization
- High level of polarization (linear or elliptical)
- Pulsed light emission (pulse durations less than one nanosecond)

The relativistic electron has an energy:

$$E = \gamma m_0 c^2$$

γ = Lorentz factor $= 1/\sqrt{1 - \frac{v^2}{c^2}}$

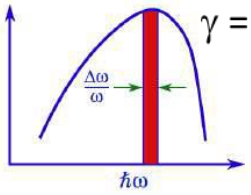

The universal curve of BM synchrotron radiation

The integrated spectral density up to the critical frequency contains half of the total energy radiated, the peak occurs approximately at 0.3 ω_c

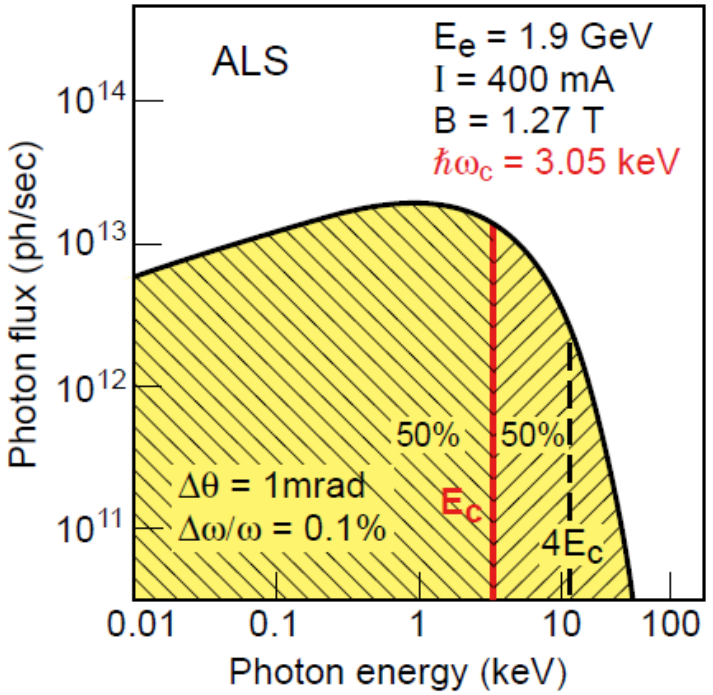

For *electrons*, the critical energy:

$$E_c = 3hc\gamma^3/(4\pi R)$$

Where R is the ring radius.

In practical units is: $E_c(keV) = 2.218\, E_{ring}^3(GeV)/R(m)$

For *electrons and positrons*, in practical units γ is:

γ = 1957 E_{ring} (GeV)

Synchrotron radiation

ESRF - Grenoble

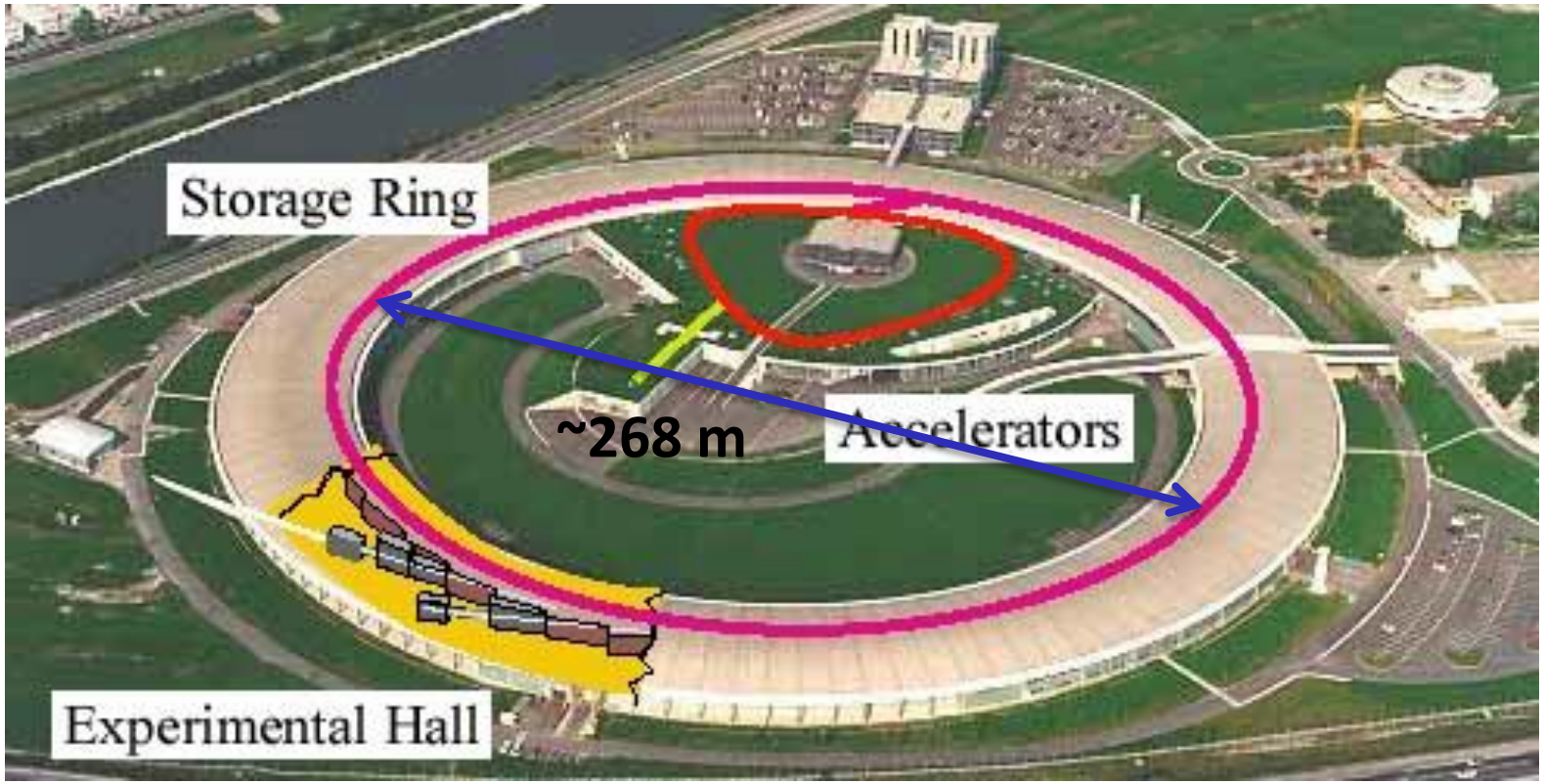

Synchrotron radiation

Injection process

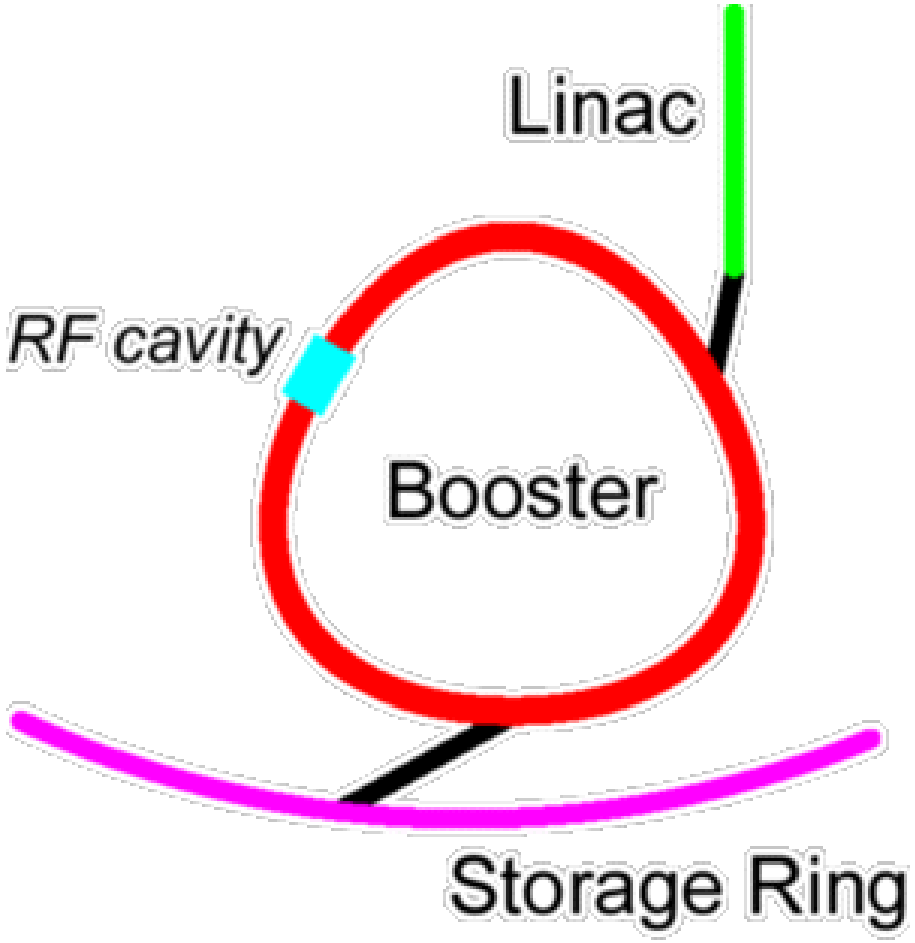

Synchrotron radiation

SR tunnel

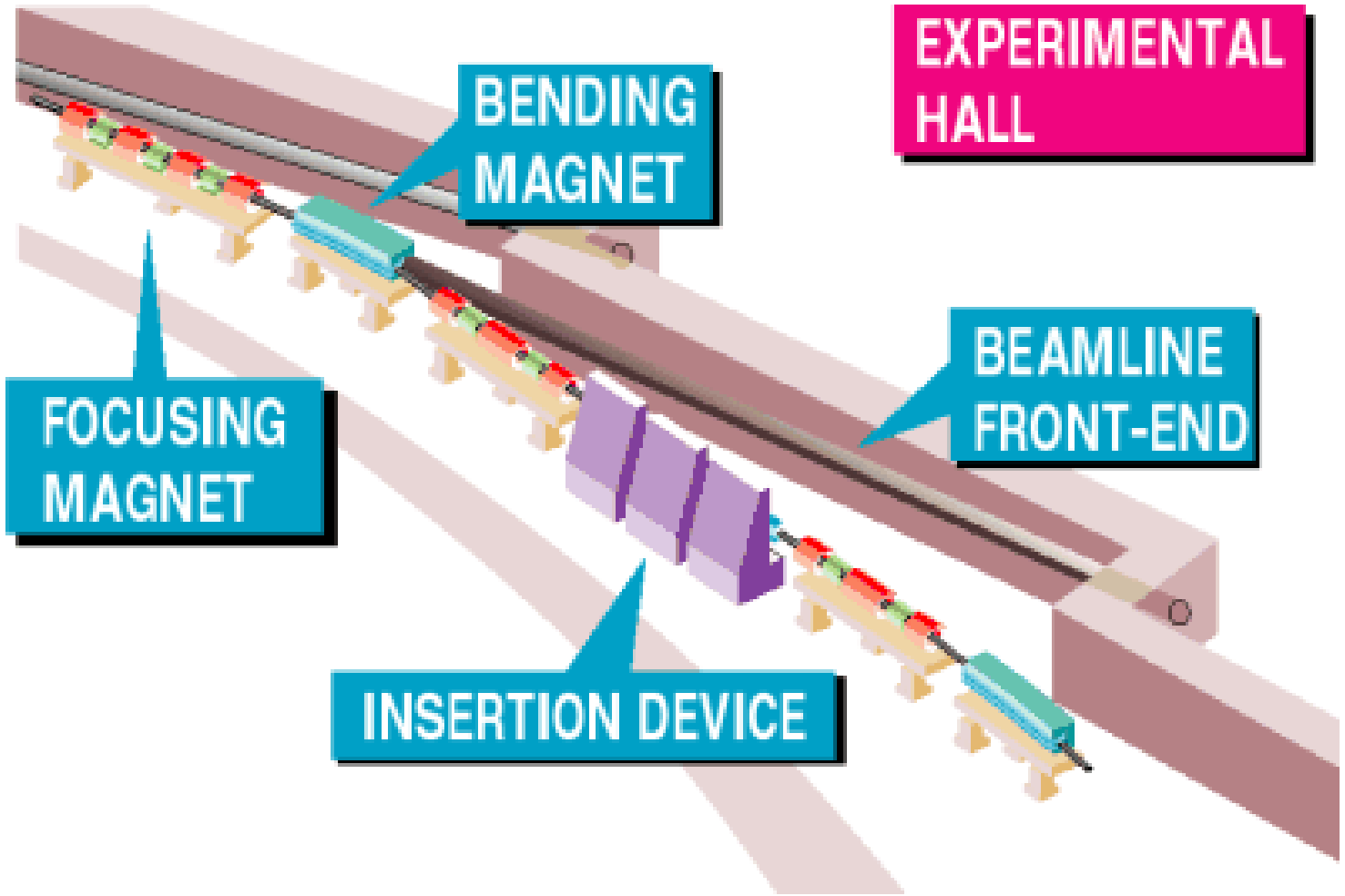

Synchrotron radiation

Bending magnet

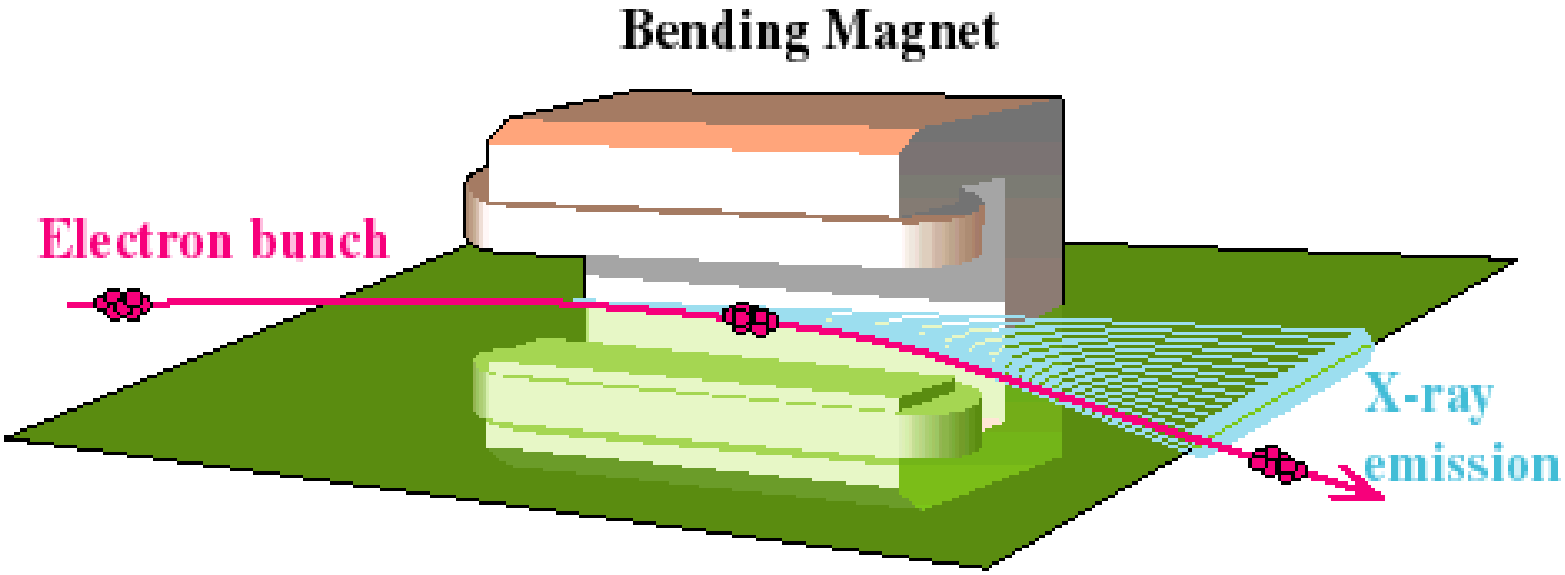

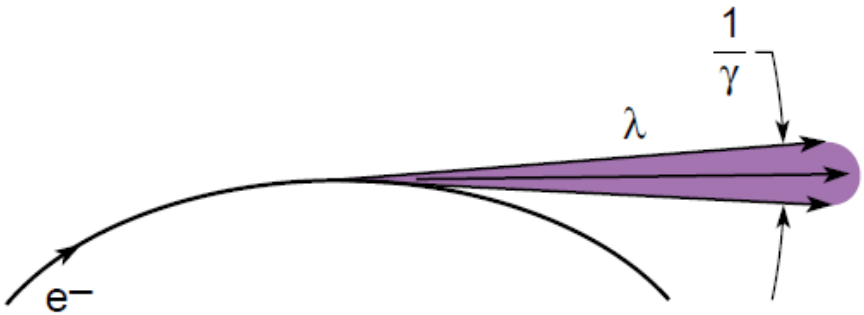

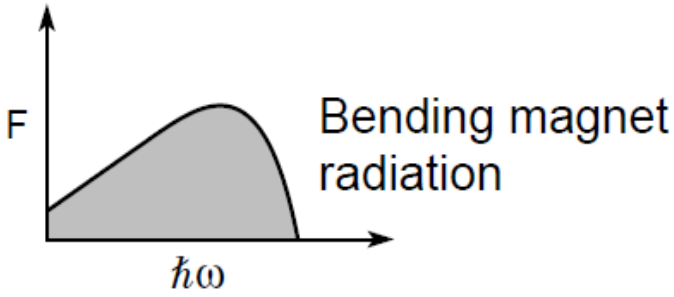

Synchrotron radiation

Wigglers

Wigglers are “insertion devices” used to increase the intensity of synchrotron radiation by lining up a series of bending magnets which enhance the intensity simply by the number of magnet poles. In order to add up the intensity of the individual emission cones, the dipoles are arranged with alternating polarity such that the electrons are essentially moving straight except for small “wiggles” where the radiation is emitted. The emission cones overlap and the intensity adds up by positive interference.

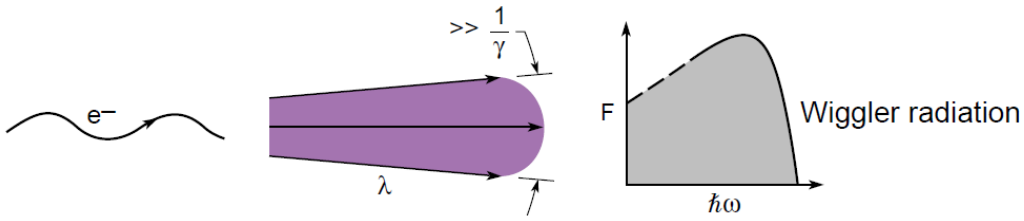

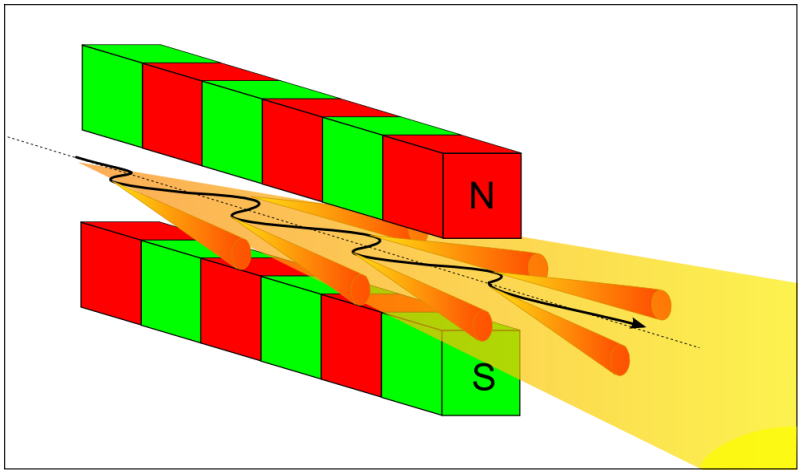

A real wiggler

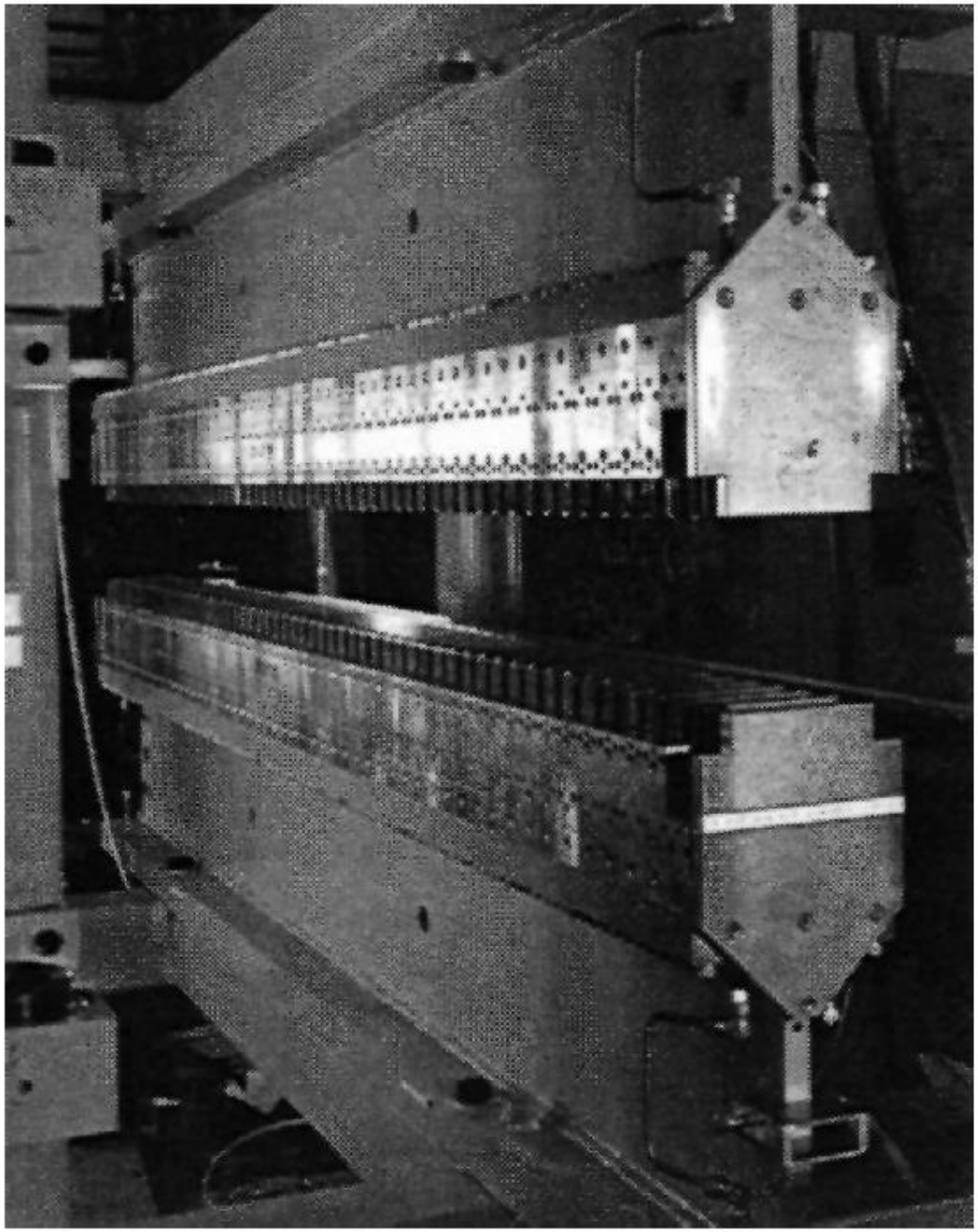

LBNL/EXXON/SSRL (1982), SSRL Beamline VI
55 pole (N = 27.5), λ_w = 7 cm

The advantage of a wiggler is that it emits intense radiation over a wide spectral range, very much like a bending magnet.

Short pulses of SR = wide spread of vawelenghts.

$$\theta_{cen} > \frac{1}{\gamma}$$

Synchrotron radiation
Undulator

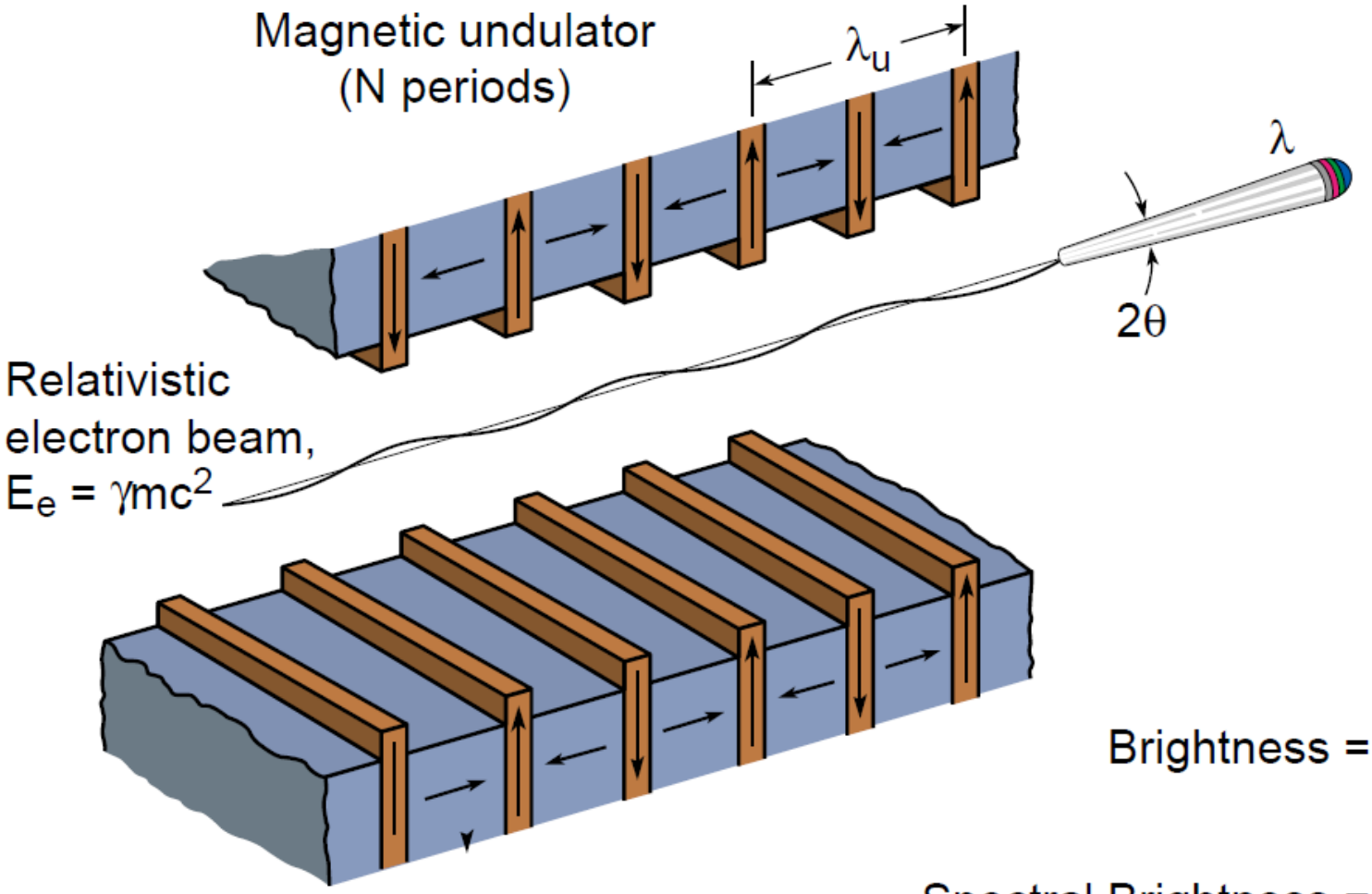

$$\lambda \simeq \frac{\lambda_u}{2\gamma^2}$$

$$\theta_{cen} \simeq \frac{1}{\gamma\sqrt{N}}$$

$$\left[\frac{\Delta\lambda}{\lambda}\right]_{cen} = \frac{1}{N}$$

$$\text{Brightness} = \frac{\text{photon flux}}{(\Delta A)\,(\Delta\Omega)}$$

$$\text{Spectral Brightness} = \frac{\text{photon flux}}{(\Delta A)\,(\Delta\Omega)\,(\Delta\lambda/\lambda)}$$

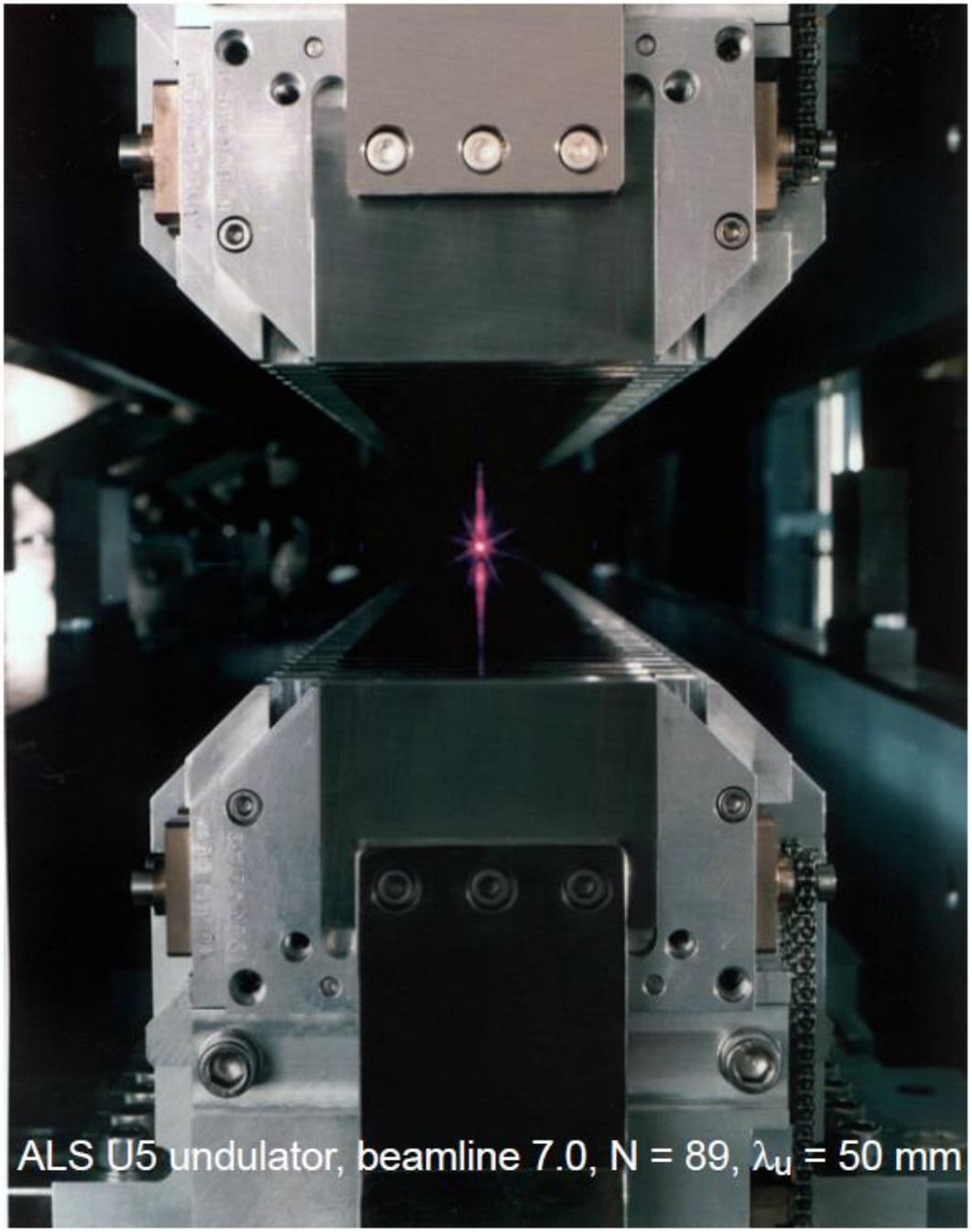

Undulator

Synchrotron radiation

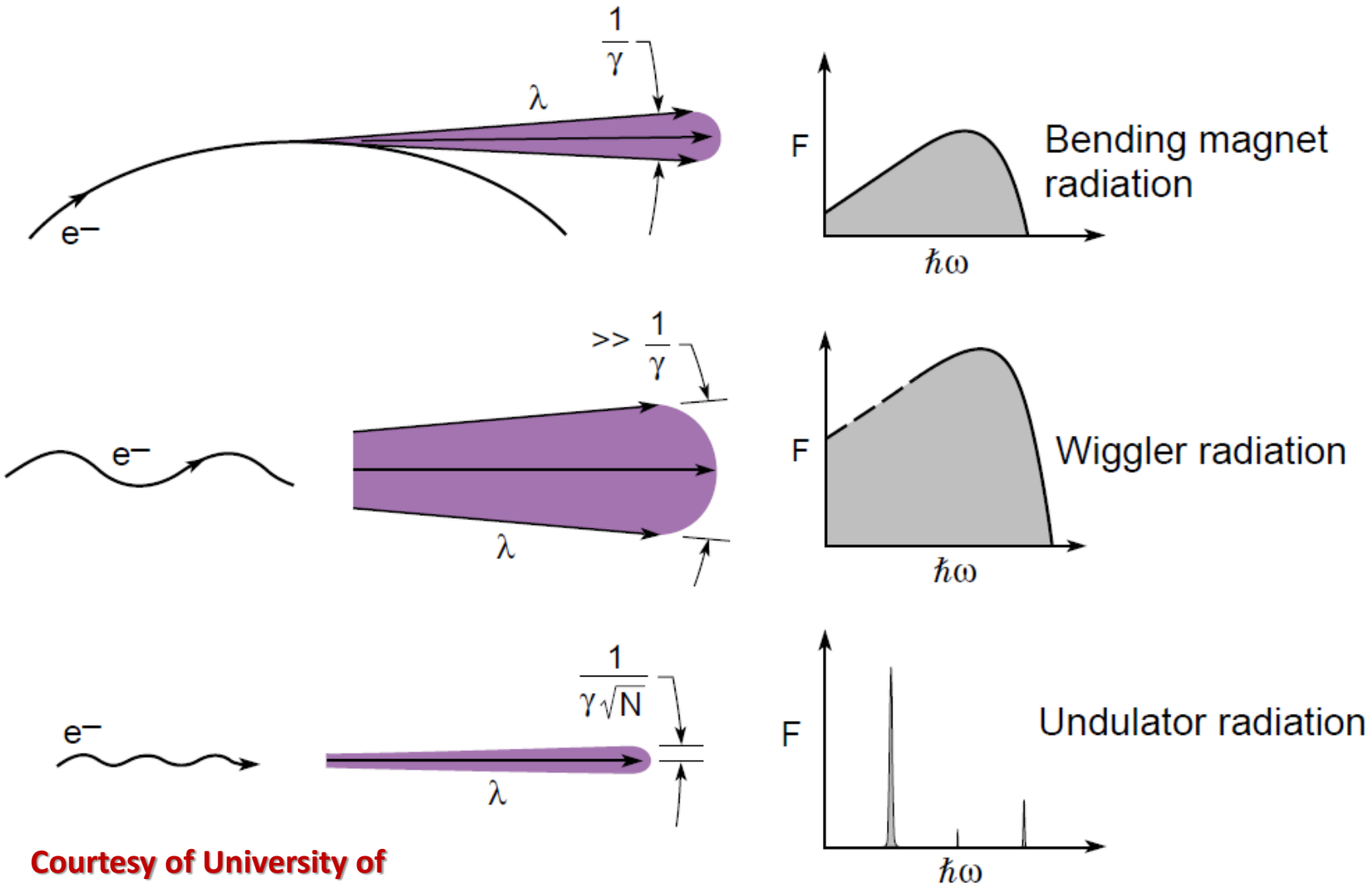

Courtesy of University of California - Berkeley

Typical Parameters for Synchrotron Radiation

Facility	ALS	BESSY II	ESRF	SP-8
Electron energy	1.90 GeV	1.70 GeV	6.04 GeV	8.00 GeV
γ	3720	3330	11,800	15,700
Current (mA)	400	200	200	100
Circumference (m)	197	240	884	1440
RF frequency (MHz)	500	500	352	509
Pulse duration (FWHM) (ps)	35-70	20-50	70	120
Bending Magnet Radiation:				
Bending magnet field (T)	1.27	1.30	0.806	0.679
Critical photon energy (keV)	3.05	2.50	19.6	28.9
Critical photon wavelength	0.407 nm	0.50 nm	0.634 Å	0.429 Å
Bending magnet sources	24	32	32	23
Undulator Radiation:				
Number of straight sections	12	16	32	48
Undulator period (typical) (cm)	5.00	4.90	4.20	3.20
Number of periods	89	84	38	140
Photon energy ($K = 1$, $n = 1$)	457 eV	373 eV	5.50 keV	12.7 keV
Photon wavelength ($K = 1$, $n = 1$)	2.71 nm	3.32 nm	0.225 nm	0.979 Å
Tuning range ($n = 1$)	230-620 eV	140-500 eV	2.6-7.3 keV	4.7-19 keV
Tuning range ($n = 3$)	690-1800 eV	410-1100 eV	7.7-22 keV	16-51 keV
Central cone half-angle ($K = 1$)	35 µrad	33 µrad	17 µrad	6.6 µrad
Power in central cone ($K = 1$, $n = 1$) (W)	2.3	0.95	14	16
Flux in central cone (photons/s)	3.1×10^{16}	1.6×10^{16}	1.6×10^{16}	7.9×10^{15}
σ_x, σ_y (µm)	260, 16	314, 24	395, 9.9	380, 6.8
σ'_x, σ'_y (µrad)	23, 3.9	18, 12	11, 3.9	16, 1.8
Brightness ($K = 1$, $n = 1$)[a] [(photons/s)/mm^2 · mrad^2 · (0.1%BW)]	2.3×10^{19}	4.6×10^{18}	5.1×10^{18}	1.8×10^{20}
Total power ($K = 1$, all n, all θ) (W)	83	32	480	2,000
Other undulator periods (cm)	3.65, 8.00, 10.0	4.1, 5.6, 12.5	2.3, 3.2, 5.2, 8.5	2.4, 10.0, 3.7, 12.0
Wiggler Radiation:				
Wiggler period (typical) (cm)	16.0	12.5	8.0	12.0
Number of periods	19	32	20	37
Magnetic field (maximum) (T)	2.1	1.15	0.81	1.0
K (maximum)	32	12.8	6.0	11
Critical photon energy (keV)	5.1	2.11	20	43
Critical photon wavelength	0.24 nm	0.59 nm	0.62 Å	0.29 Å
Total power (max. K) (kW)	13	1.8	4.8	18

[a]Using Eq. (5.65). See comments following Eq. (5.64) for the case where $\sigma'_{x,y} \simeq \theta_{cen}$.

Courtesy of University of California - Berkeley

Synchrotron radiation

Focusing magnet

Synchrotron radiation

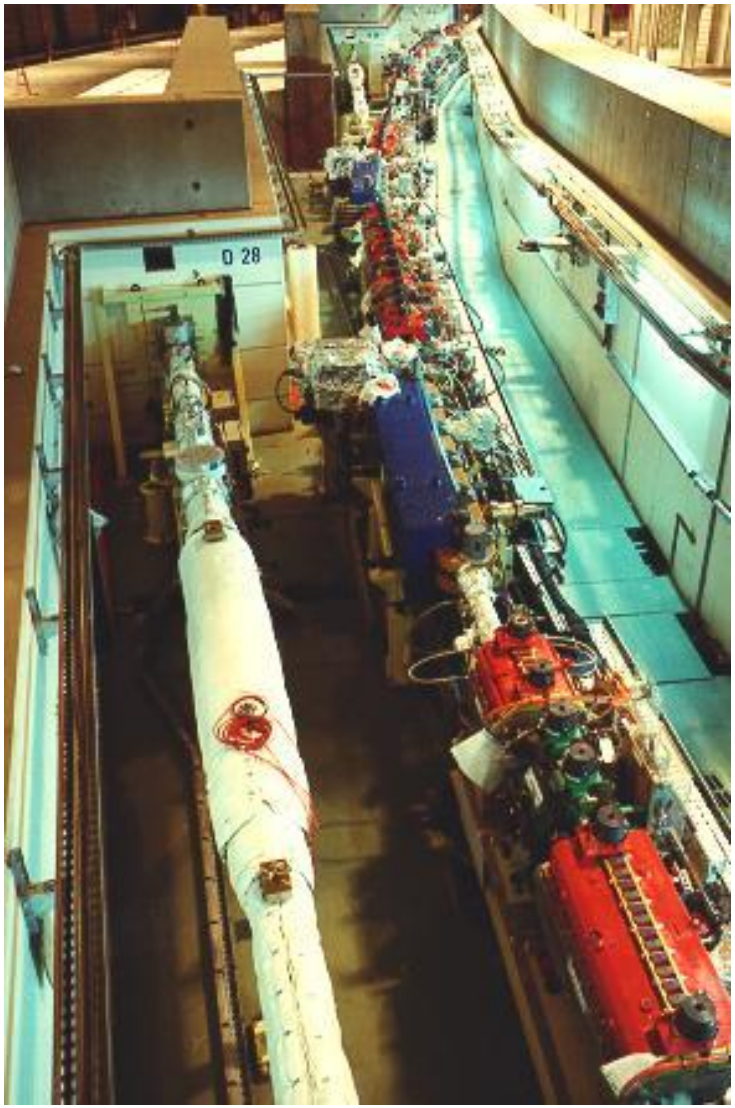

Front - end

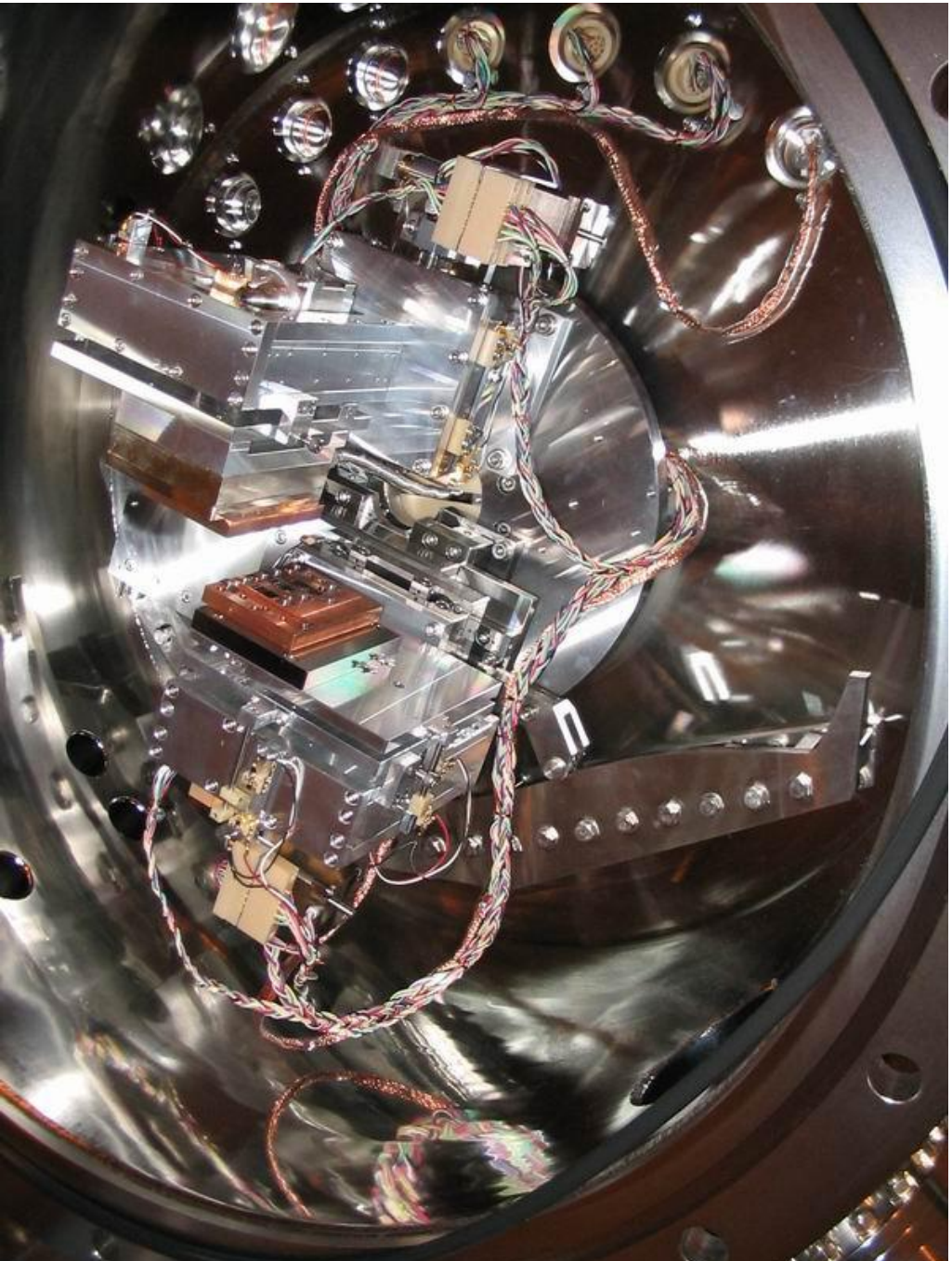

Double crystal monochromator

Si(111), Si(220), Si(311),
Ge(111)

Synchrotron radiation

Beamline

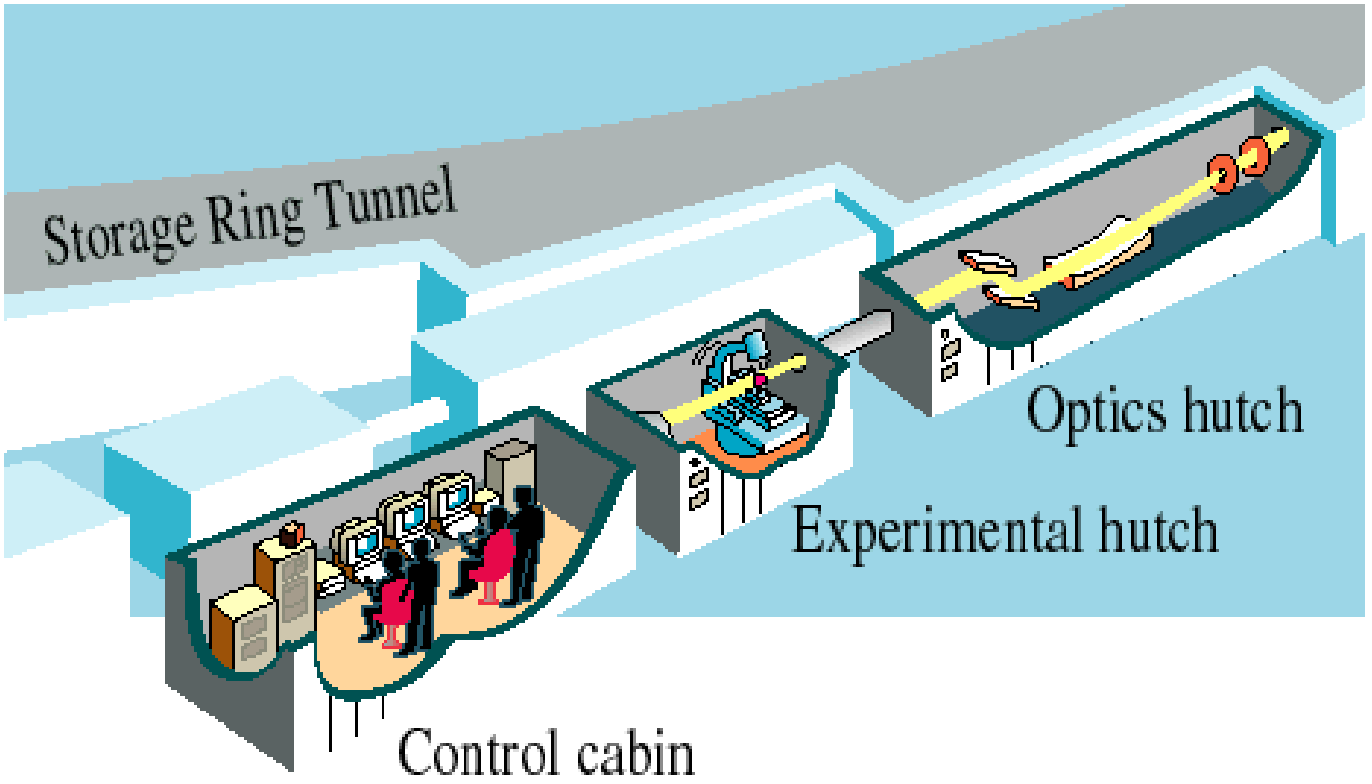

X-ray Absorption Spectroscopy

Acronyms

XAS X-ray Absorption Spectroscopy: Generic term for various techniques involving absorption of X-rays

XAFS X-ray Absorption Fine Structure: Name resuming the following two techniques

XANES(NEXAFS) X-ray Absorption Near Edge Structure: Studies the region just before and after the edge (about -20 eV +50 eV from edge). It is a ***spectroscopic*** technique

EXAFS Extended X-ray Absorption Fine Structure: Studies the region from about 50 eV up to 1000 (or more) eV from the edge. It is a ***structural*** technique

X-ray Absorption Spectroscopy

What is XAS?

• X-ray Absorption Spectroscopy exploits the x-ray photoelectric effect and the wave nature of the electron to study the modulation of the X-ray absorption coefficient at energies in the vicinity of the absorption edge of selected atomic species in the sample. The edge region and the extended region of the spectrum contain information about the chemical state and coordination environment of the absorber.

• Unlike X-ray diffraction, it does not require long range translational order – it works equally well in amorphous materials, liquids, (poly)crystalline solids and molecular gases.

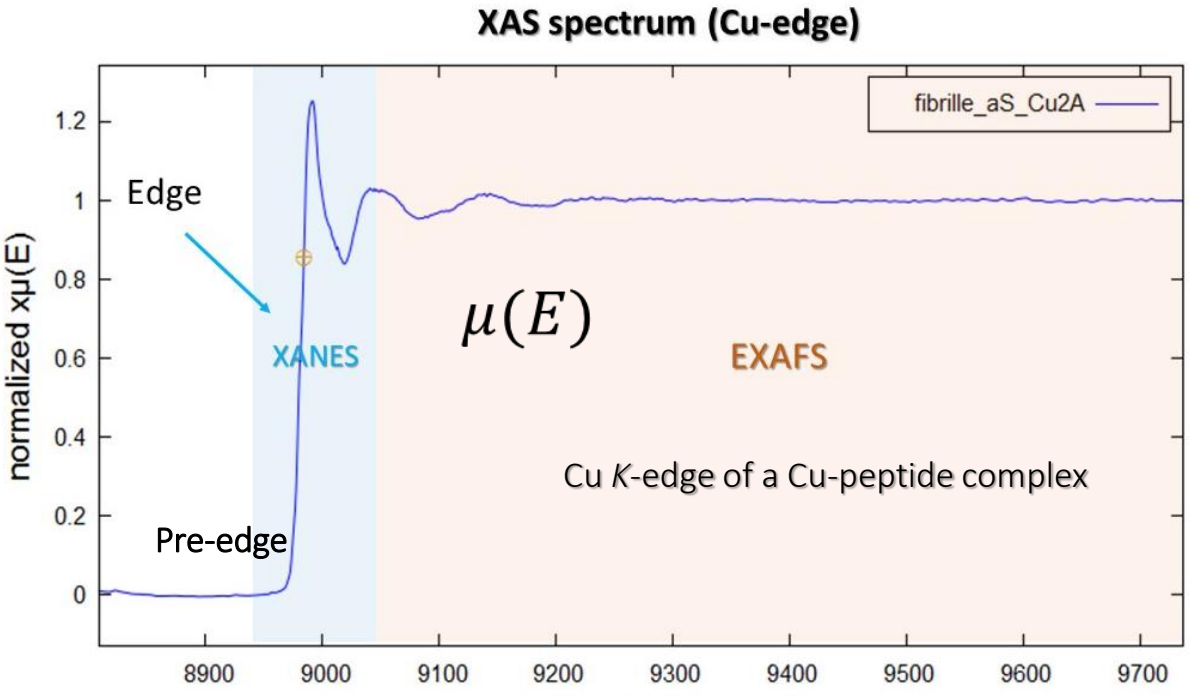

XAS characteristics

- interatomic distances, atom types
- coordination number (geometry) of absorber
- oxidation state of absorber
- covalency of coordination bonds

X-ray Absorption Spectroscopy

Mass absorption coefficient vs. E of different elements

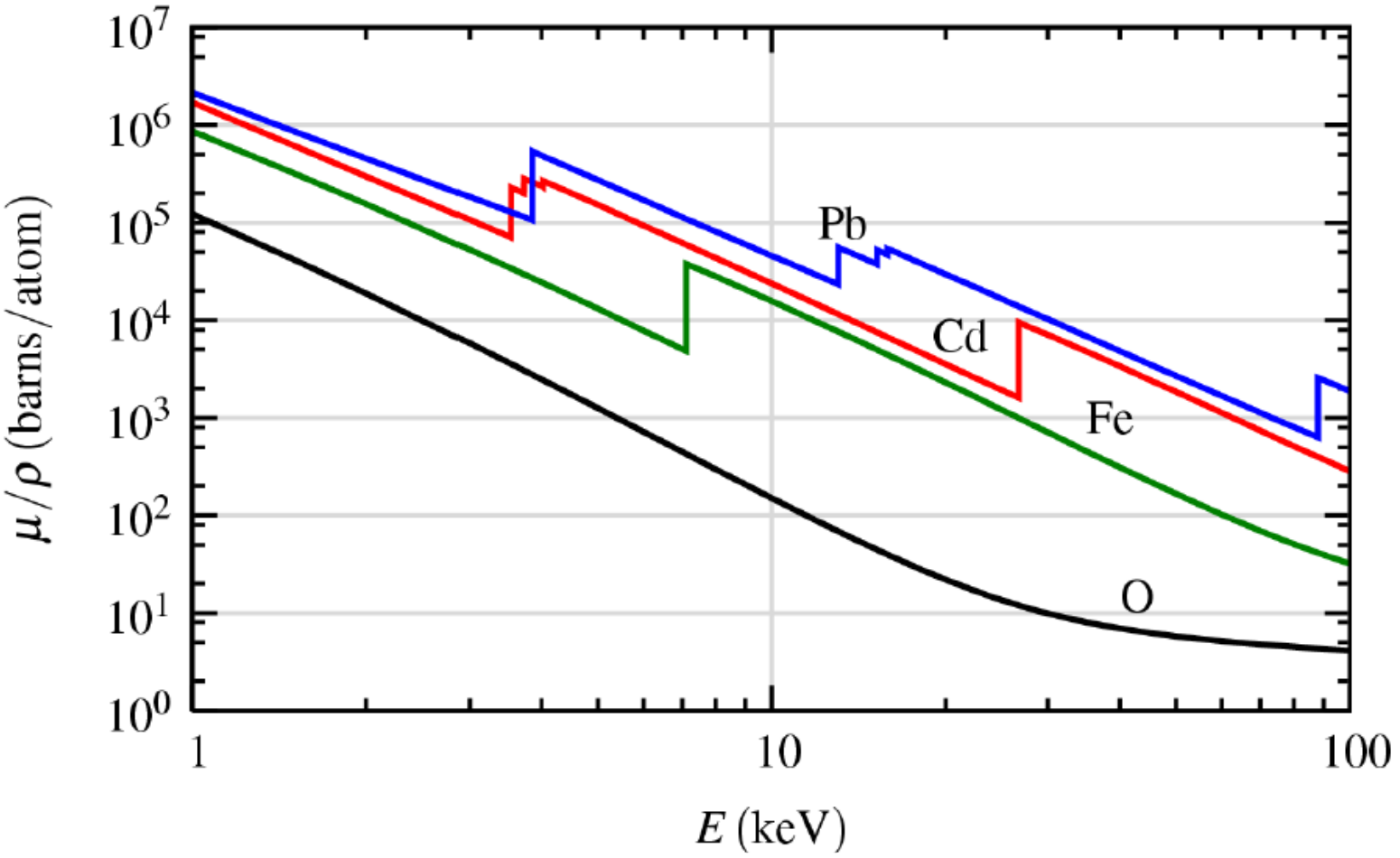

X-ray Absorption Spectroscopy

The photoelectric effect

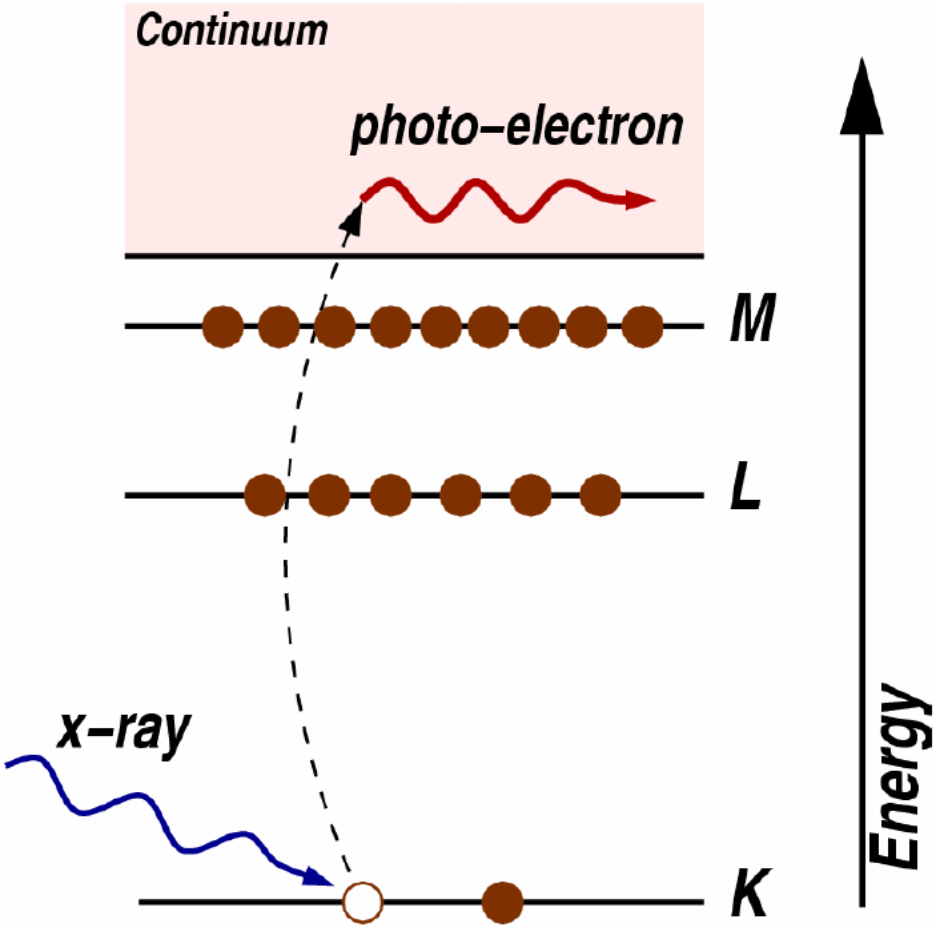

A core-level electron is extracted out of the absorbing atom that is now in an ***excited state***.
The kinetic energy of the free photoelectron is the *difference* between that of the absorbed photon and that of the initial electron state.

X-ray Absorption Spectroscopy

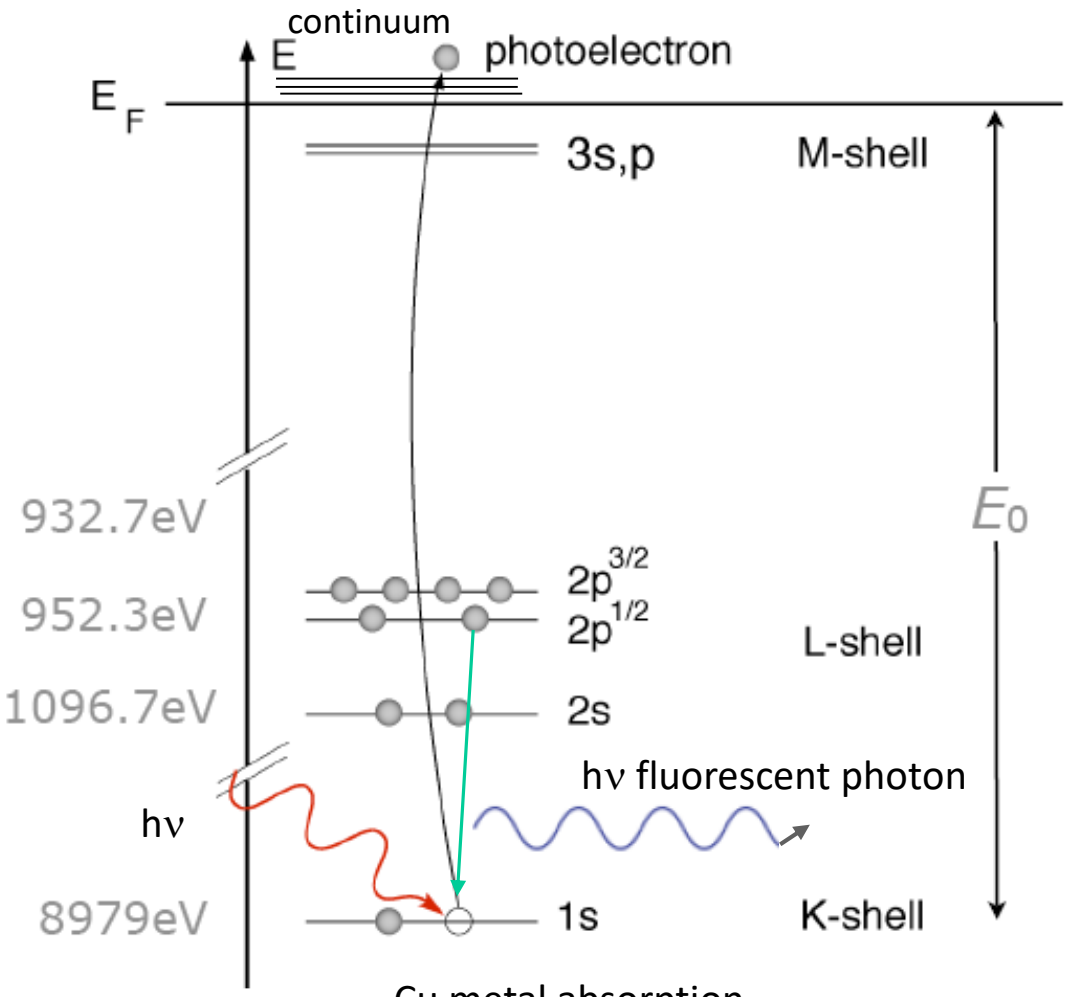

Cu metal absorption

Electrons are arranged in shells.
Photoionization: atom can be ionized by absorption of an (X-ray) photon if:

$E_{photon} > E_{ionization}$

Absorption/Emission Selection rules:

$\Delta L = \pm 1; \Delta S = 0; \Delta J = 0, \pm 1$

Core-hole decay may occur by ***x-ray fluorescence emission*** or by ***Augier*** electron emission

X-ray Absorption Spectroscopy

How XAS happens – the physical process:

photoabsorption/photoionization

Transition rate: The Fermi golden rule

$$\mu(E) \propto \left|\langle \psi_f | \boldsymbol{\varepsilon} \cdot \boldsymbol{p} | \psi_i \rangle\right|^2$$

Here $\boldsymbol{\varepsilon}$ is the electric dipole vector associated with the photon and $\boldsymbol{p}$ is the electron momentum, ψ_i and ψ_f are the electron initial and final states wave-functions.

This relation is valid if considering only «*elastic transitions*», (i.e. all the photon energy is transferred to the photoelectron so that only one core electron changes its state and the remaining N − 1 electrons, passive electrons, simply relax their orbitals around the core hole) and under the so-called «*electric dipole approximation*», i.e. when the photon electric field is constant over (almost all) the extension of the electron wave function. Under such approximation, the electromagnetic field interacts only with a core orbital, whose extension is smaller than the X-ray wavelength. For 1s electrons, this is the case.

X-ray Absorption Spectroscopy

How XAS happens – the physical process:

photoabsorption/photoionization

Example: Cu 1s orbital

Cu 1s electron radius:

Bohr radius of H in ground state

$$\frac{a_0}{Z} = \frac{0.53\ \text{Å}}{29} = 0.02\ \text{Å}$$

Wavelength of photon at the Cu absorption edge:

$$\lambda = \frac{hc}{E} = \frac{12.4\ keV\text{Å}}{8.9282\ keV} = 1.38\ \text{Å}$$

$\lambda \gg \frac{a_0}{Z}$: dipole approximation is well fullfilled

X-ray Absorption Spectroscopy

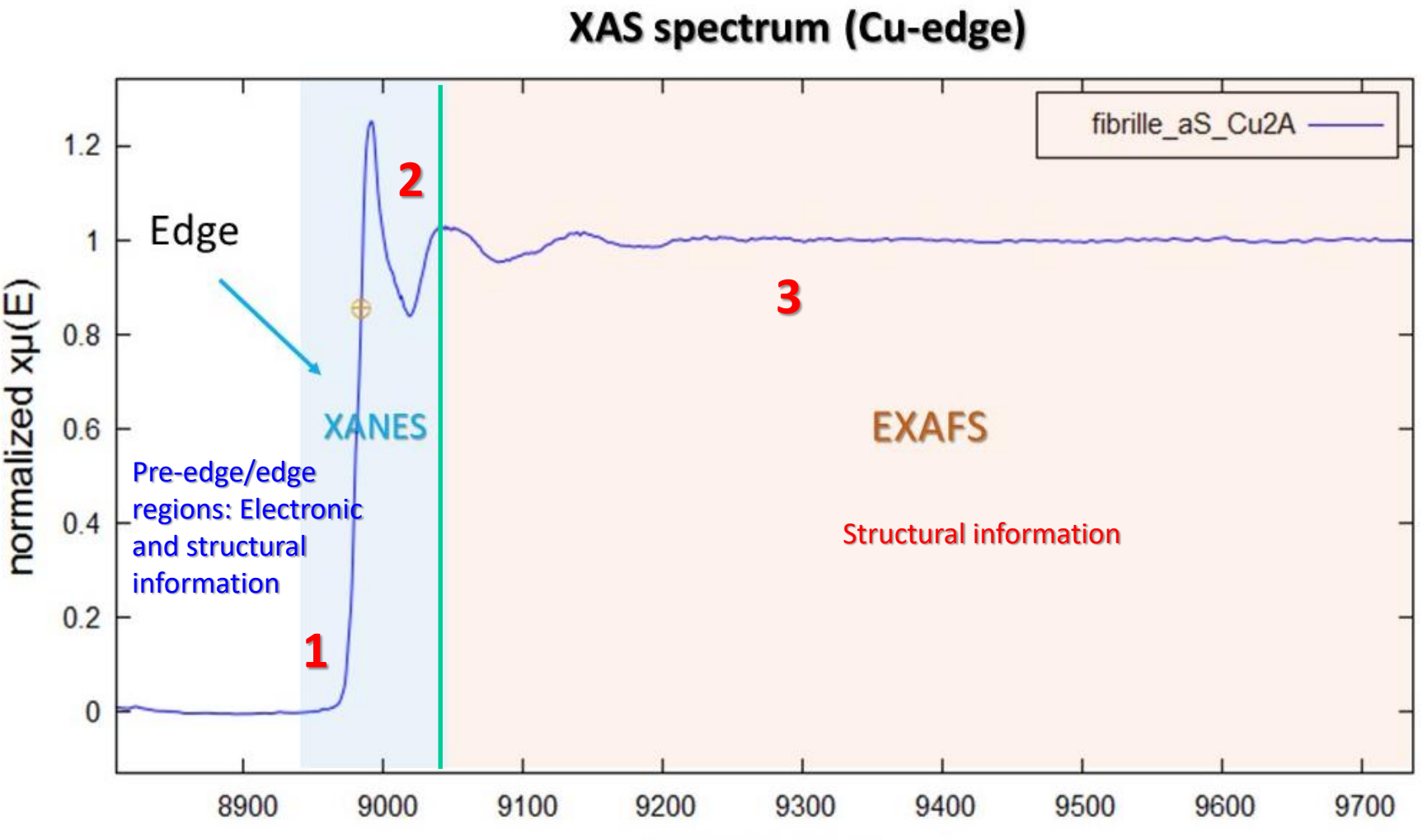

X-ray Absorption Spectroscopy

How XAS happens – the physical process

Electric-dipole electronic transitions between atomic quantum states.

$$\mu(E) \propto \left|\langle \psi_f | \boldsymbol{\varepsilon} \cdot \boldsymbol{p} | \psi_i \rangle\right|^2$$ **Transition probability**

$$\mu(E) \propto |\langle \psi_e | \boldsymbol{\varepsilon} \cdot \boldsymbol{p} | \psi_i \rangle|^2$$

1. *Core* to *bound* states (pre-edge, edge regions): the excited electron remains within the atom nuclear potential. The electronic structure of the emitter bound to the molecule is probed.
2. *Core* to *quasi-bound* states (XANES): multiple scattering resonances between the excited electrons with low kinetic energy dominate. Low kinetic energy electrons - Multiple scattering (typically up to ~ 50 eV above the threshold, the region where bound to quasi-bound transitions take place); e is scattered primarily by valence and shallow inner shell electrons of the neighboring atoms - XANES region.

X-ray Absorption Spectroscopy

How XAS happens – the physical process

3. *core* to *continuum* (electron with sufficient kinetic energy to escape into the continuum) - photoelectric effect. (EXAFS). High kinetic energy electrons (50 -1000 eV) are scattered primarily by the core electrons of the neighboring atoms, single scattering pathway dominates - EXAFS region.

It is suggested that the boundary between XANES and EXAFS regions is that where the wavelength of excited electron is equal to the distance between the absorbing atom and its nearest neighbors. ($\lambda(\text{Å}) = 12/[E(\text{eV})]^{1/2}$).

X-ray Absorption Spectroscopy

How XAS happens – electron scattering

Free electron (plane wave) scattered by an atom (spherical potential) travels away as a spherical wave.
Electron with kinetic energy: KE > 0 in a molecular environment is scattered be the surrounding atoms.
Low KE e^- is scattered by valence electrons, undergoes multiple scattering in a molecular environment (XANES).
High KE e^- is scattered by core electrons, favors single scattering (EXAFS).

The number of absorbed photons is proportional to the absorption probability (the absorption cross-section for the absorber A is given by: $\sigma = \frac{\mu}{\rho} \cdot \frac{m_a}{N_A}$; where $\frac{\mu}{\rho}$ is the mass absorption coefficient, m_a is the atomic molar mass and N_A is the Avogadro's number.

X-ray Absorption Spectroscopy

Example: Linear Absorption Coefficient of Cu & Ag

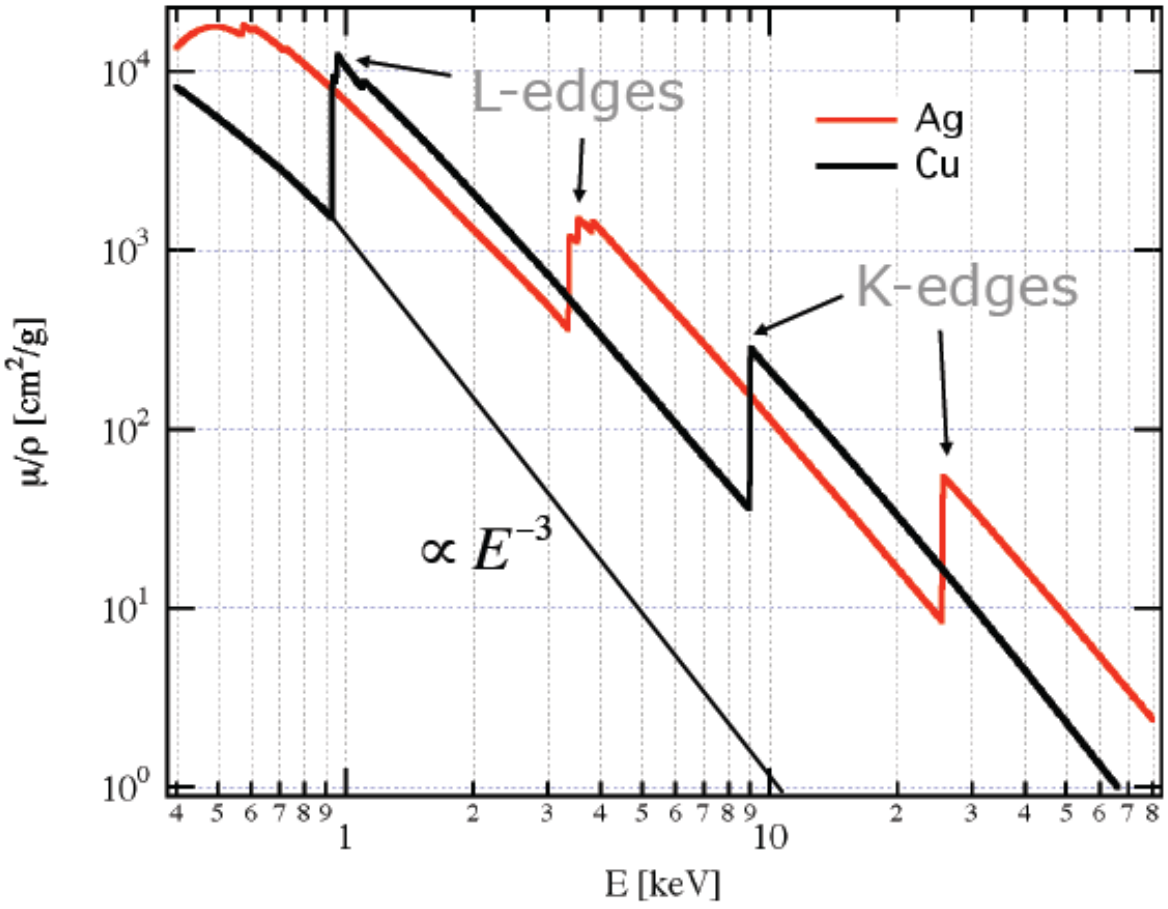

- mainly atomic effect!
- strong dependence on energy

$$\propto E^{-2.78}$$

- strong dependence on atomic number:

$$\propto Z^{2.7}$$

- inner shell electr. contribute most strongly!

X-ray Absorption Spectroscopy

The EXAFS equation

Absorber has neighboring atoms in condensed matter. They scatter back the emitted photoelectron.

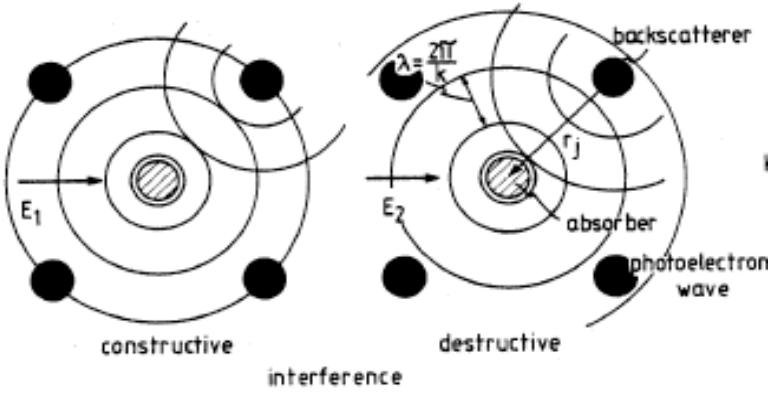

Interference occurs between outgoing and incoming waves

EXAFS monitors the variable behavior of theabsorpion coefficient above the edge energy

$$\chi(k) = \frac{\mu - \mu_0}{\mu_0}$$

$$\lambda = \frac{2\pi}{k}, \quad k = \frac{1}{\hbar}\sqrt{2m(E - E_0)}$$

where E_0 is the absorption edge energy and m is the electron mass. $k = 0.513\ \Delta E^{1/2}(\text{Å}^{-1})$

X-ray Absorption Spectroscopy

The EXAFS equation

EXAFS: Oscillatory Part of μ beyond the edge

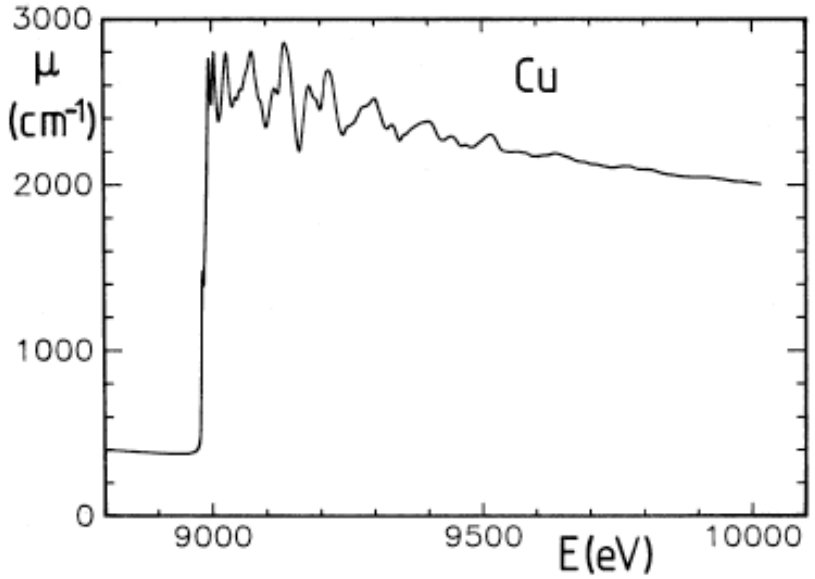

$$\chi(k) = \frac{\mu - \mu_0}{\mu_0}$$ EXAFS

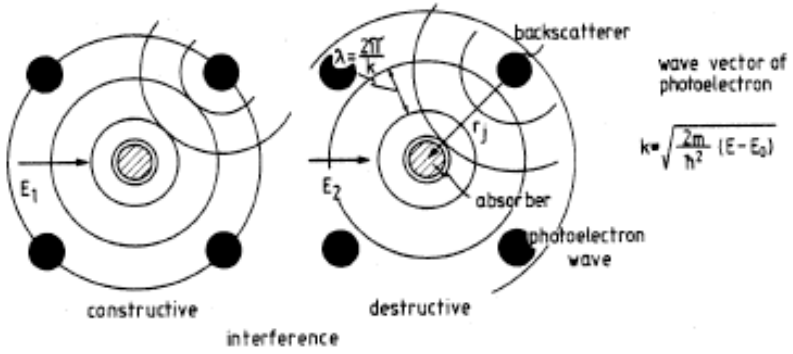

Constructive (destructive) interference:

probability to excite electron is increased (reduced)

μ has maximum (minimum)

X-ray Absorption Spectroscopy

EXAFS

How can the emitted electron influence the absorption of the photon?

Naive picture:

1. photon is absorbed
2. electron is emitted
3. electron is scattered back by neighbors

How can scattering of electron (step 3) influence absorption (step 1)?

X-ray Absorption Spectroscopy

EXAFS

How can the emitted electron influence the absorption of the photon?

Quantum mechanical process:

photon (with given energy) is absorbed by atom and electron is excited into (free) state!

This is a one step process!

Final state of electron is given by the local environment of the atom!

Final state determines transition probability!

$$\mu(E) \propto |\langle \psi_e | \boldsymbol{\varepsilon} \cdot \boldsymbol{p} | \psi_i \rangle|^2$$

X-ray Absorption Spectroscopy

EXAFS

How can the emitted electron influence the absorption of the photon?

Other way of looking at the same process:

absorption of photon takes a certain time τ_0
[given by the length of the wave train of the photon (monochromaticity)]

During that time the excited electron has time to probe the local environment of the atom.

X-ray Absorption Spectroscopy

EXAFS: Monochromaticity and Coherence Time

Example:
energy: 9000eV
band width: ~1eV

1eV = 1.60218 x 10^{-19} J
h =4.13667×10^{-15} eV·s =
= 6.62607×10^{-34} J·s

$$\nu = \frac{E}{h} = 2.3 \cdot 10^{18}\ \mathrm{s}^{-1}, \quad T = 4.4 \cdot 10^{-19}\ \mathrm{s}$$

wave train contains ~ 9000 oscillations:
$\tau_0 = 4 \cdot 10^{-15}$ s

In copper:

energy of electron: ~ 20-100 eV

In time τ_0 electron could travel ~ 50 – 100 Å and back!

In practice, travel range limited by inelastic scattering processes to about 10Å.

X-ray Absorption Spectroscopy: the experiment

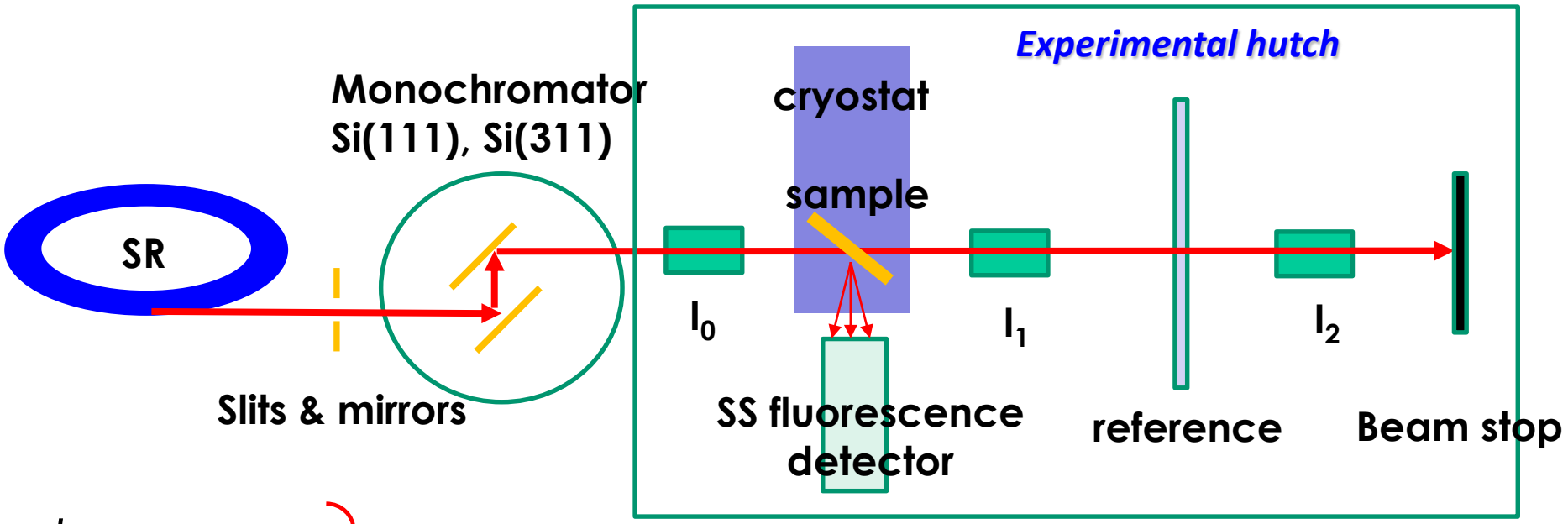

$$\frac{I}{I_0} = e^{-\mu(E)x}$$

$$\mu(E)x = \ln\frac{I_0}{I}$$

Absorption mode

$$\mu(E) = \frac{I_F}{I_0}$$

Fluorescence mode

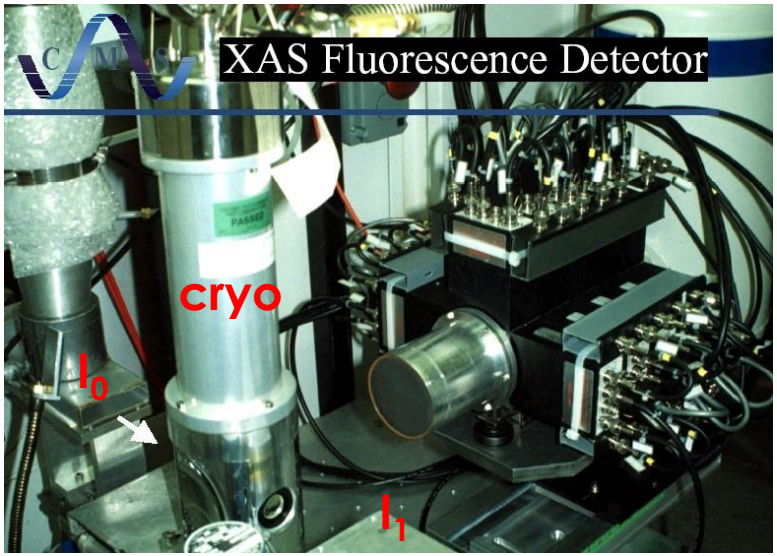

X-ray Fluorescence Emission

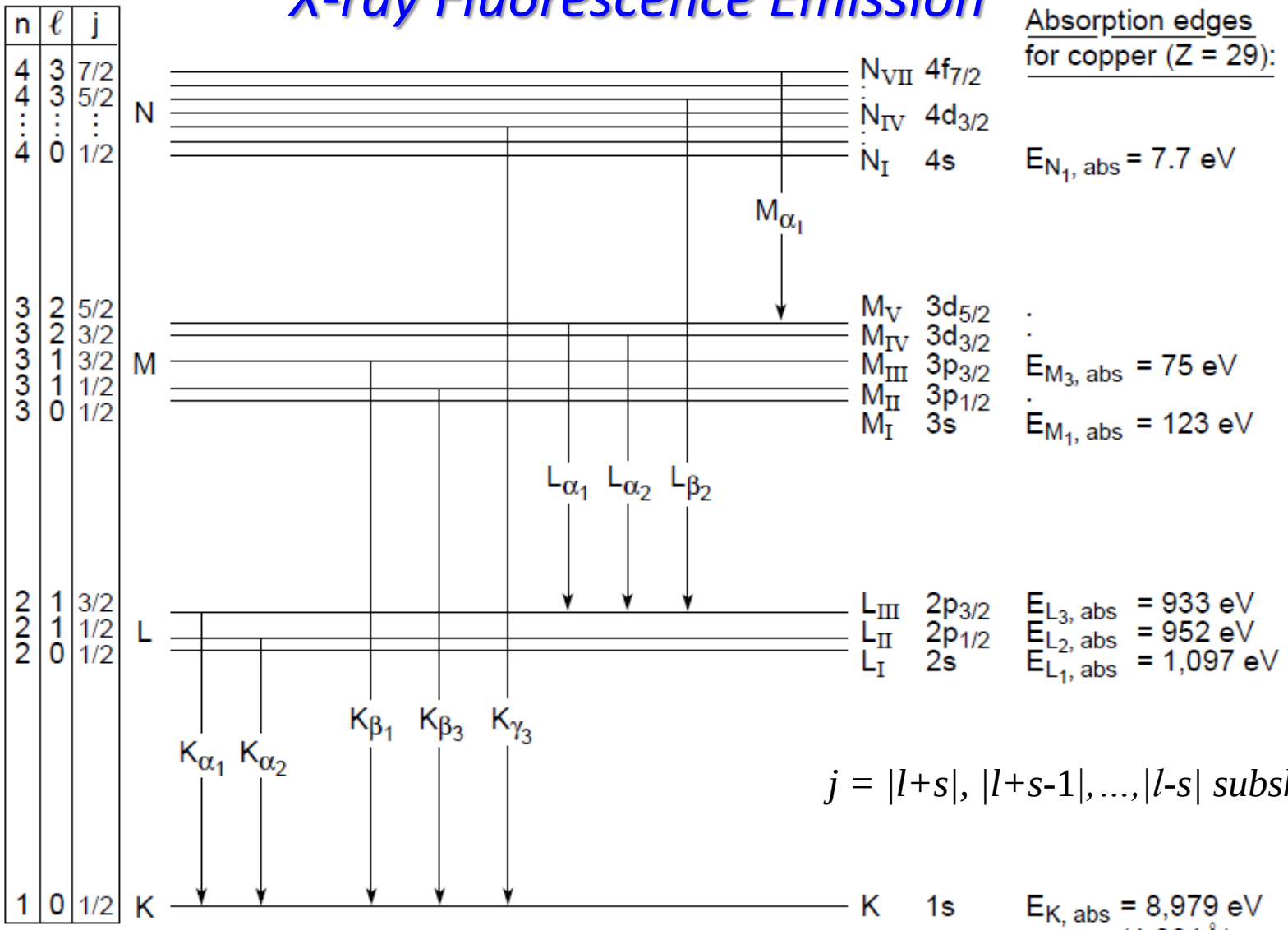

Absorption edges for copper (Z = 29):

$E_{N_1, abs}$ = 7.7 eV

$E_{M_3, abs}$ = 75 eV

$E_{M_1, abs}$ = 123 eV

$E_{L_3, abs}$ = 933 eV

$E_{L_2, abs}$ = 952 eV

$E_{L_1, abs}$ = 1,097 eV

$E_{K, abs}$ = 8,979 eV (1.381Å)

$j = |l+s|, |l+s-1|, \ldots, |l-s|$ *subshells*

Cu K_{α_1} = 8,048 eV (1.541Å)
Cu K_{α_2} = 8,028 eV (1.544Å)
Cu K_{β_1} = 8,905 eV

Cu L_{α_1} = 930 eV
Cu L_{α_2} = 930 eV
Cu L_{β_1} = 950 eV

Sample requirements and limitations

- ✓ Samples can be measured in any state:
- Solid (pure or solution)
- Liquid (pure or solution)
- Gas (also mixtures)
- Frozen solutions

- ✓ Concentrations and volume requirements depend on energy, flux, beamline characteristics
- 1 mM (typical) - 50 μM (possible)
- Small volume (10 μL with focused beam)

The experimental XAS spectrum

Example: Absorption of Cu

μ(E): linear absorption coefficient

metallic copper:

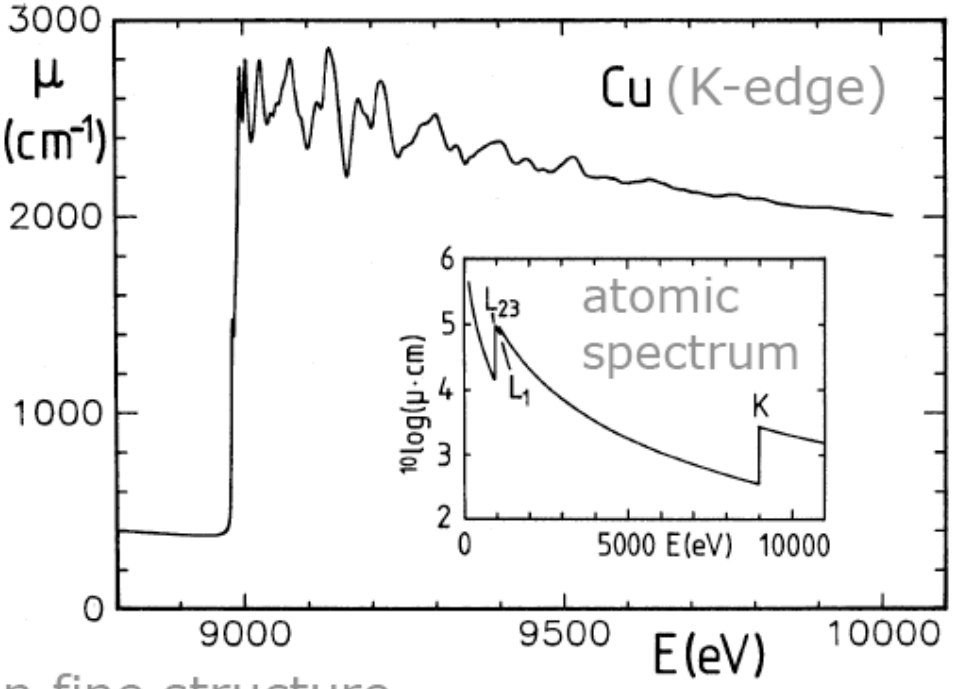

In condensed matter: absorption fine structure

X-ray Absorption Fine Stucture

X-RAY & ABSORPTION EDGE ENERGIES (keV)

Element	K_{abs}	$K\alpha_1$	$K\beta_1$	L-III_{abs}	$L\alpha_1$	$L\beta_1$	M-V_{abs}	$M\alpha_1$	$M\beta$
9 F	0.687	0.677							
11 Na	1.072	1.041	1.067						
12 Mg	1.305	1.253	1.295						
13 Al	1.559	1.486	1.553						
14 Si	1.838	1.740	1.829						
15 P	2.142	2.013	2.136						
16 S	2.472	2.307	2.464						
17 Cl	2.822	2.622							
18 Ar	3.202	2.957	3.190						
19 K	3.607	3.313	3.589						
20 Ca	4.038	3.691	4.012	0.346	0.341	0.345			

X-RAY & ABSORPTION EDGE ENERGIES (keV)

21 Sc	4.496	4.090	4.460	0.403	0.395	0.400			
22 Ti	4.965	4.510	4.931	0.454	0.452	0.458			
23 V	5.465	4.951	5.426	0.513	0.511	0.519			
24 Cr	5.989	5.414	5.946	0.574	0.573	0.583			
25 Mn	6.540	5.898	6.489	0.641	0.637	0.649			
26 Fe	7.112	6.403	7.057	0.709	0.705	0.718			
27 Co	7.709	6.929	7.648	0.779	0.776	0.791			
28 Ni	8.333	7.477	8.263	0.855	0.851	0.869			
29 Cu	8.979	8.046	8.904	0.932	0.930	0.950			
30 Zn	9.659	8.637	9.570	1.021	1.012	1.034			
38 Sr	16.105	14.163	15.833	1.940	1.806	1.871			
40 Zr	17.998	15.772	17.665	2.223	2.042	2.124			
56 Ba	37.441	32.188	36.372	5.247	4.465	4.827			
57 La	38.925	33.436	37.795	5.483	4.650	5.041			0.854
58 Ce	40.449	34.714	39.251	5.724	4.839	5.261			0.902
60 Nd	43.571	37.355	42.264	6.208	5.229	5.721			0.996
72 Hf	65.351	55.781	63.222	9.561	7.898	9.021			1.697
82 Pb	88.006	74.965	84.922	13.035	10.550	12.612	2.484	2.345	2.442
90 Th	109.646	93.334	105.591	16.300	12.967	16.199	3.332	2.996	3.145
92 U	115.036	98.422	111.281	17.167	13.612	17.217	3.552	3.170	3.336

The experimental XAS spectrum

X-Ray Absorption Spectrum

- edge position:

  oxidation state

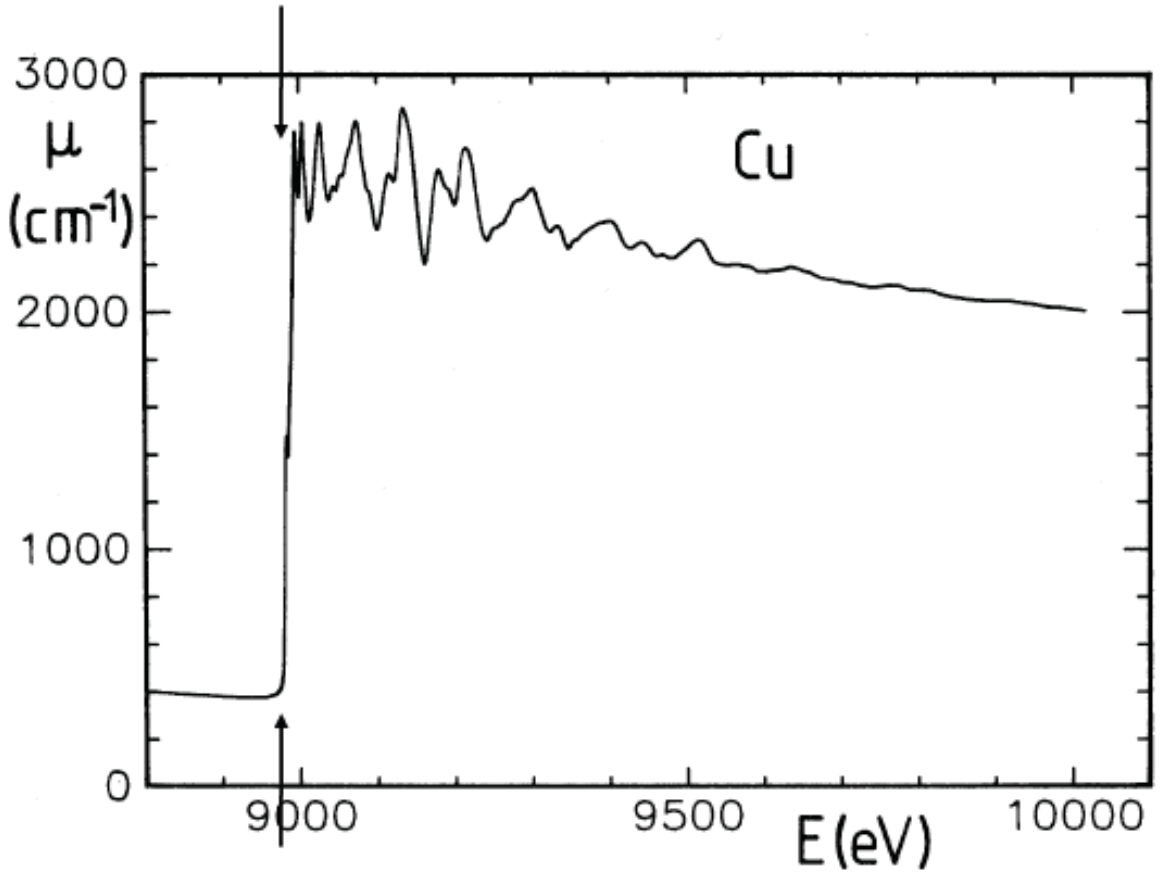

The experimental XAS spectrum

X-Ray Absorption Spectrum

- edge position:

  oxidation state

- near edge spectrum:

  local free projected density of states

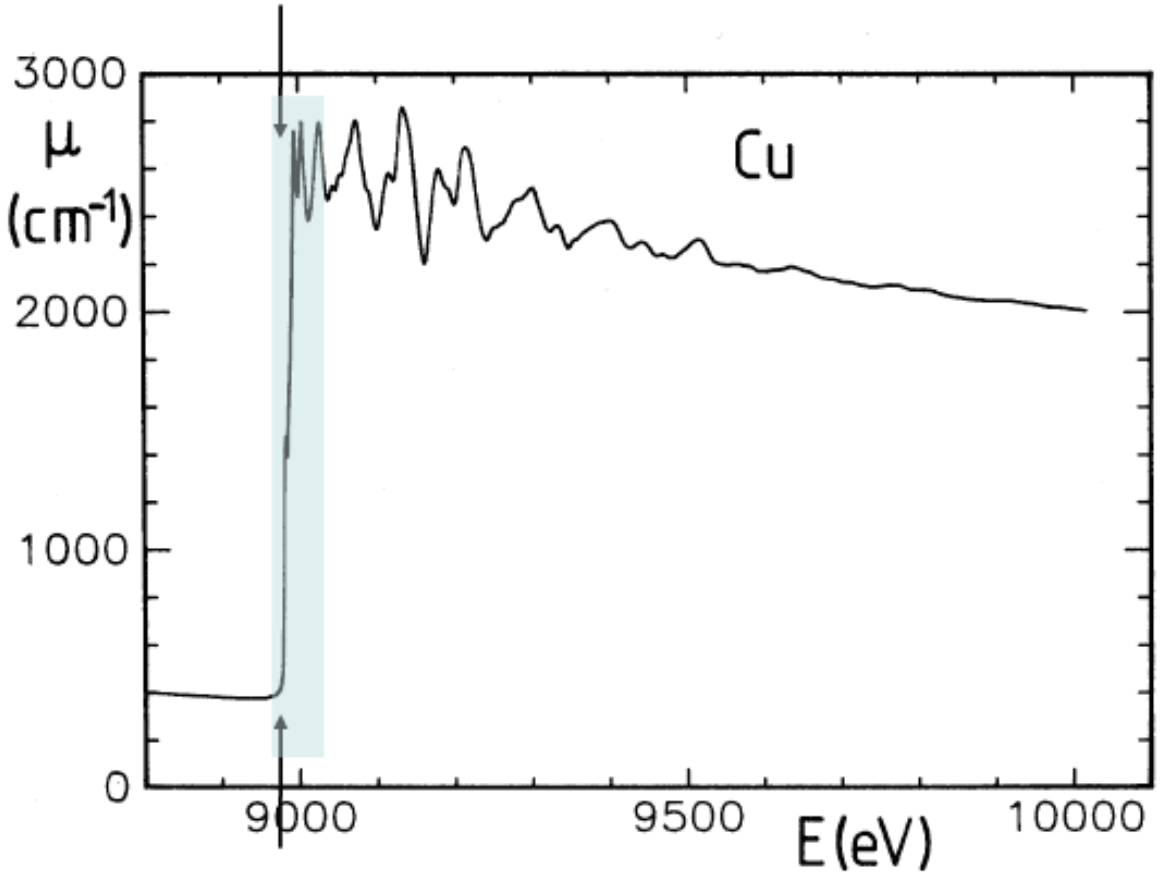

The experimental XAS spectrum

X-Ray Absorption Spectrum

- edge position:

  oxidation state

- near edge spectrum:

  local free projected density of states

- extended fine structure:

  local atomic neighborhood

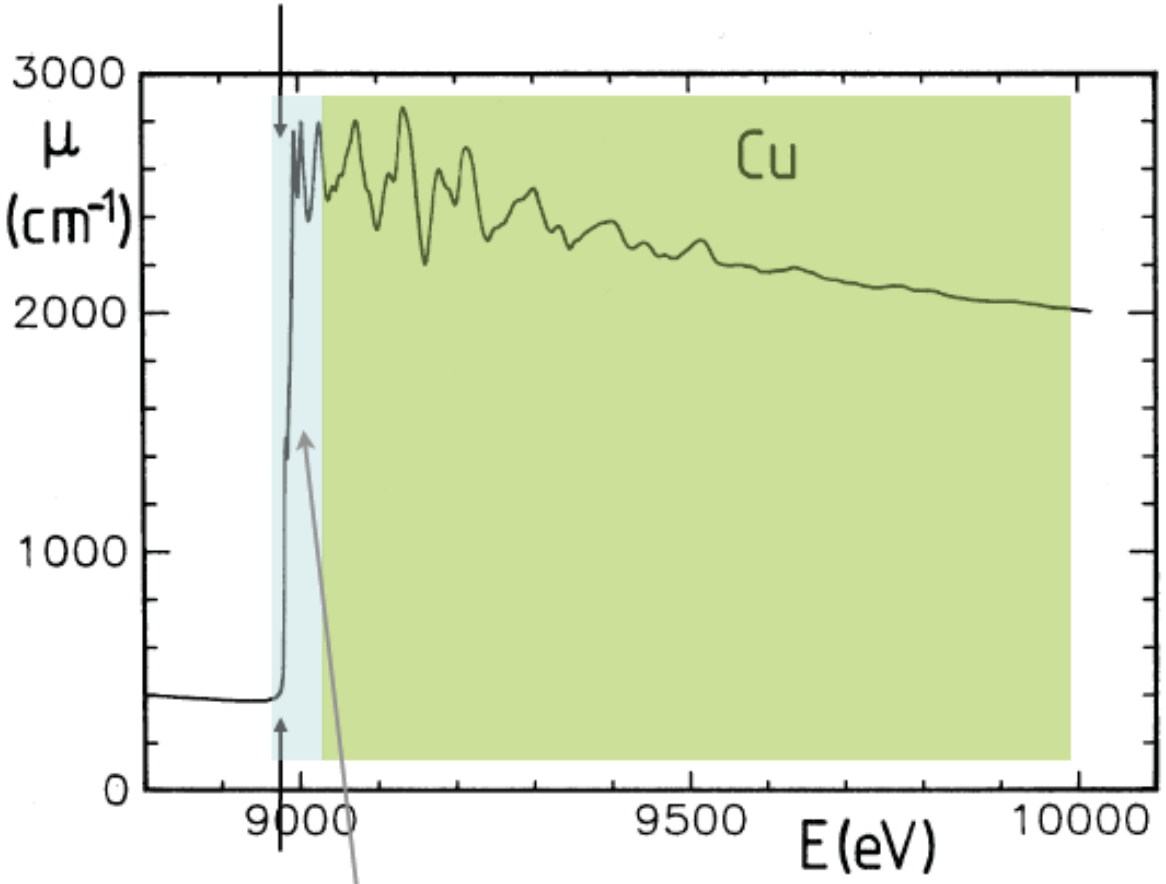

XANES

X-ray Absorption Near Edge Structure

The experimental XAS spectrum

EXAFS: Data Analysis

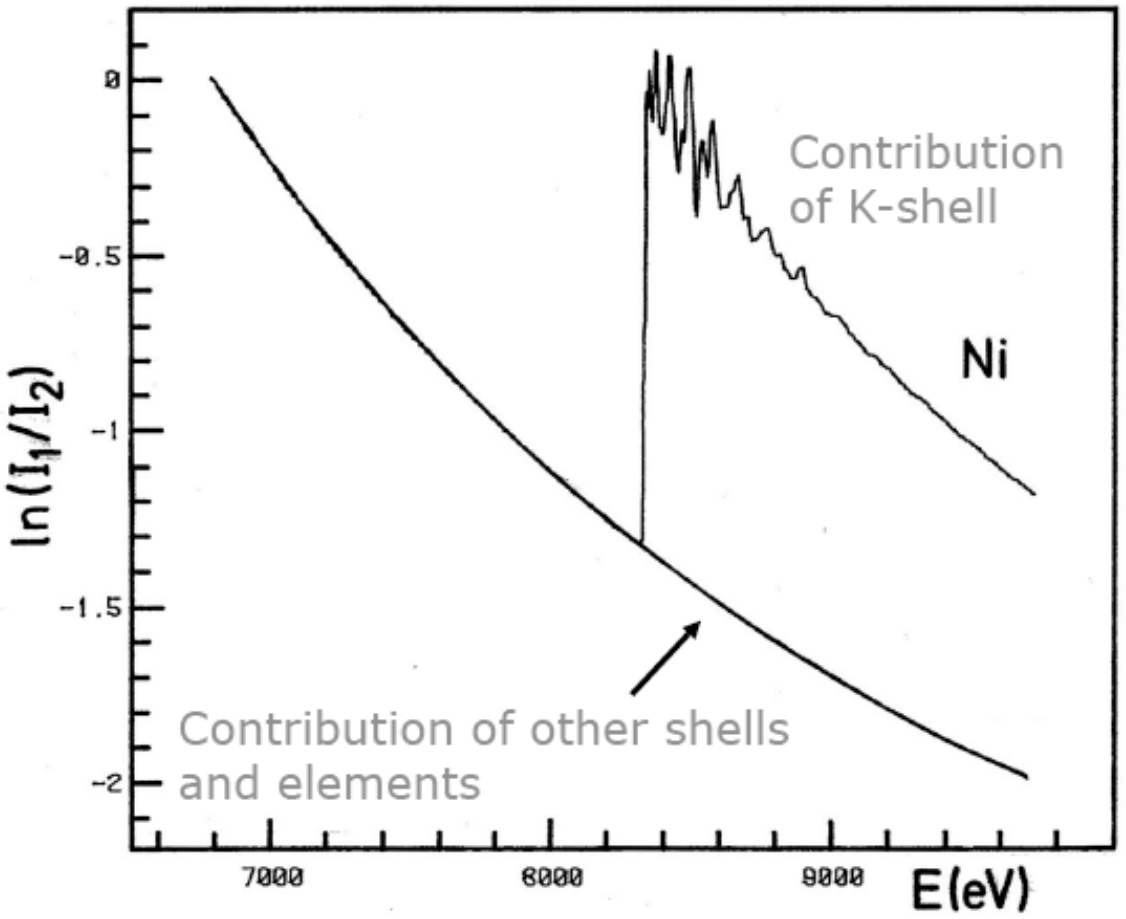

Subtract contribution of other shells and elements

The experimental XAS spectrum

EXAFS: Data Analysis

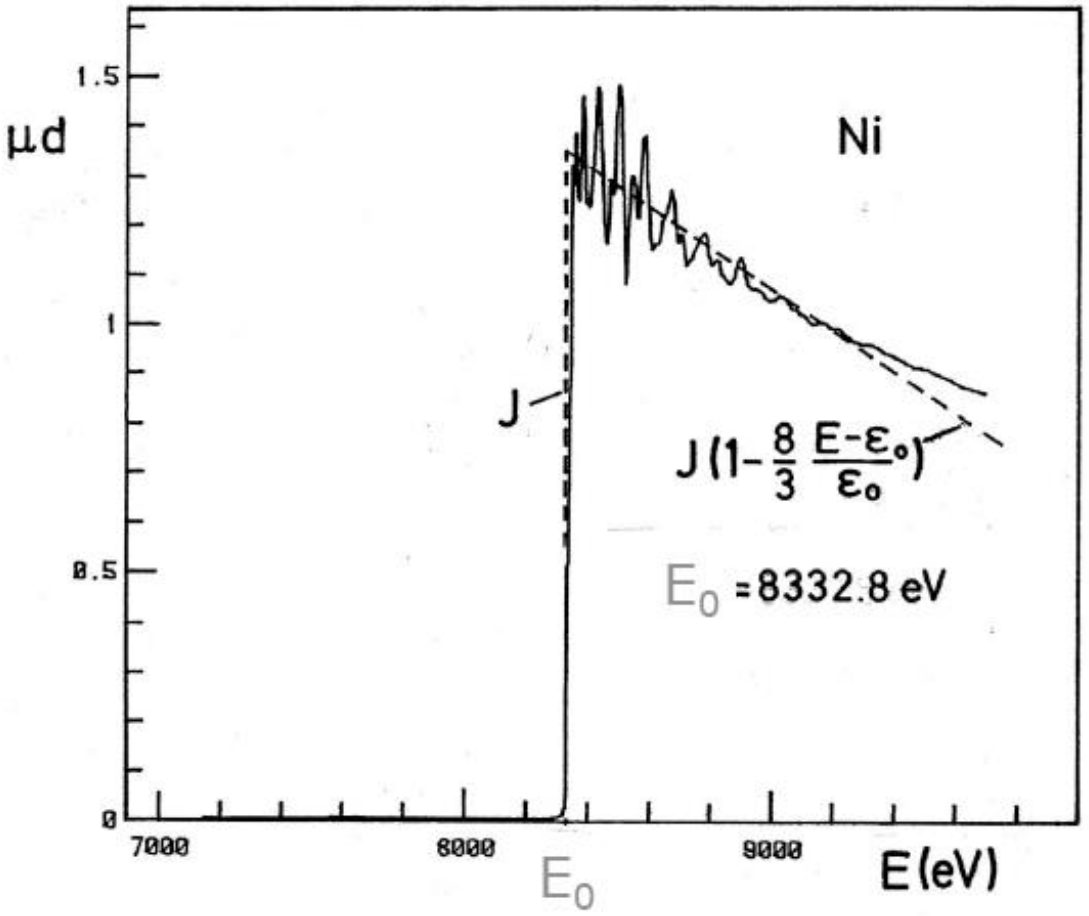

Position of absorption edge:

E_0 not well defined

rule of thumb: first inflection point on edge

The experimental XAS spectrum

EXAFS: Data analysis

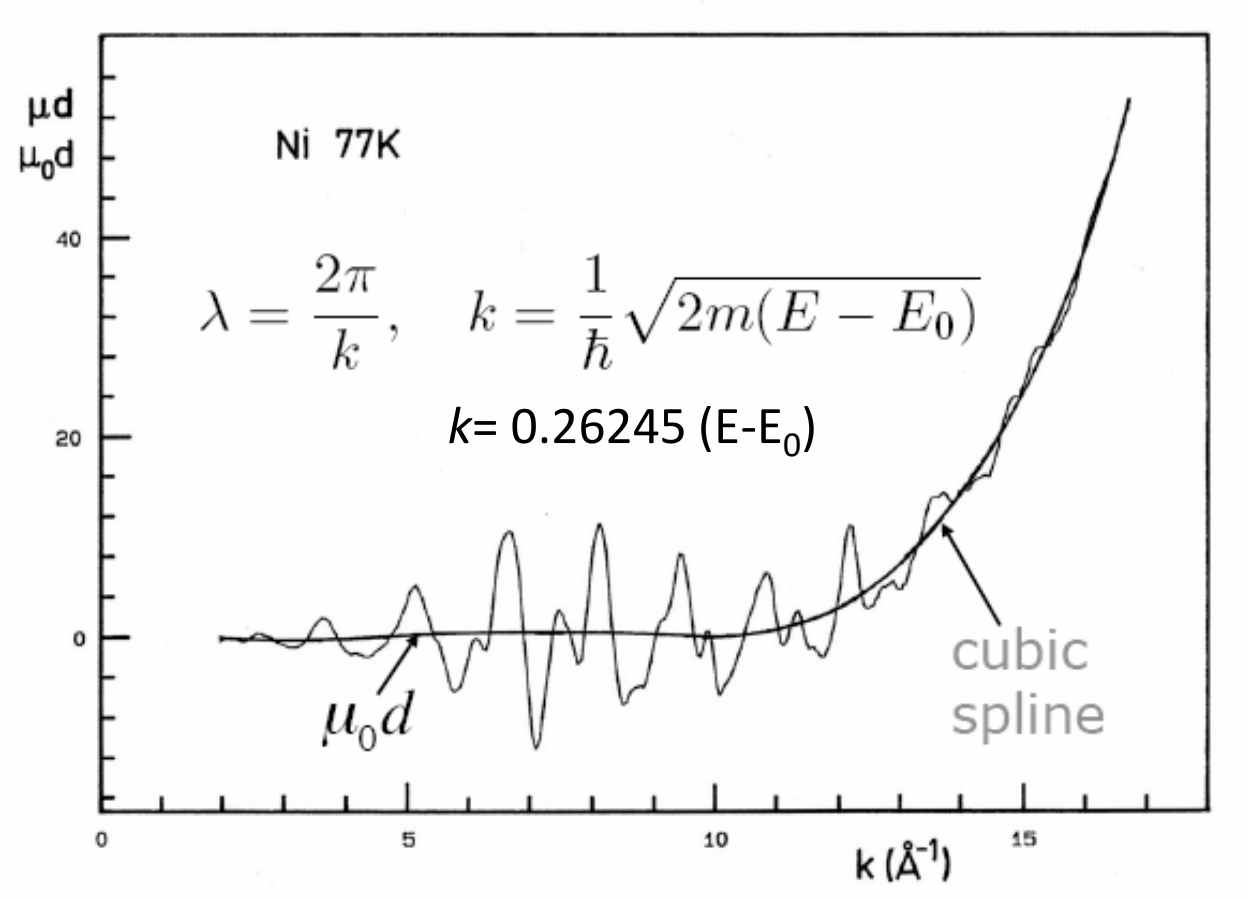

subtract background (without introducing additional oscillations)

Oscillations:

$$\chi(k) = \frac{\mu - \mu_0}{\mu_0}$$

Plot oscillations over *k* rather than *E*.

The experimental XAS spectrum

EXAFS: Data Analysis

Input to EXAFS data analysis:

oscillations:

$$\chi(k) = \frac{\mu - \mu_0}{\mu_0}$$

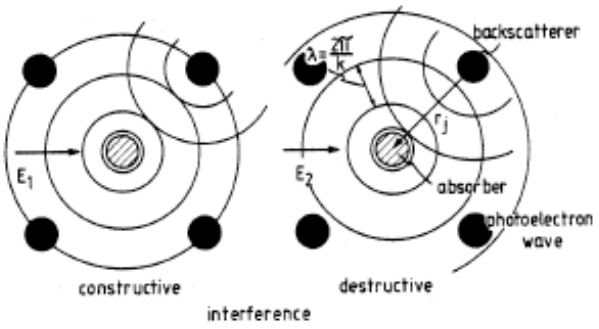

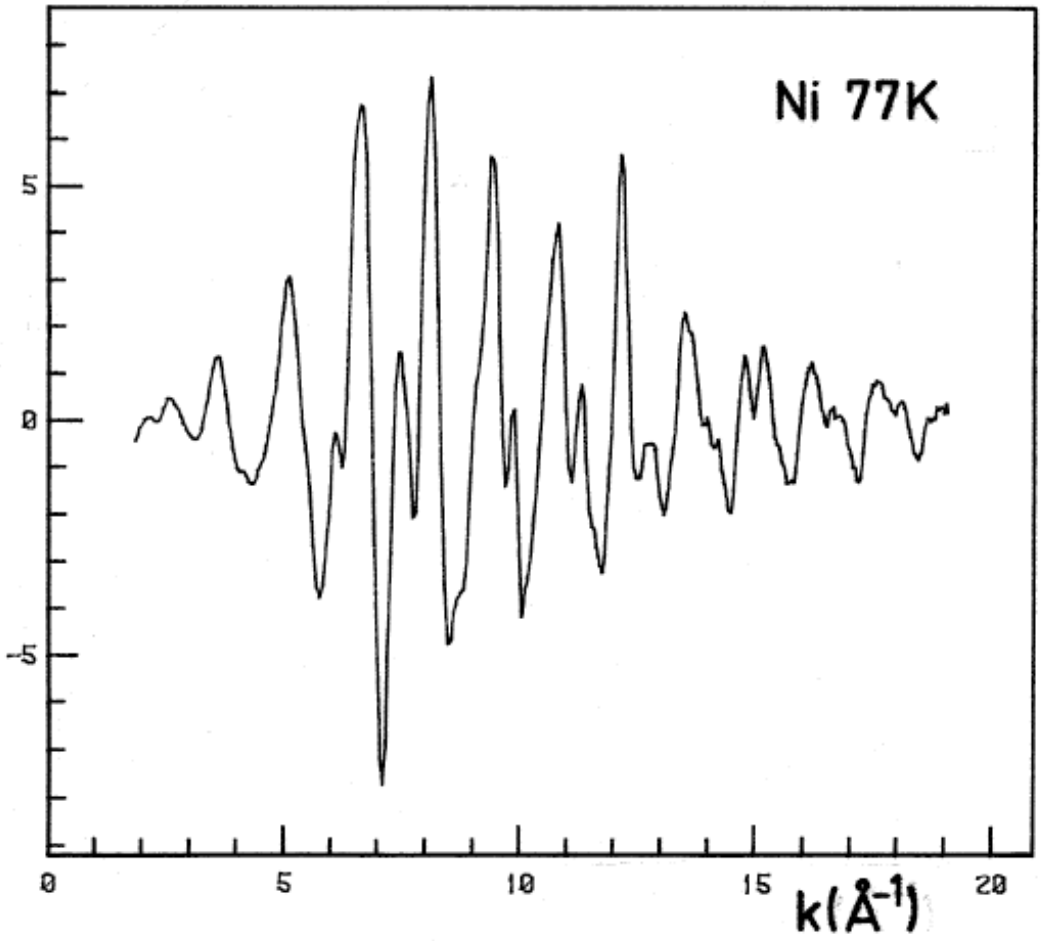

The EXAFS formula

Elementary EXAFS formula (Lytle, Sayers, Stern)

$$\chi(k) = \sum_j \frac{N_j S_0^2}{k r_j^2} F_j(k) D_j(k) \exp\left(-2\sigma_j^2 k^2\right) \sin(2kr_j + \Phi_j(k))$$

interference:

$$\sin(2kr_j) = \sin\left(\frac{2\pi}{\lambda} 2r_j\right)$$

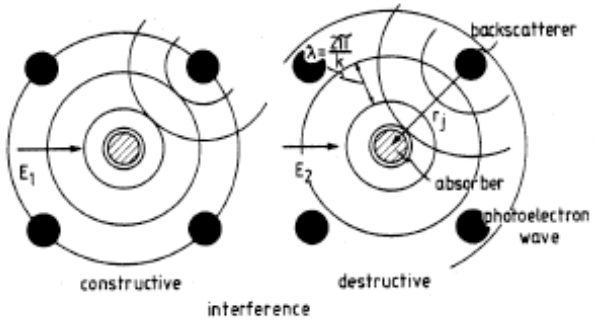

r_j: distance to neighboring shell j

$F_j(k)$: backscattering amplitude

$\Phi_j(k)$: scattering phases in absorber and backscatterer

N_j: number of neighbors in shell j.

S_0^2 : amplitude reduction factor due to intrinsic inelastic effects within the absorbing atom (0.7 – 0.9)

The EXAFS formula

Elementary EXAFS formula (Lytle, Sayers, Stern)

$$\chi(k) = \sum_j \frac{N_j S_0^2}{k r_j^2} F_j(k) D_j(k) \exp\left(-2\sigma_j^2 k^2\right) \sin(2kr_j + \Phi_j(k))$$

interference:

$$\sin(2kr_j) = \sin\left(\frac{2\pi}{\lambda} 2r_j\right)$$

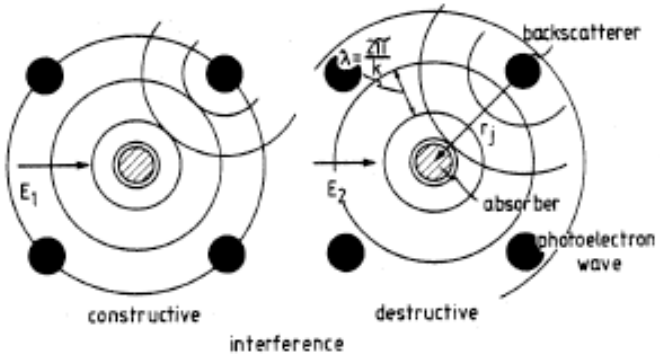

r_j: distance to neighboring shell j

$F_j(k)$: backscattering amplitude

$\Phi_j(k)$: scattering phases in absorber and backscatterer

N_j: number of neighbors in shell j.

$$D_j = \exp(-\frac{2r_j}{\Lambda(k)})$$

$$\Lambda^{-1} \cong \sqrt{3}\frac{a_0 R}{E_{kin}} r_s^{3/2} \ln\left[(\frac{4}{9\pi})^{3/2} \frac{E_{kin}}{R} r_s^2\right]$$

Essential structural information from EXAFS

Observable	Information	Accuracy
Frequency of oscillations	distance	0.005 – 0.02 Å
Phase shift	Type of atoms in shell	$Z \pm 2$ ($Z = 6 – 17$) $Z \pm 3$ ($Z = 20 – 35$)
Amplitude of oscillations	Type of atoms in shell Number of atoms in shell (coordination number	$N \pm 5 – 25$ % Depending on the system and data quality

The EXAFS signal

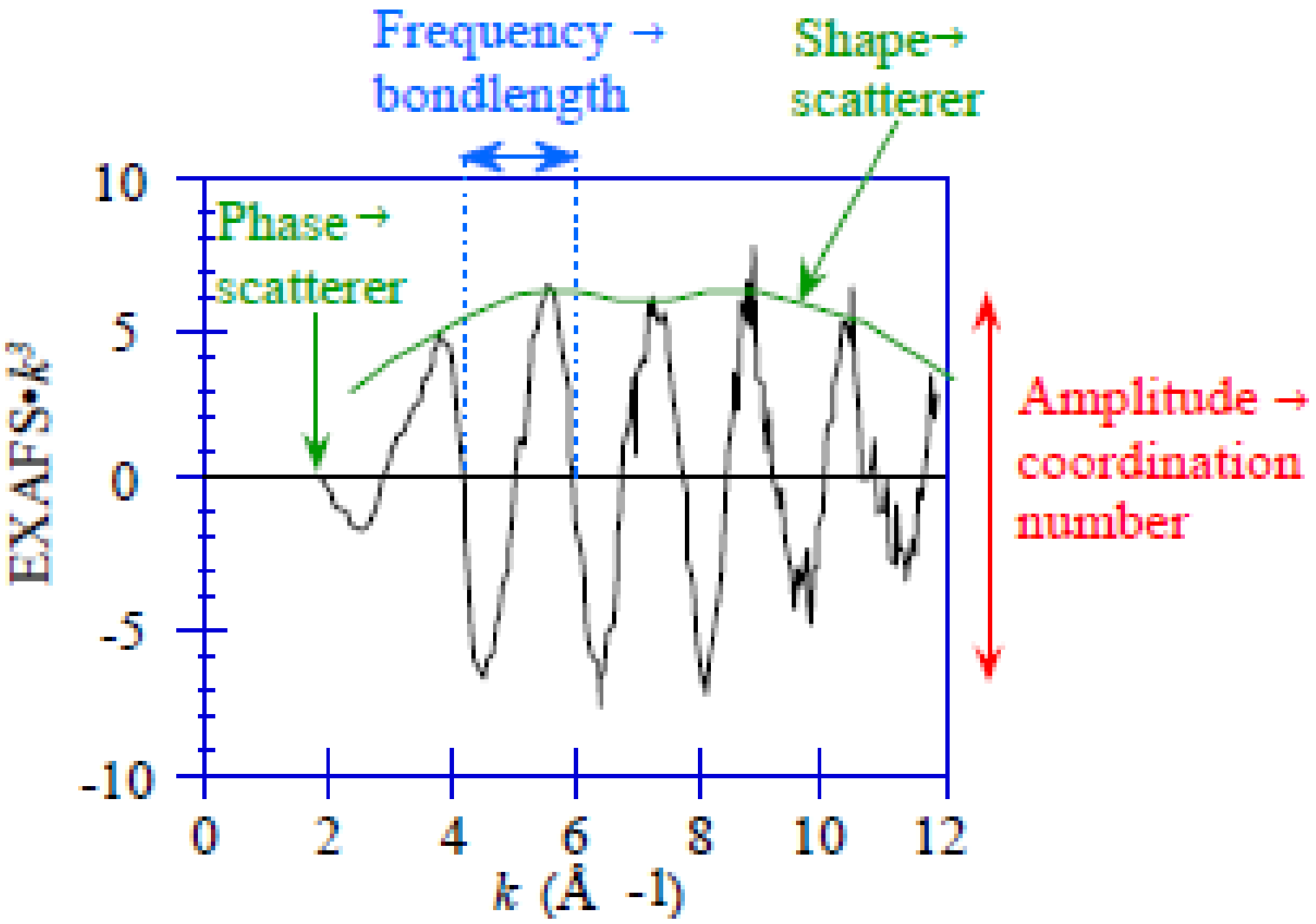

The EXAFS formula

Elementary EXAFS formula (Lytle, Sayers, Stern)

$$\chi(k) = \sum_j \frac{N_j S_0^2}{k r_j^2} F_j(k) D_j(k) \exp\left(-2\sigma_j^2 k^2\right) \sin(2kr_j + \Phi_j(k))$$

Too many unknowns for measured data:

Some parameters must be determined in reference experiments or by theory:

- amplitudes $F_j(k)$
- phases $\Phi_j(k)$
- loss factors $D_j(k)$

EXAFS: local probe of atomic arrangement

N_j, r_j, σ_j, (E_0: additional fit parameter)

in neighborhood of atomic species of interest.

Backscattering Amplitudes (and Phases)

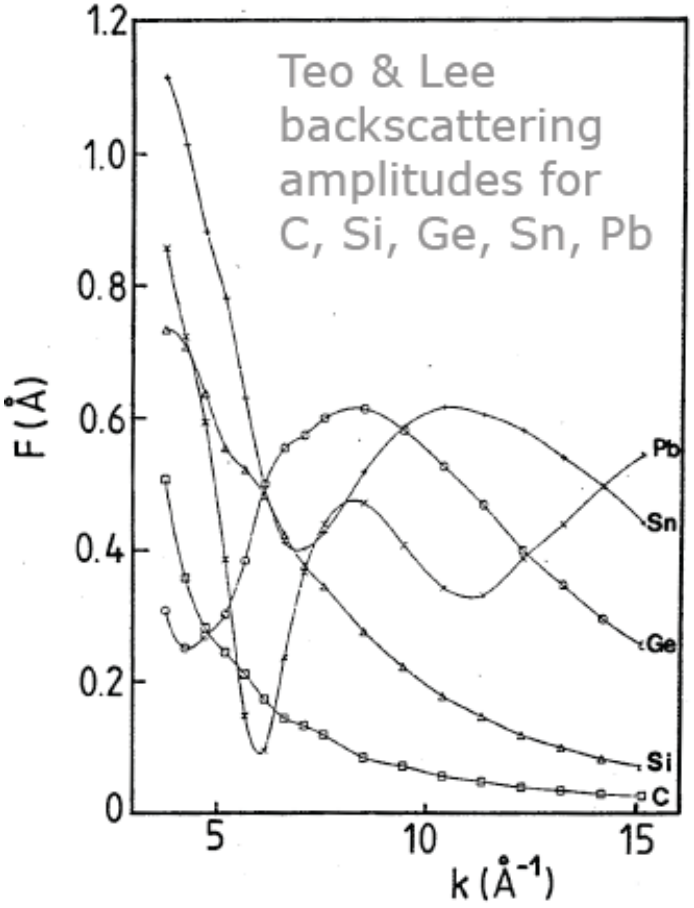

photoelectron is scattered in absorber and backscatterer:

k-dependent

- backscattering amplitude $F(k)$
- phases $\Phi(k) = \Phi_a(k) + \Phi_b(k)$

- $F(k)$ decreases with increasing k.
- superposed may be 1, 2 or 3 resonances:

  Ramsauer-Townsend-resonances

(Backscatterer becomes transparent for certain energies of the photoelectron!)

Scattering Phases

backscatterer

absorber

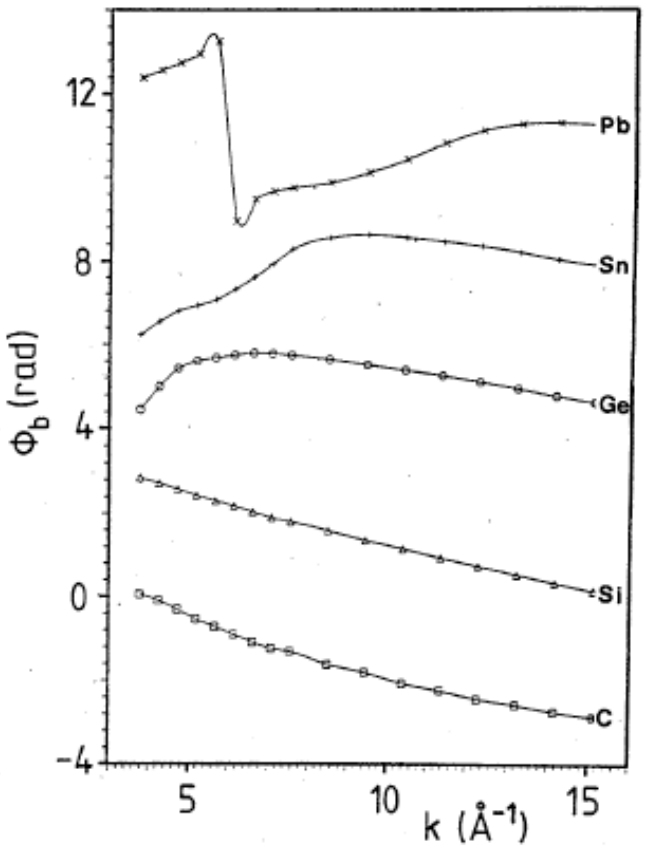

$$\Phi(k) = \Phi_b(k) + \Phi_a(k)$$

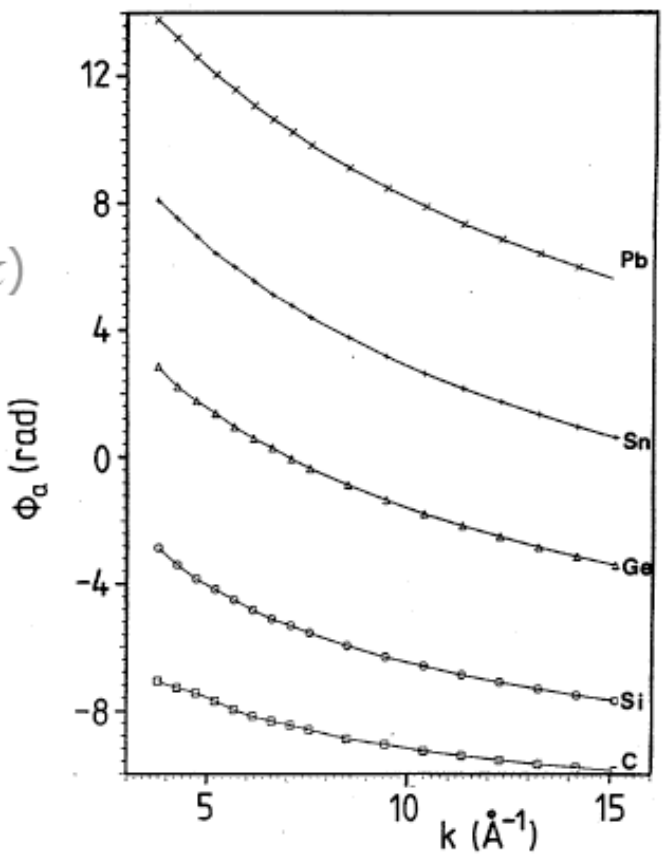

with Ramsauer-Townsend-Osc.

monotone in k

Fourier analysis

Identify Different Shells: Fourier Transform of $\chi(k) \cdot k^n$

$$\chi(k) = \sum_j \frac{N_j S_0^2}{k r_j^2} F_j(k) D_j(k) \exp\left(-2\sigma_j^2 k^2\right) \sin(2kr_j + \Phi_j(k))$$

Multiplication with k^n

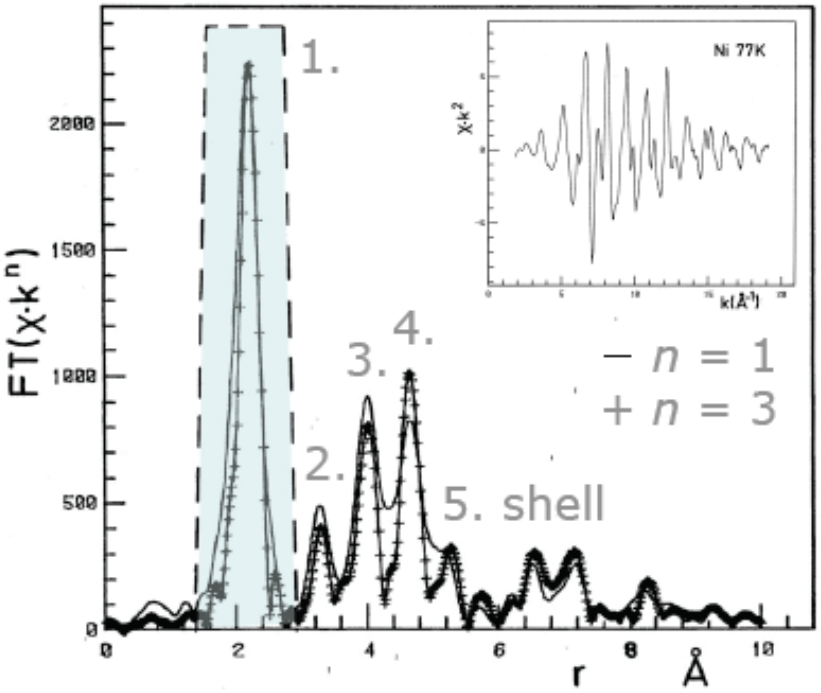

n = 0, 1: short data set
n = 2, 3: long data set
(with low noise)

n = 3: enhances high *k* data, makes data set effectively longer and separates shells better in Fourier transform

Fourier analysis

Isolate Shell

For given shell *j* fit

$$\chi_j(k) = \frac{N_j S_0^2}{k r_j^2} F_j(k) D_j(k) \exp\left(-2\sigma_j^2 k^2\right) \sin(2kr_j + \Phi_j(k))$$

Example:

determine Φ_1(k) from model substance

oscillations:

$$2kr_1 + \Phi_1(k)$$

with known r_1 = 2.486Å

$$\longrightarrow \Phi_1(k)$$

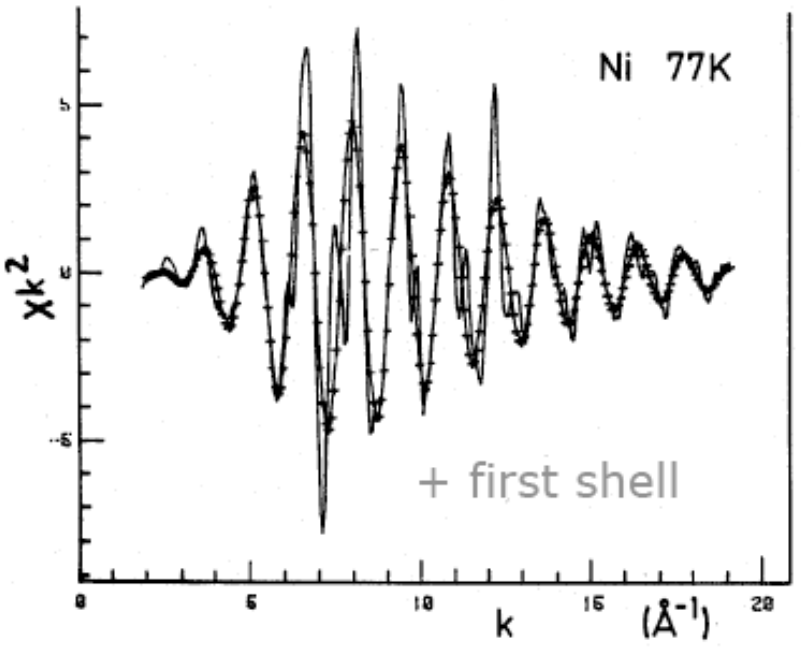

Fourier analysis

Isolate Shell

For given shell *j* fit

$$\chi_j(k) = \frac{N_j S_0^2}{k r_j^2} F_j(k) D_j(k) \exp\left(-2\sigma_j^2 k^2\right) \sin(2kr_j + \Phi_j(k))$$

Example:

determine $\Phi_1(k)$ from model substance

oscillations:

$$2kr_1 + \Phi_1(k)$$

with known r_1 = 2.486Å

$$\longrightarrow \Phi_1(k)$$

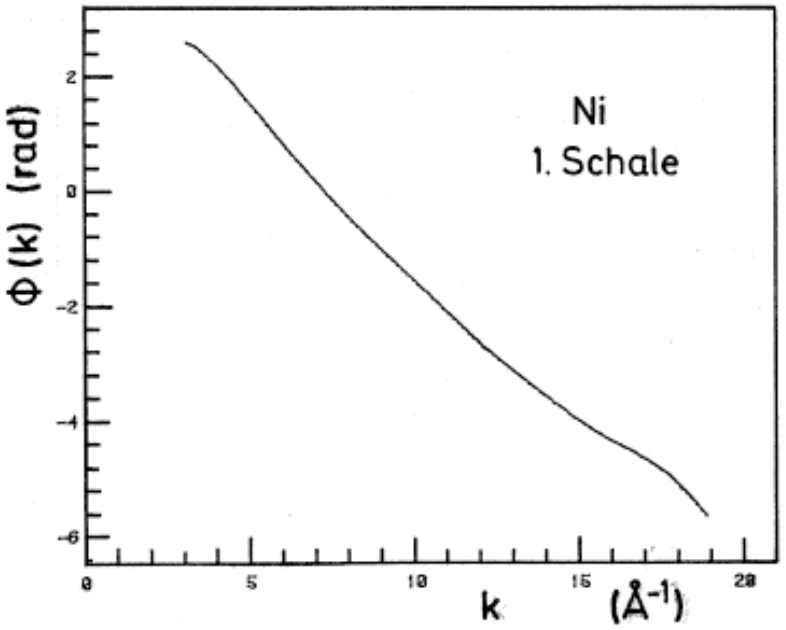

Fourier analysis

Example: Cu at Room Temp. Analysed with 77K Data

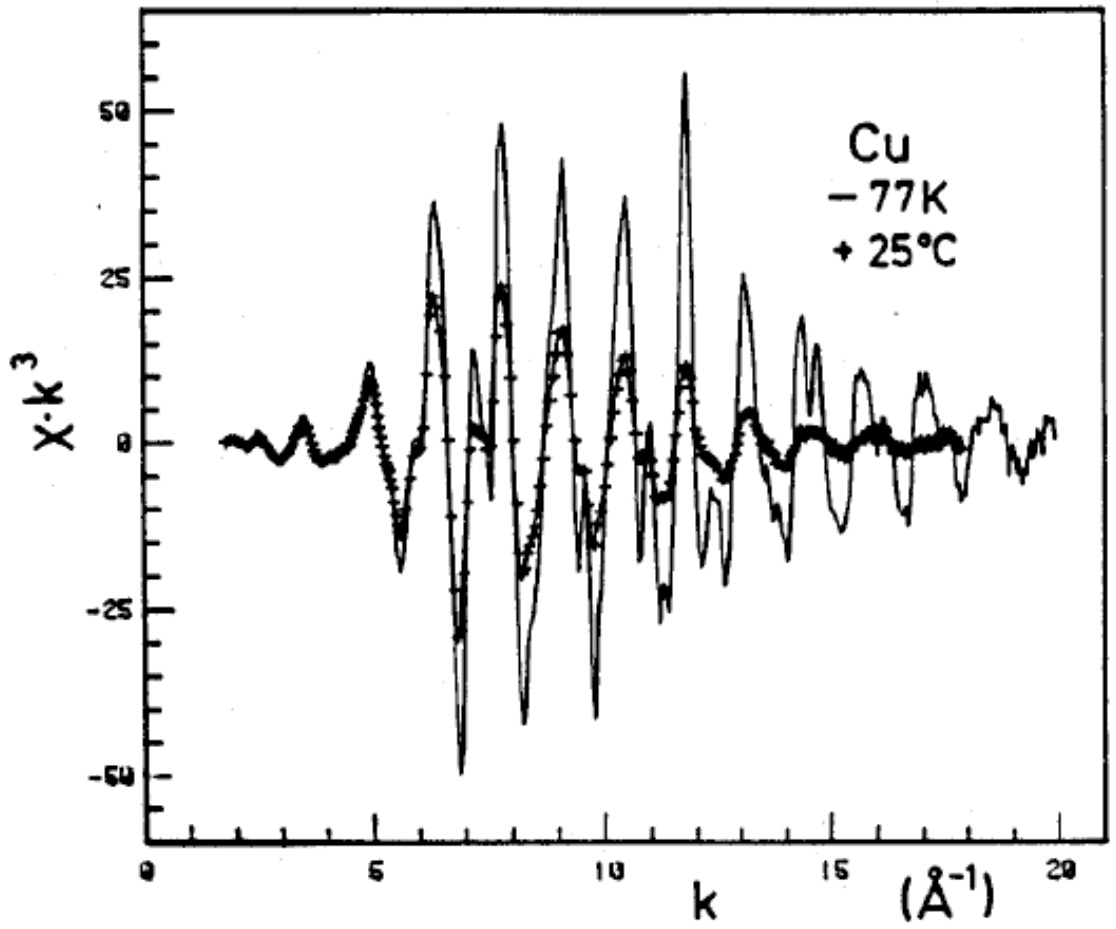

reference data for $\Phi(k)$ and $F(k)$:

copper at 77K

Fourier analysis

Example: Cu at Room Temp. Analysed with 77K Data

Fourier transform:

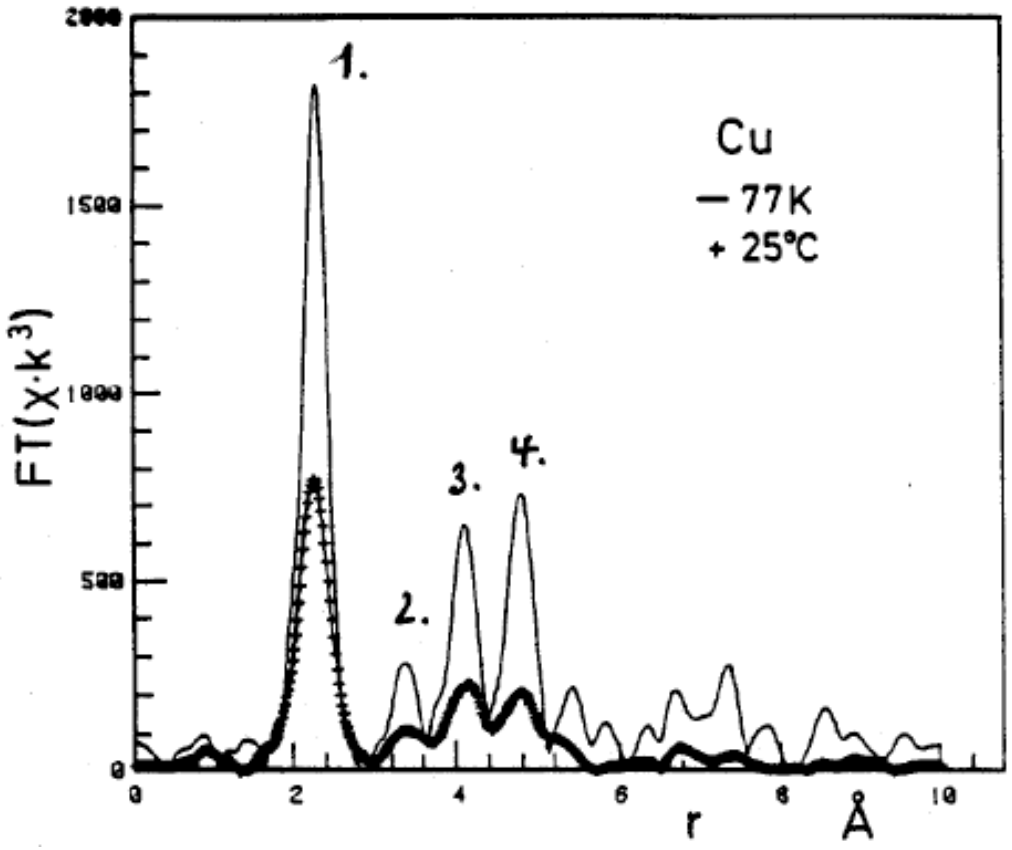

Main difference:

damped oscillations due to thermal motion of atoms

Fit of first shell at RT with 77K data

Fourier analysis

Example: Cu at Room Temp. Analysed with 77K Data

Input: F_f, Φ_j, D_j, r_j, N_j, σ_j, E_{0j}

for Cu at 77K

	fit	expected
r_1	2.546Å	2.556Å
N_1	12.06	12
$\delta\sigma_1^2$	0.0044Å^2	
δE_{01}	-1.48eV	

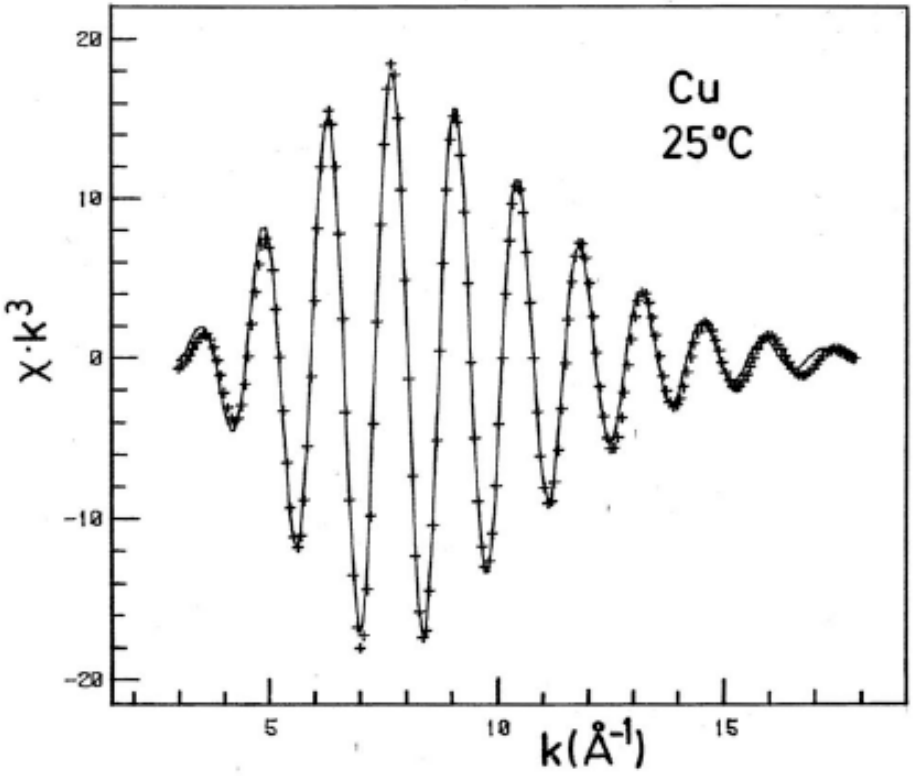

Fourier analysis

Example: Cu at Room Temp. Analysed with 77K Data

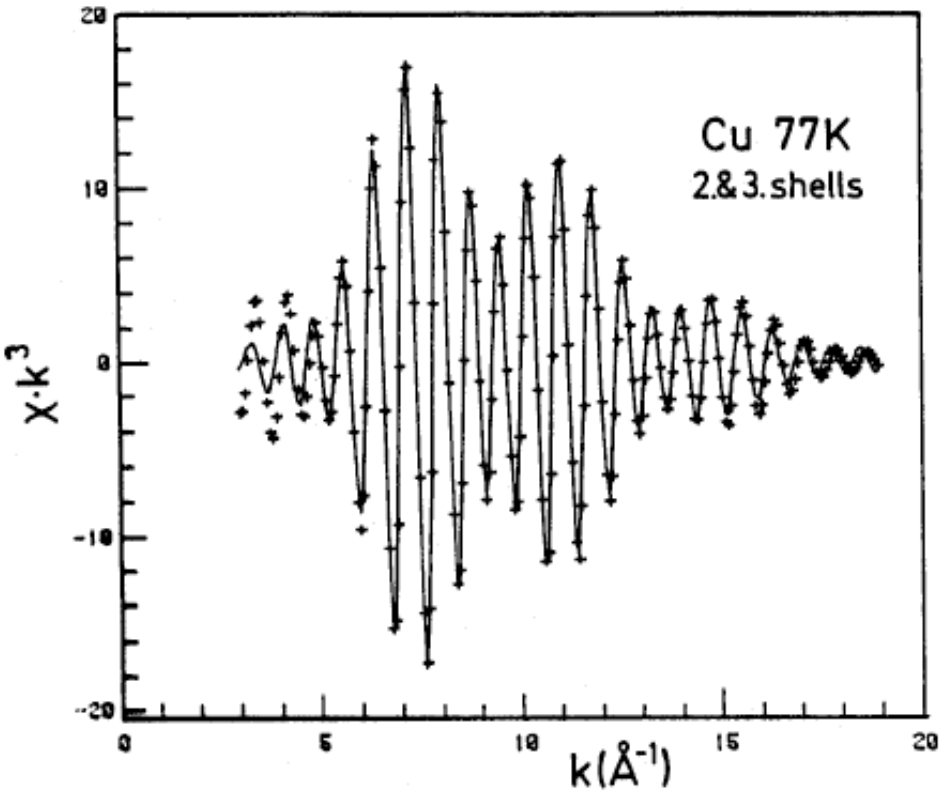

	fit	expected
r_2	3.609Å	3.603Å
N_2	6.4	6
$\delta\sigma_2^2$	0.0030Å^2	
δE_{02}	2.57eV	

	fit	expected
r_3	4.409Å	4.413Å
N_3	19.4	24
$\delta\sigma_3^2$	0.0020Å^2	
δE_{03}	-4.61eV	

inelastic scattering length: Λ = 21Å

Accuracy

Accuracy of r, E_0, N & σ^2

$$\chi_j(k) = \frac{N_j S_0^2}{k r_j^2} F_j(k) D_j(k) \exp\left(-2\sigma_j^2 k^2\right) \sin(2kr_j + \Phi_j(k))$$

r_j has little correlation with other parameters:

$$\chi(k) \propto \sin(2r_j k + \Phi(k))$$

$$k = \frac{1}{\hbar}\sqrt{2m(E - E_0)}$$

High accuracy r_j: 0.01Å and less

However:

N and σ are 100% correlated!

⟶ errors are compensated

⟶ accuracy: 5 – 25 %

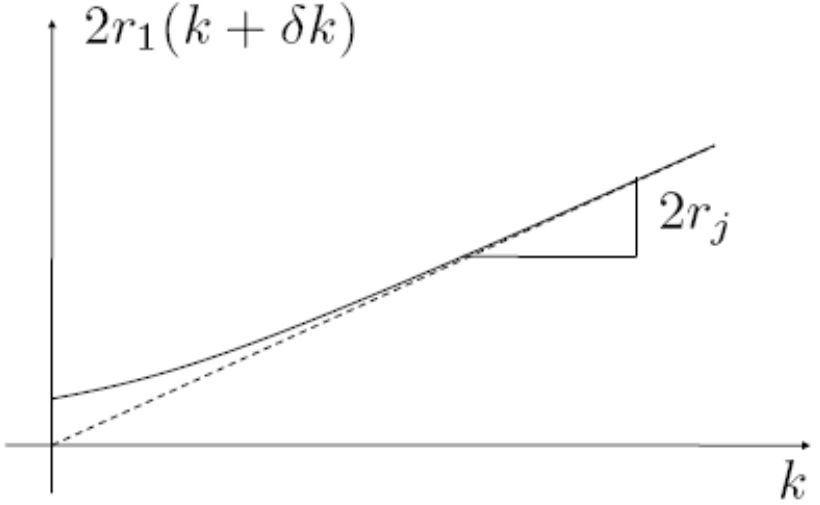

The X-ray Absorption Edge

Position of Absorption Edge

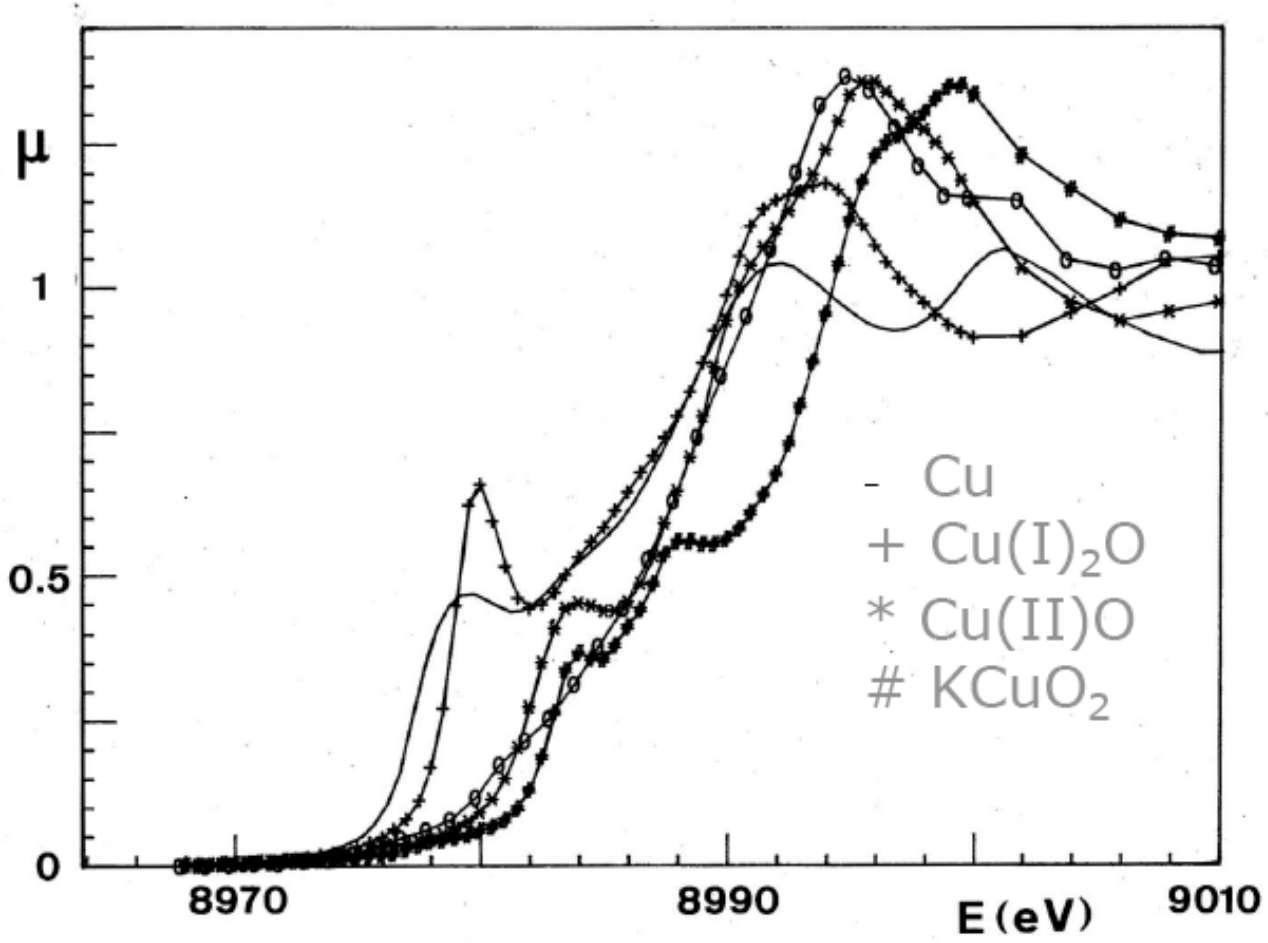

Edge is shifted toward higher energies with increasing formal valence

Screening of nucleus by valence electrons decreases:

Core electrons are more tightly bound!

The X-ray Absorption Edge

Position of Absorption Edge

Shift increases with electronegativity of ligants

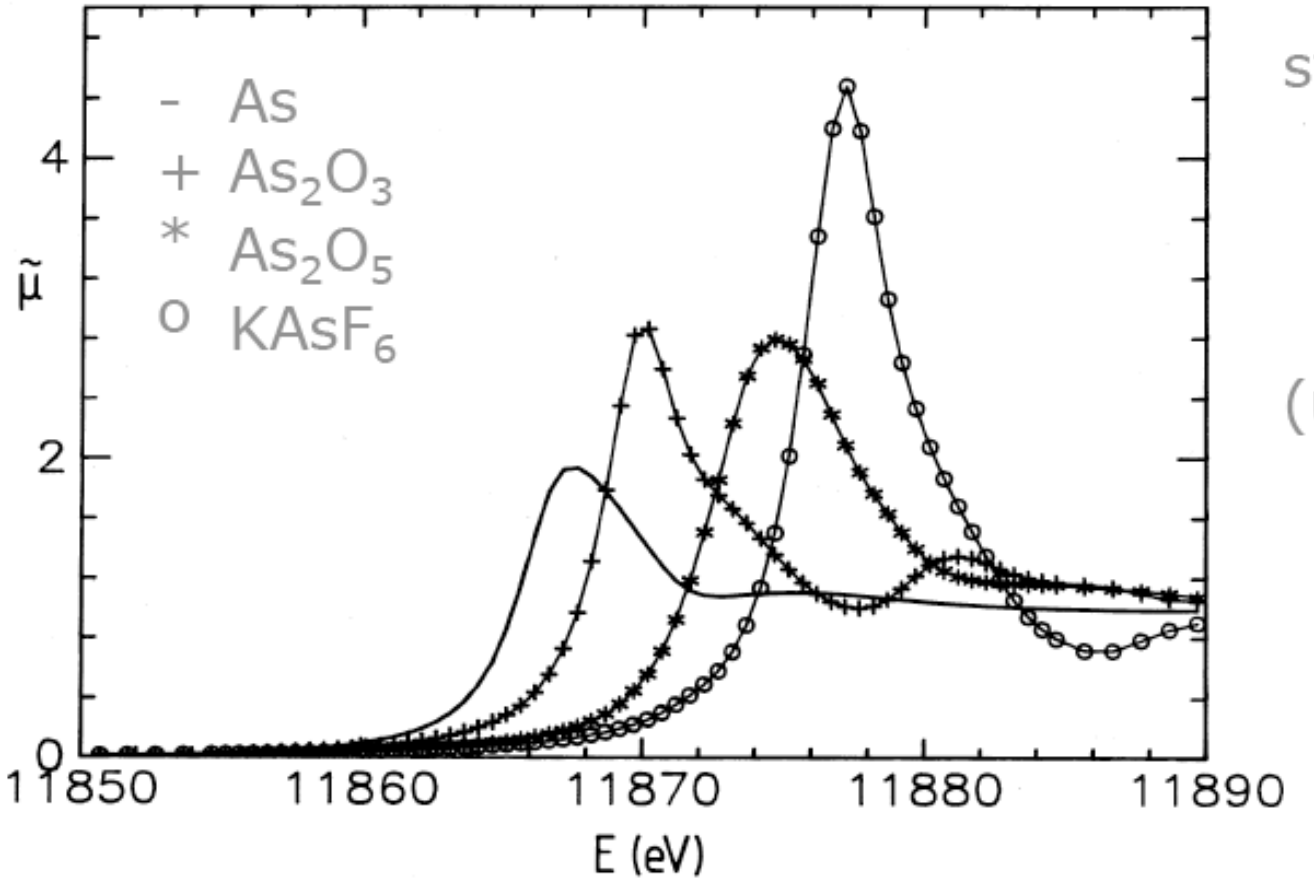

strongest for:

oxides and fluorides

(up to 13eV)

The X-ray Absorption Edge

Shape of Absorption Edge

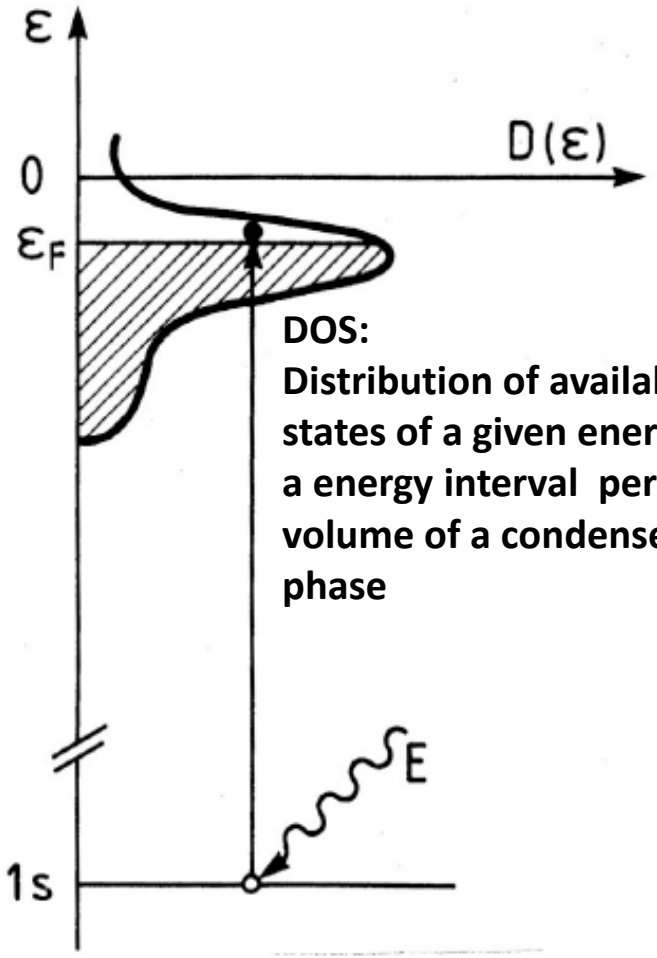

local projected density of empty states:

μ proportional to transition rate:

$$R_{fi} = \frac{2\pi}{\hbar} \sum_f |\langle f|H_1|i\rangle|^2 \, \delta(E_f - E_i - \hbar\omega)$$

matrix element $M(E) = \langle f|H_1|i\rangle$ only weakly energy dependent:

$$\mu \propto M(E) \cdot \rho(E)$$

density $\rho(E)$ of free final states determines edge structure.

local: at atom of interest
free: Pauli-principle
projected: selection rule $\Delta L = \pm 1$

The X-ray Absorption Edge

Shape of Absorption Edge

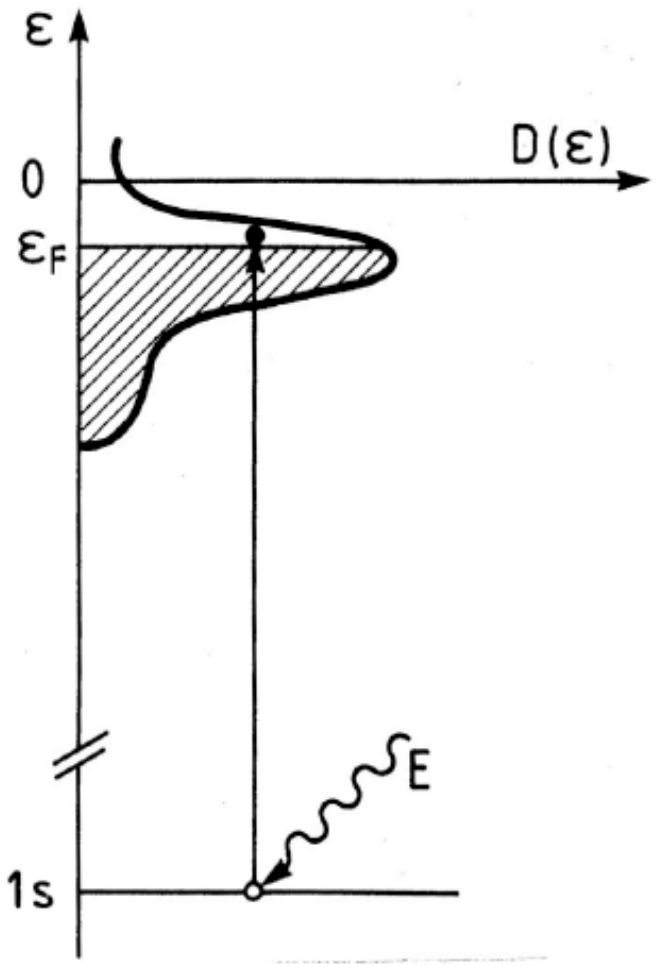

local projected density of empty states:

density $\rho(E)$ of free final states determines edge structure.

local: at atom of interest
free: Pauli-principle
projected: selection rule $\Delta L = \pm 1$

Angular momentum conservation:

K-, L_1-shell: s ⟶ p

L_2-, L_3-shell: p ⟶ d, (s)

The X-ray Absorption Edge

Shape of Absorption Edge

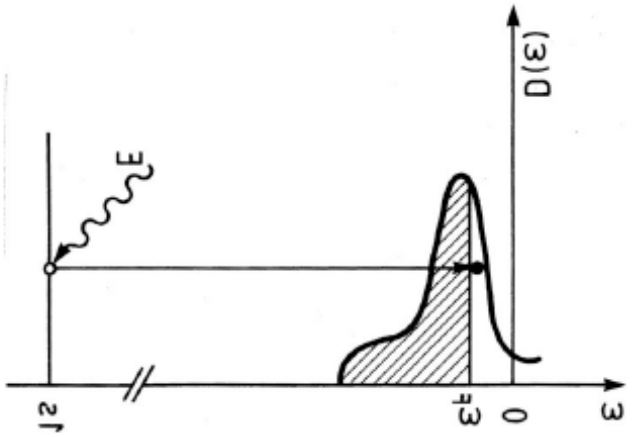

life time of excitation and experimental energy resolution:

⟶ edge smoothed

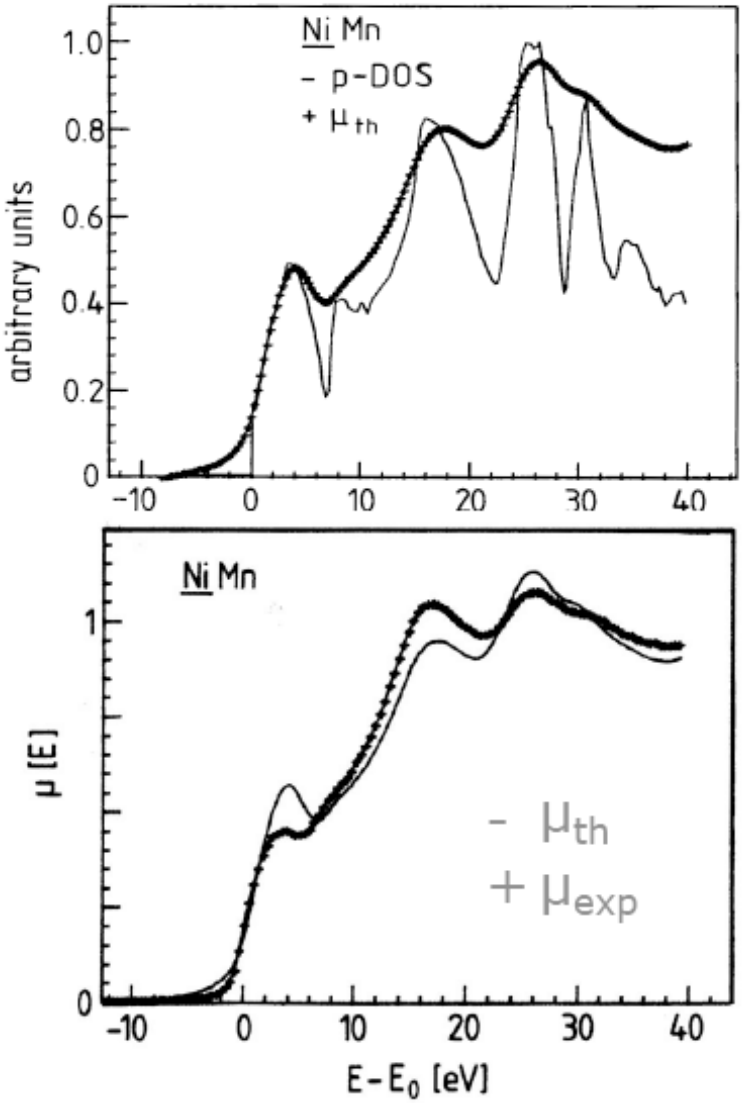

The X-ray Absorption Edge

Near Edge Spectrum

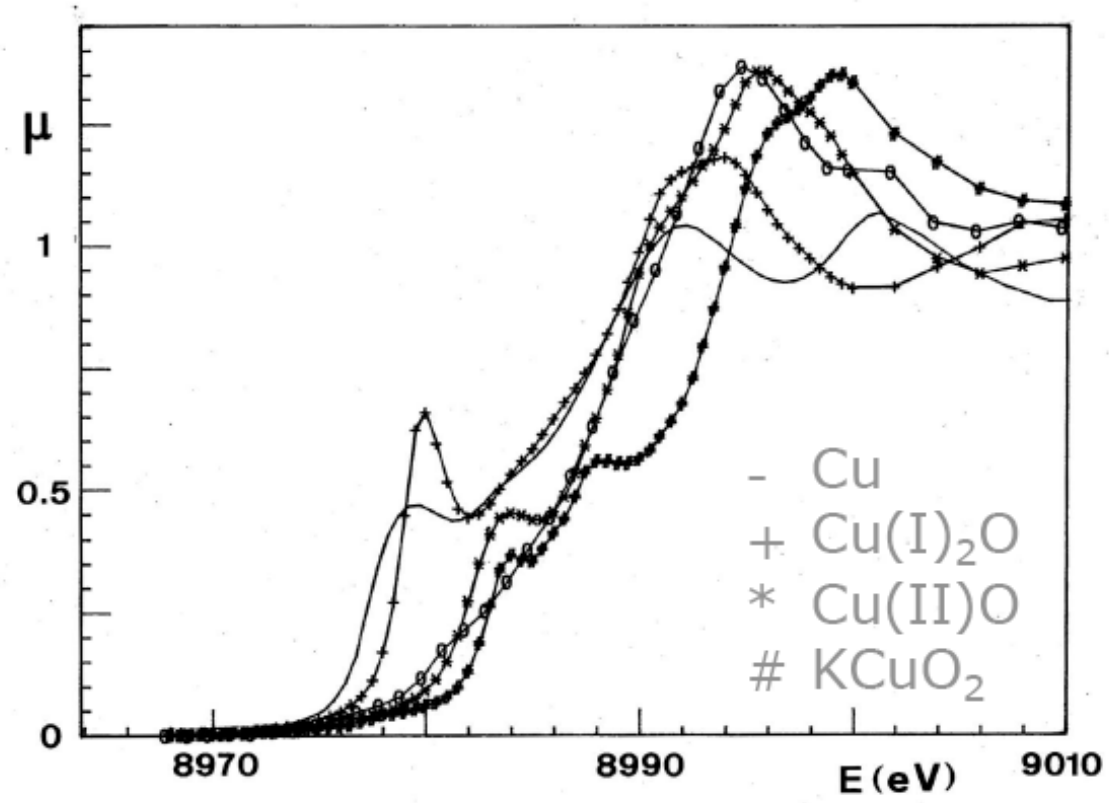

Finger print for chemical state of element of interest

Determine concentration of chemical compounds in mixtures

Example: inhomogeneous specimens

X-ray Absorption Spectrum

Summary: X-Ray Absorption Spectrum

- edge position:

  oxidation state

- near edge spectrum:

  local free projected density of states

- extended fine structure:

  local atomic neighborhood

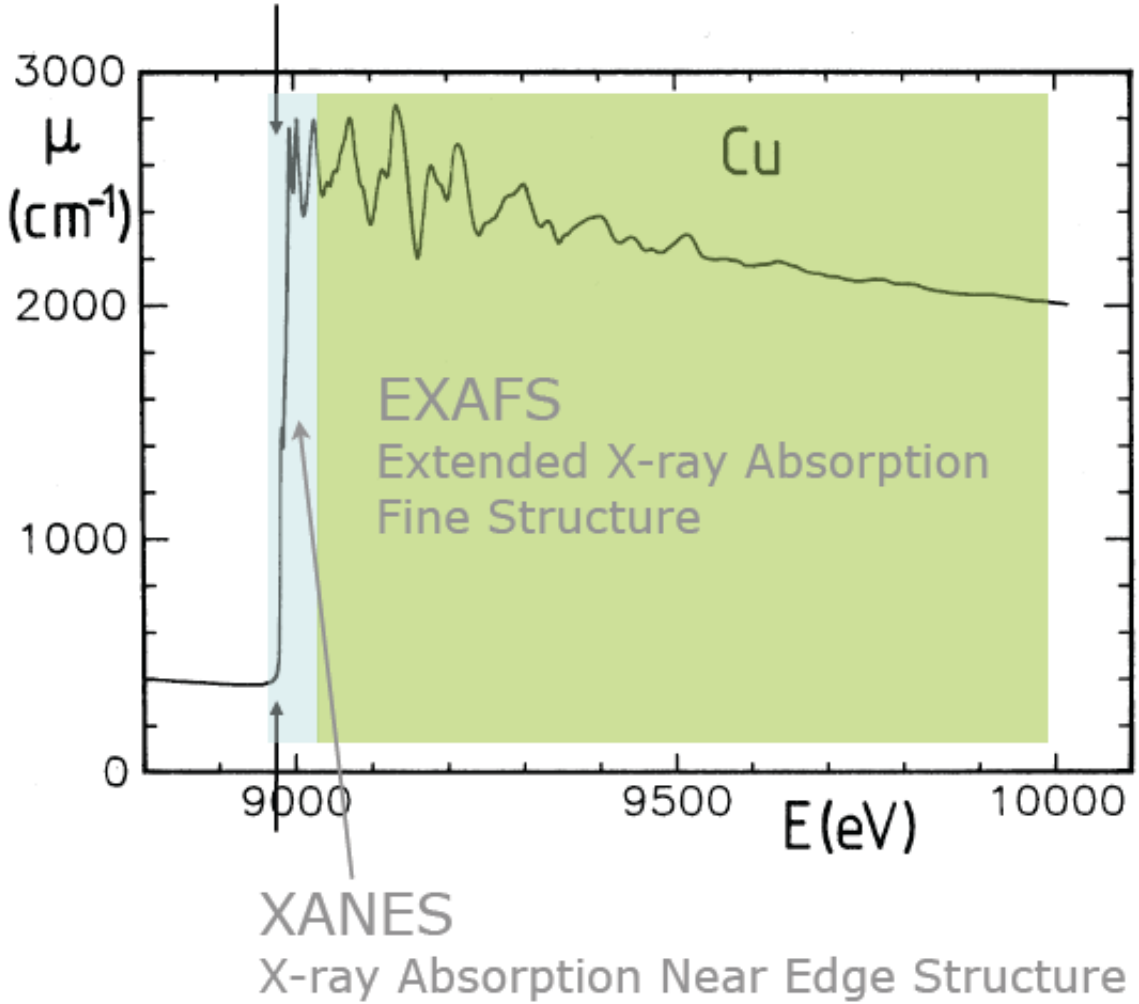

EXAFS spectrum analysis

EXAFS Curve fitting

- Evaluate data quality (how many shells can be analysed?)
- Make hypothesis about the structure of atom shells around absorber
- Use theoretical amplitude and phase shift functions for each atom species
- Choose initial values for r_j, N_j, σ_j^2 (for each shell)
- Optimize fit of $\chi(k)$ by varying r_j, N_j, σ_j^2, ΔE_0

BioXAS case studies

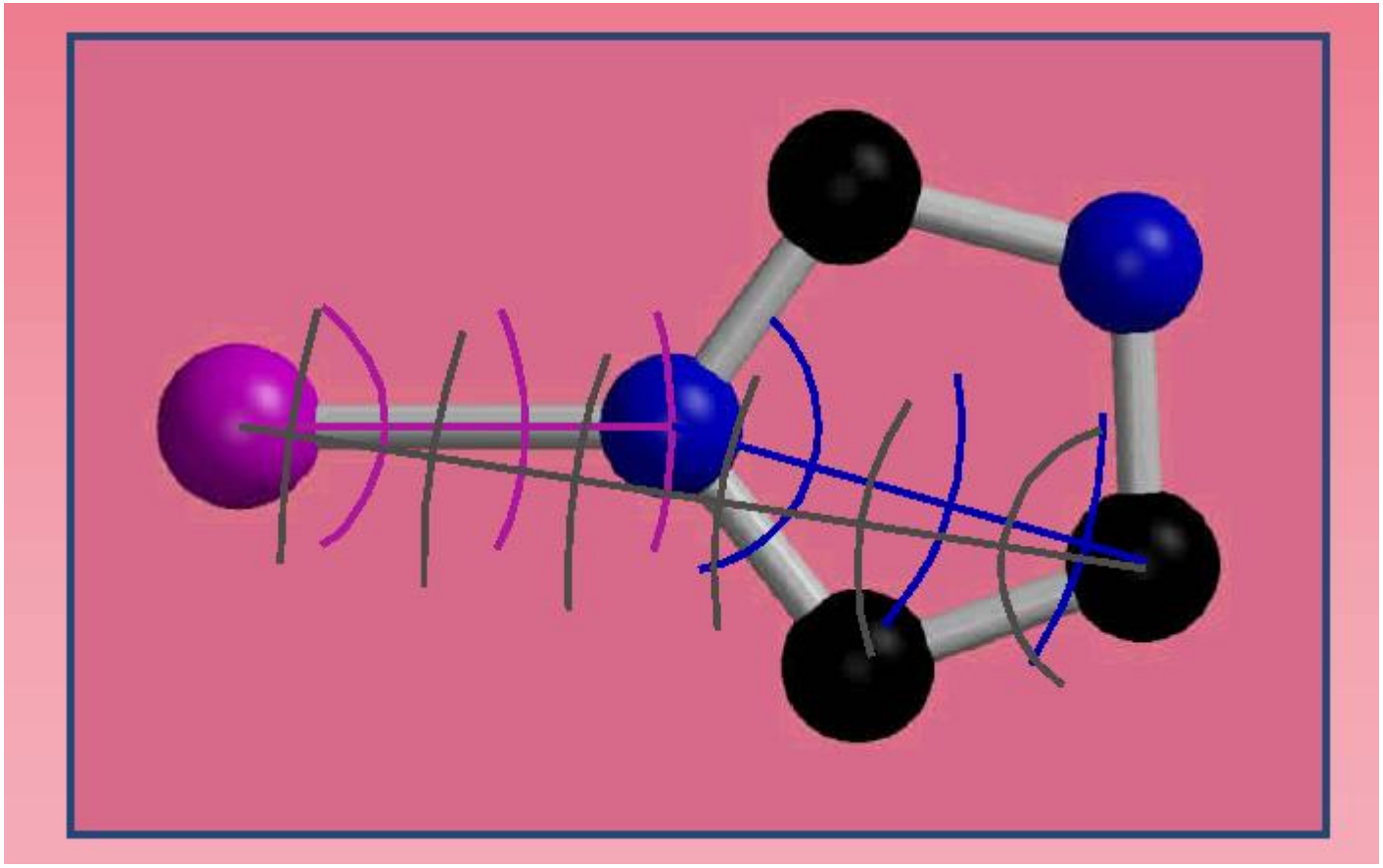

The case of Ni-UreE

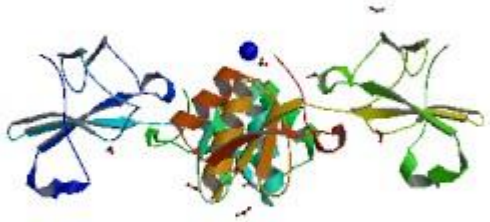

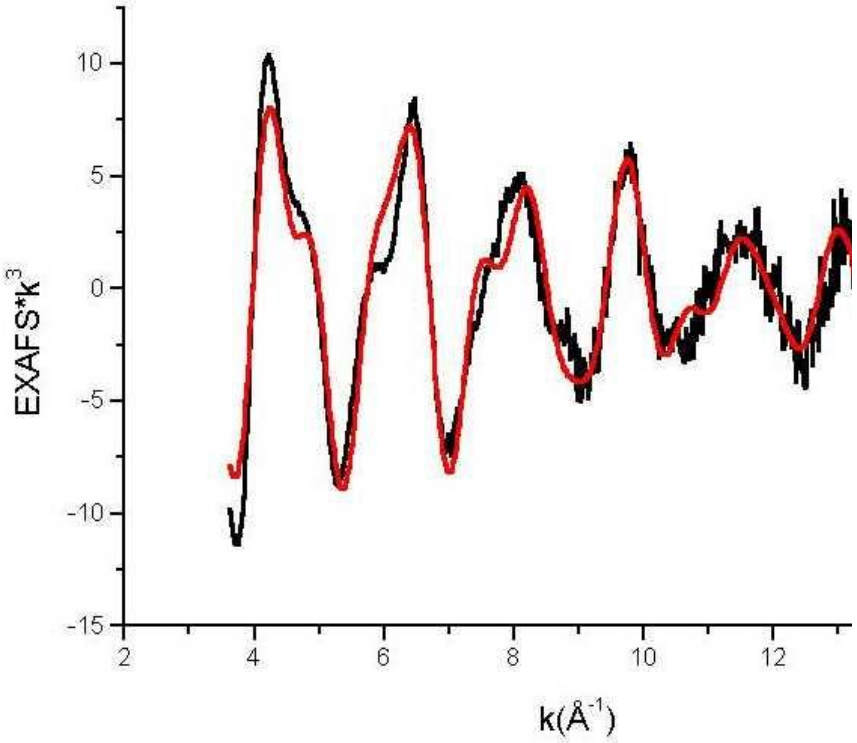

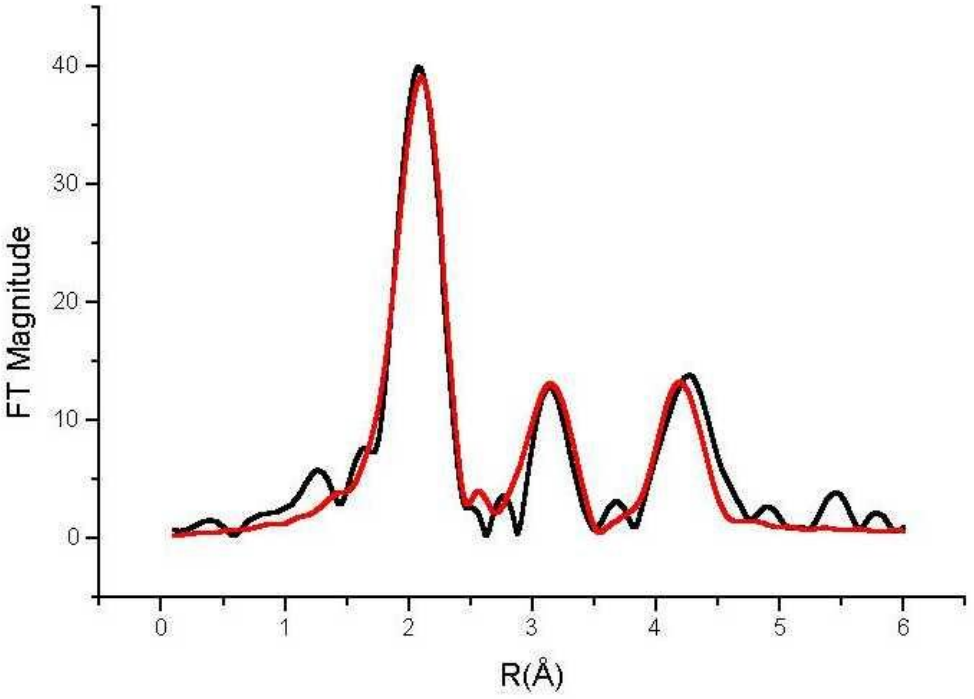

Ni – UreE

Biochemistry 2006, 45, 6495-6509

Close shells in Cu(I)-CopZ

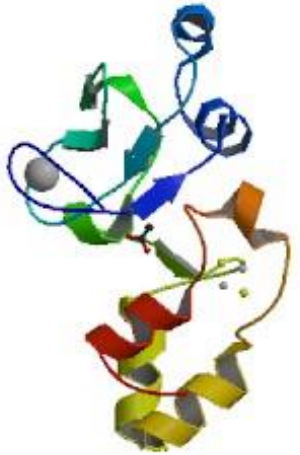

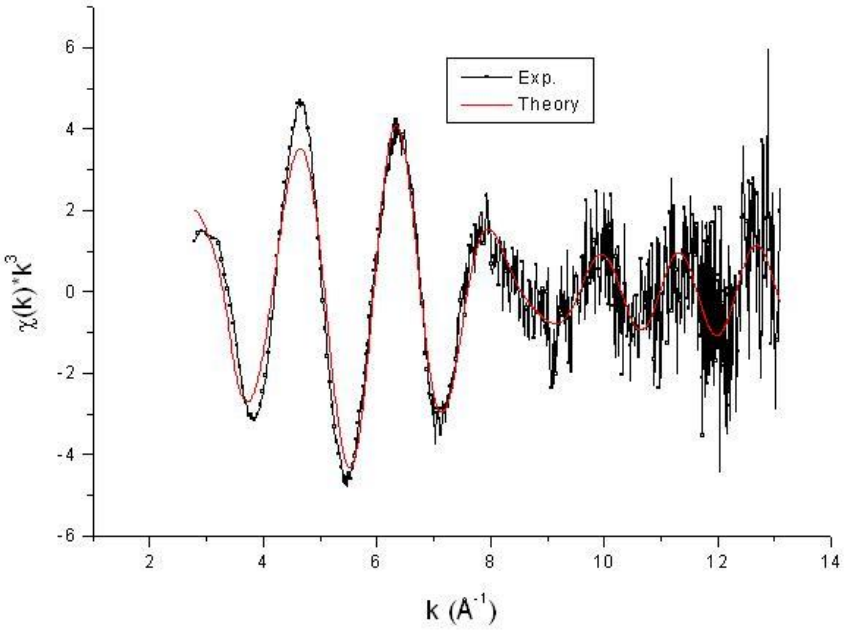

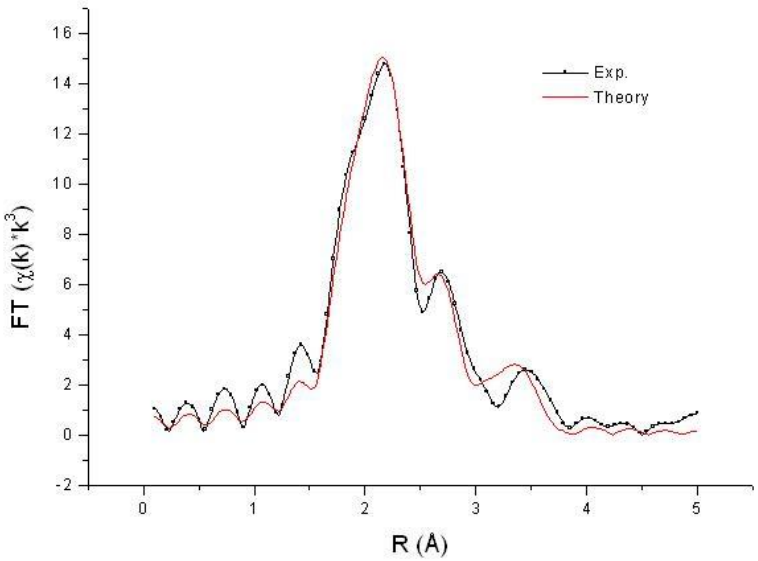

Biochemistry **2003,** *42,* 2467-2474

Bond Valence Sum to check EXAFS fitting results

Bond Distances and Formal Valence

For inorganic solid-state chemistry:

- there are nearly universal ionic sizes.
- Bond lengths between atoms are correlated with formal valences of the species.

Pauling's "2nd Rule" of electrostatic valence (Pauling, 1929) gives a common sense view of charge balance at the atomic scale:

> The total strength of the valency bonds which reach an ion from all neighboring atoms is equal to the charge of the ion.

This works well for ionic and covalent bonds, and considers only the *near neighbors*.

How can we use this information in EXAFS analysis?

L. Pauling, *J. Am. Chem. Soc.*, 51, pp 1010 (1929)

L. Pauling, *J. Am. Chem. Soc.*, 69, pp 542–553 (1947).

A. Byström and K. A. Wilhelmi, *Acta Chem. Scand.*, 5, pp 1003-1010 (1953).

W. H. Zachariasn, *Acta Cryst.*, 16, pp 385–389 (1963).

I. D. Brown, *Chem. Soc. Rev.* 7, pp.359–376 (1978).

Bond Valence Sum to check EXAFS fitting results

The Bond Valence Model

Following the description of I. D. Brown and D. Altermatt:

1. For inorganic structures, "bond" means all neighboring cation-anion distances (a local structural view).
2. The oxidation state of a cation i can be written as

$$V_i = \sum_j s_{ij}$$

   where the sum is over neighboring atoms j, with each bond between atoms i and j having bond valence s_{ij}.

3. This bond valence is most commonly parameterized as

$$s_{ij} = \exp[(R'_{ij} - R_{ij})/b]$$

   where R_{ij} is the bond distance between atoms i and j and
4. R'_{ij} and b are parameters to be determined empirically.

D. Altermatt and I. D. Brown, *Acta Cryst.* B41, pp.240-244 (1985).
I. D. Brown and D. Altermatt, *Acta Cryst.* B41, pp.244-247 (1985).
N. E. Brese and M. O'Keefe *Acta Cryst.* B47, pp.192–197 (1991).

Bond Valence Sum to check EXAFS fitting results

The Bond Valence Model

Brown and Altermatt considered other functional forms, such as

$$s_{ij} = (R_{ij}/R'_{ij})^N$$

but preferred the exponential form, because there seemed to be a universal value for the empirical parameter b:

$$b = 0.37\,\text{Å}$$

Which makes a *One-Parameter Model* relating Formal Valence V, coordination number N, and bond distance R:

$$V_i = \sum_{j=1}^{N} \exp[(R'_{ij} - R_{ij})/0.37]$$

D. Altermatt and I. D. Brown, *Acta Cryst.* B41, pp.240-244 (1985).

I. D. Brown and D. Altermatt, *Acta Cryst.* B41, pp.244-247 (1985).

Bond Valence Sum to check EXAFS fitting results

Bond Valence Parameters

Altermatt and Brown (1985) analyzed ∼15000 cation environments from the Inorganic Crystal Structure Database, and determined reliable bond valence parameters R' for ∼150 bonds, mostly metal-oxygen, and metal-sulfur.

Some Typical Bond Valence Parameters R' (in Å) for metal-oxides from Altermatt and Brown:

Bond	R' (Å)	Bond	R' (Å)
Cu(I)-O	1.593	Cu(II)-O	1.679
Fe(II)-O	1.734	Fe(III)-O	1.759
Mn(II)-O	1.790	Mn(III)-O	1.760
Mn(IV)-O	1.753		

Brese and O'Keefe (1991) and others have tabulated additional bond valence parameters for more anions (F, Cl, Br, Se, H . . .).

N. .E. Brese and M. O'Keefe *Acta Cryst.* B47, pp.192–197 (1991).

Bond Valence Sum to check EXAFS fitting results

Bond Valence Examples: Does it work?

$$V_{sum} = \sum_{j=1}^{N} \exp[(R'_{ij} - R_{ij})/0.37]$$

Mineral/Site	Oxygen Coordination	V_{sum}	V_{formal}
Cu_2O (cuprite)			
Cu(I)	2 @ 1.849Å	1.002	1
CuO (tenorite)			
Cu(II)	2 @ 1.951Å, 2 @ 1.961Å, 2 @ 2.784Å.	1.993	2
FeO (ferrous oxide)			
Fe(II)	6 @ 2.1387Å	2.010	2
Fe_2O_3 (hematite)			
Fe(III)	3 @ 1.946Å, 3 @ 2.226Å.	2.955	3
$CuFeO_2$ (cuprous ferrite)			
Cu(I)	2 @ 1.898Å	0.877	1
Fe(III)	6 @ 1.982Å	3.284	3

Bond Valence Sum to check EXAFS fitting results

Using Bond Valence Sums in EXAFS Analysis

Several groups (G. E. Brown, *et al.*) have used Bond Valence Sums as an *a posteriori* check on results of EXAFS analysis:

1. Do EXAFS Analysis.
2. Do Bond Valence Sum on Resulting Local Structure.
3. Check for "Reasonableness".

This has proven successful and useful for several real experimental systems (Pb-O, Ti glasses, . . .)

Conclusion #2:

> Bond Valence Sums provide a simple, independent check on the Formal Valence, Coordination Number, and Bond Lengths determined from EXAFS analysis.

F. Farges, G. E. Brown, Jr., A. Navrotsky, H. Gao, J. J. Rehr, *Geochim. Cosmichim. Acta* 60, pp.3039–3053 (1996).

J. R. Bargar, G. E. Brown, Jr., and G. A. Parks, *Geochim. Cosmichim. Acta* 61, pp.2617–2637 (1997).

K. Xia, W. Bleam, P. A. Helmke, *Geochim. Cosmichim. Acta* 61, pp.2223–2235 (1997).

F. Farges, D. Neuville, G. E. Brown, Jr., *Am. Mineralogist* 84, pp.1562–1568 (1999).

M. I. Davis, *et al.*, *Inorg. Chem.* 38, pp.3676–3683 (1999).

X-ray Absorption Edges in proteins

edge energy reflects redox state

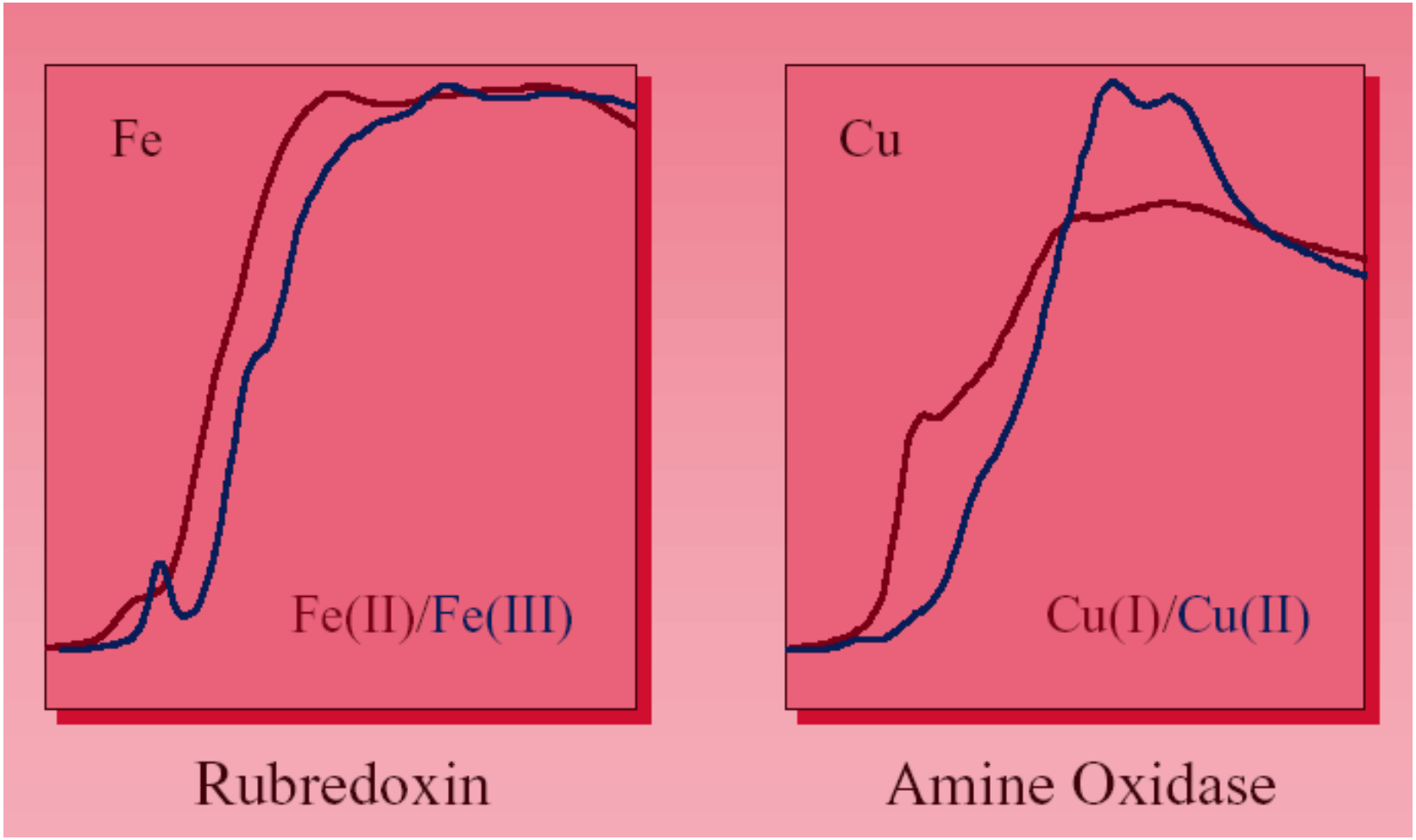

X-ray Absorption Edges in proteins

Cu(I)-edges In different coordination environments

a) DTT reduced 3mM Cu(I)
b) DTT reduced 1 mM Cu(I)
c) Dithionite reduced 3mM Cu(I)
d) Ascorbate reduced 3mM Cu(I)

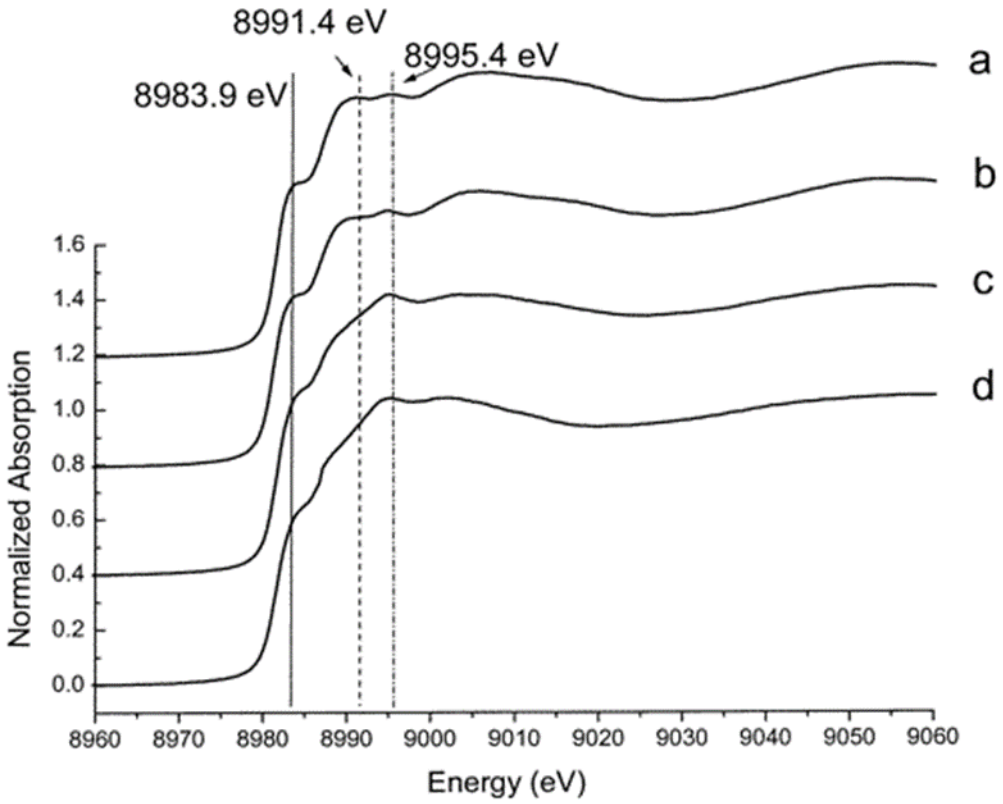

X-ray Absorption Edges in proteins

pre-edge transitions reflect coordination symmetry (model compounds)

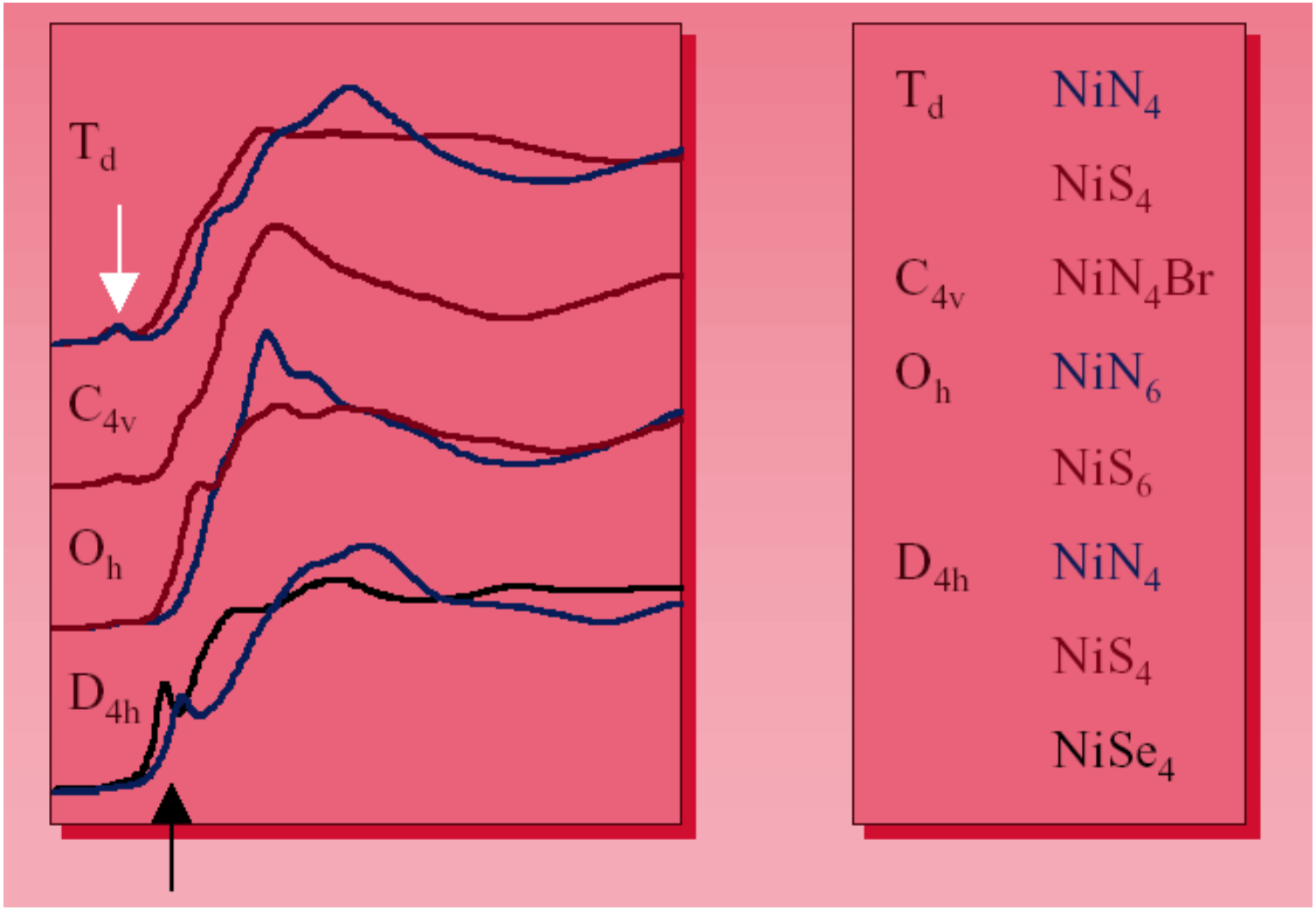

Support coordination number determination from EXAFS analysis

X-ray Absorption Edges in proteins (and model compounds)

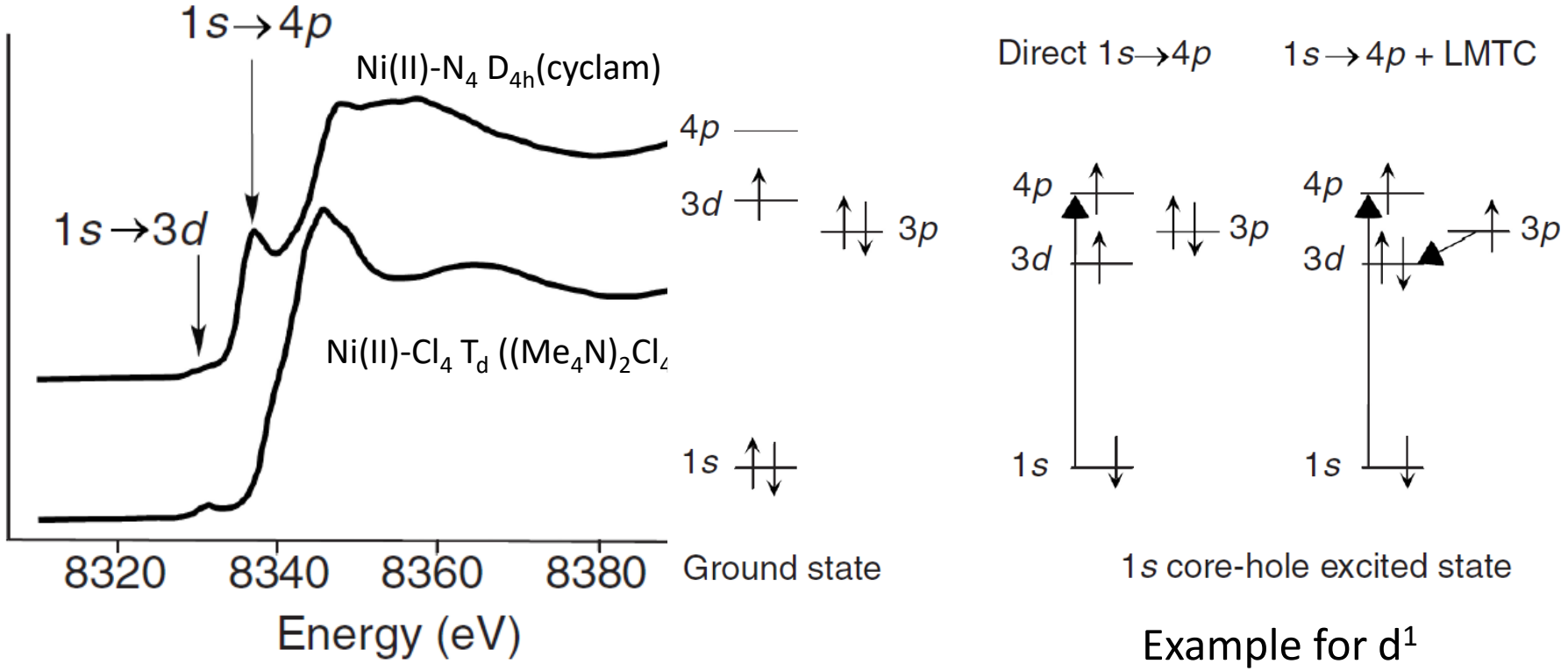

Example for d^1

Colpas, G. J et al. **Inorg. Chem**. 1991, 30, 920–928

The greater intensity for square–planar complexes may be due to decreased mixing between the empty 4p orbital ($4p_z$) and the ligand orbitals. This intensity of the 1s→4p transition is even more dramatic for 2-coordinate Cu(I)

X-ray Absorption Edges in proteins (an model compounds)

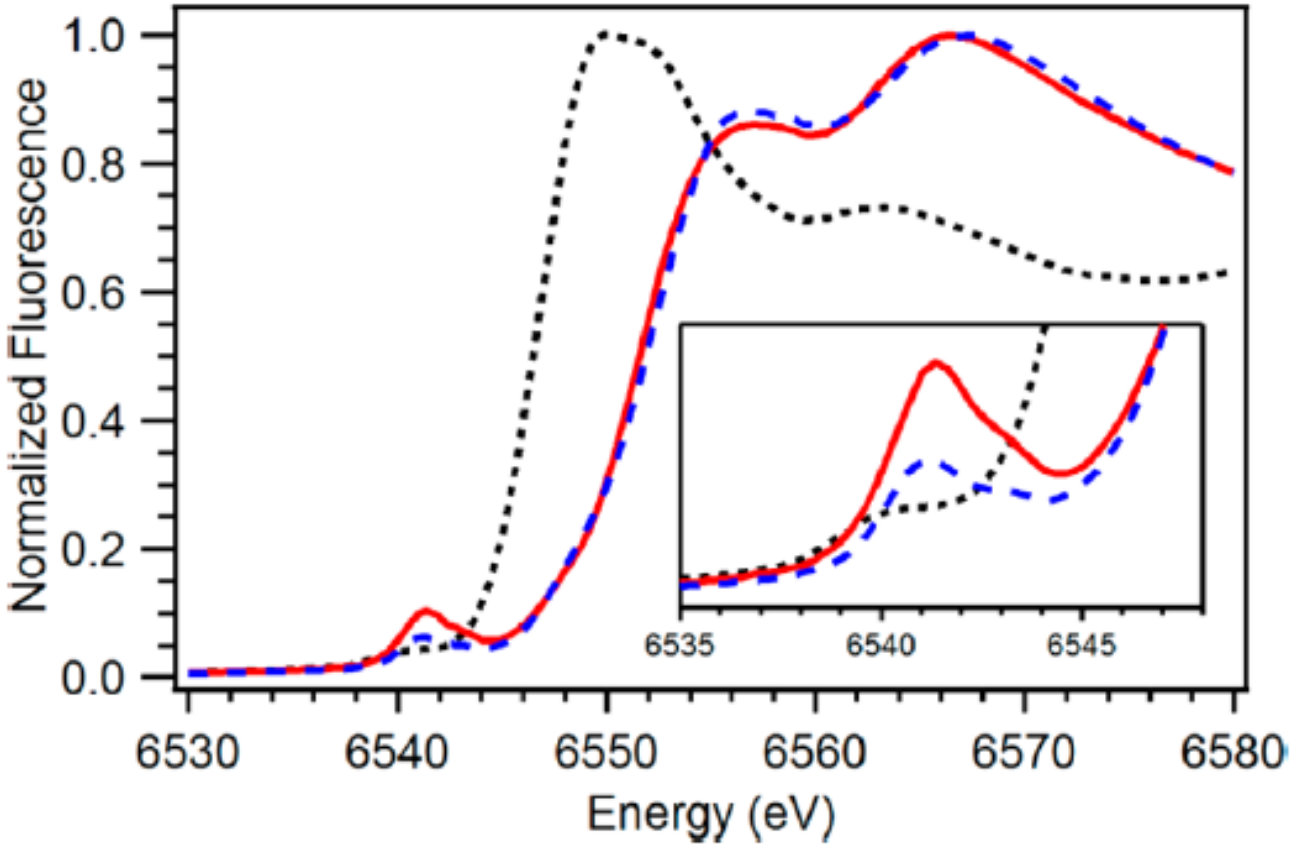

..... $Mn(II)N_4Cl_2$

- - - $Mn(IV)N_4(OH)_2$

___ $Mn(IV)N_4(O)(OH)$

6-coordinated complexes with different ligands

D.F. Leto & T.A. Jackson **Inorg. Chem**. 2014, 53, 6179-61-94

Multi-technique approach for determining the structure of a metallo-protein

Establishing the nature, the oxidation state and the coordination parameters of a metal ion bound to a protein is usually beyond the capability of either X-ray crystallography or NMR spectroscopy

Many experimental difficulties:

- Limitations of the technique
- Redox reactions occurring during data acquisition
- Radiation damage (X-ray)
- Chemistry occurring with sample components (buffer, additives)
- Contamination of the sample by other metal ions

Multi-technique approach for determining the structure of a metallo-protein

NMR ⇒ structure of the protein in solution (little info on the metal center)

PX ⇒ structure of the protein in the crystal

XAS-EXAFS ⇒ Accurate metal-ligand distances (constraints for NMR). Oxidation state, electronic structure, and coordination geometry of the metal ion

XAS-NMR; XAS-PX ⇒ complete structure determination of the protein in solution or solid state

Banci, Bertini, Mangani *J. Synchrotron Rad.* **12**, 94 (2005)

Multi-technique approach for determining the structure of a metallo-protein

One example from previous work:

The structure of the copper resistance protein CopC from *P. syringae*

The copper resistance system in Gram negative bacteria (*P. syringae* – *E. coli*)

Plasmid for Cu resistance

Cha and Cooksey, *PNAS* 88, 8915 (1991)
Puig, Rees & Thiele *Structure,* 10, 1292 (2002)

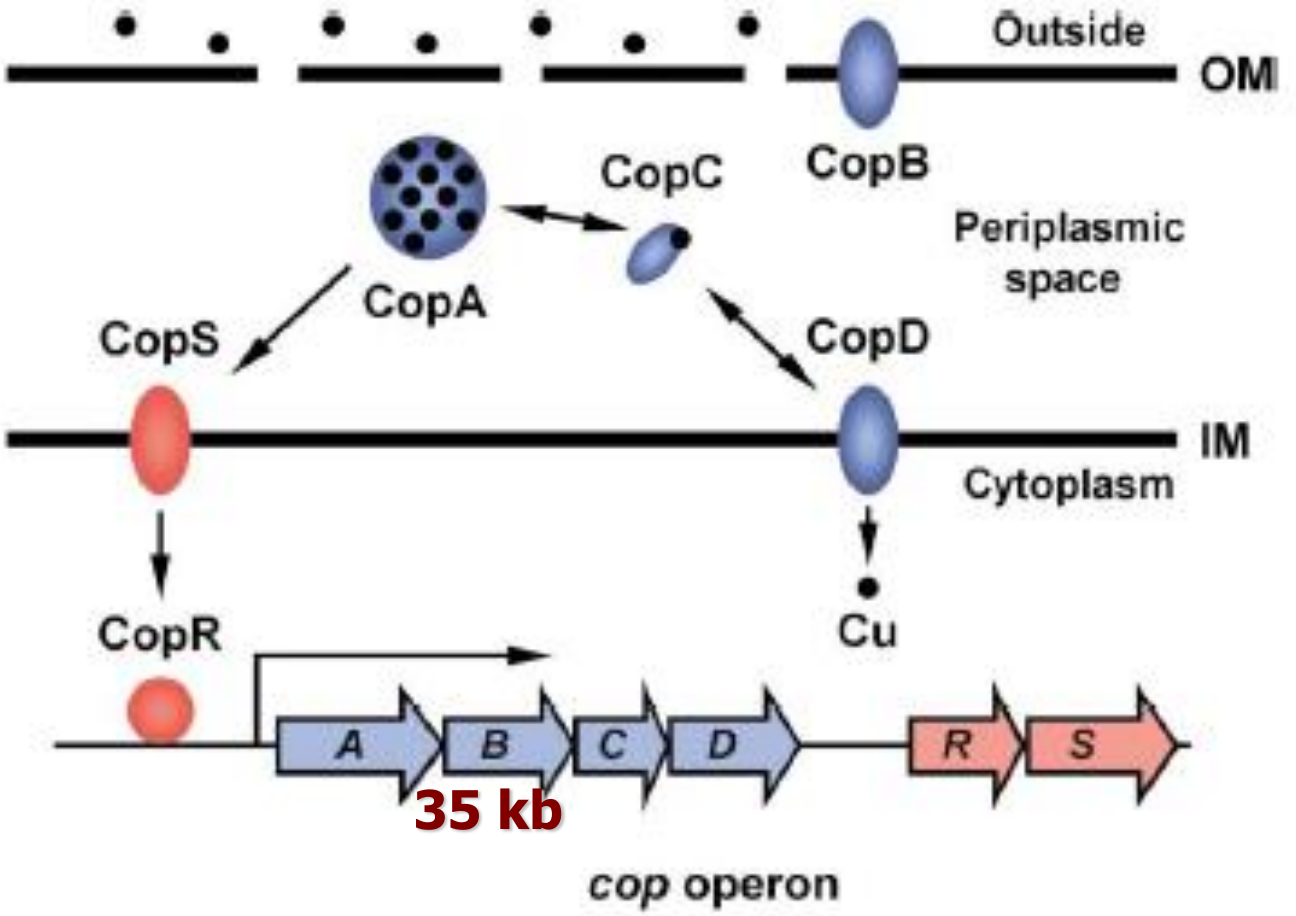

Solution structure of apoCopC

A cupredoxin-like protein involved in copper homeostasis

β-sandwich cupredoxin fold

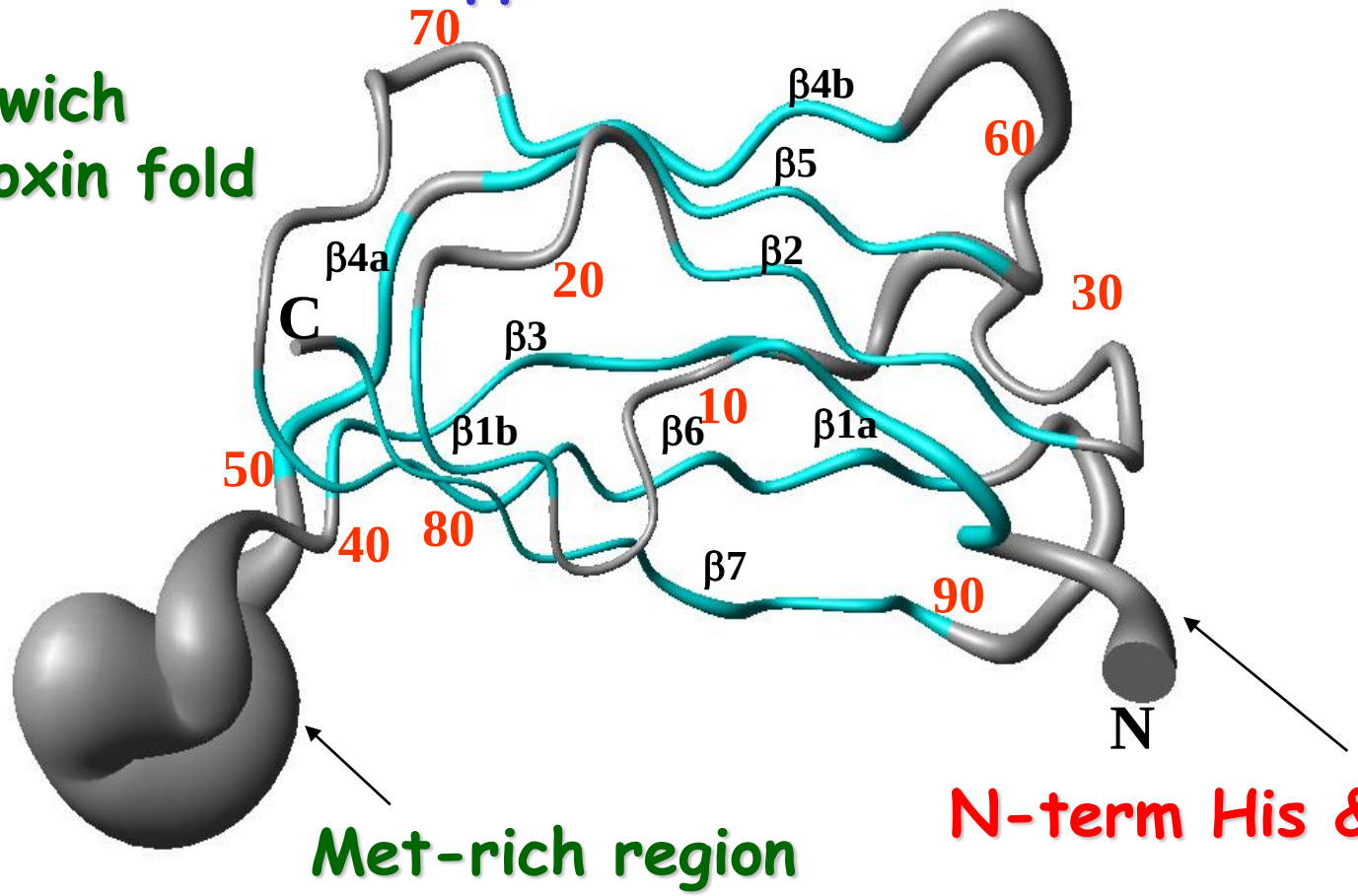

Met-rich region

N-term His & Glu

Arnesano, Banci, Bertini, Mangani, Thompsett, *PNAS* 100, 3814 (2003)

Redox-driven metal transfer

The Cu(II) – CopC sample

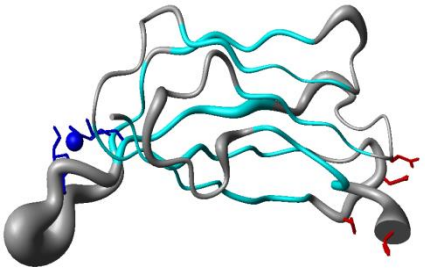

EXAFS results:
2 Cu – His 1.99 Å
2 Cu – O/N 1.97 Å

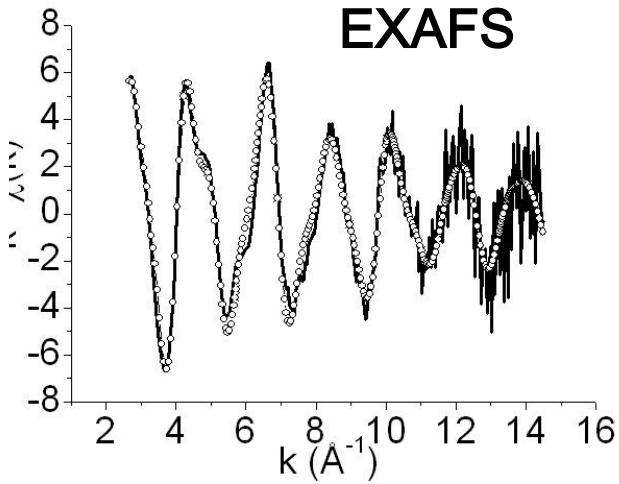

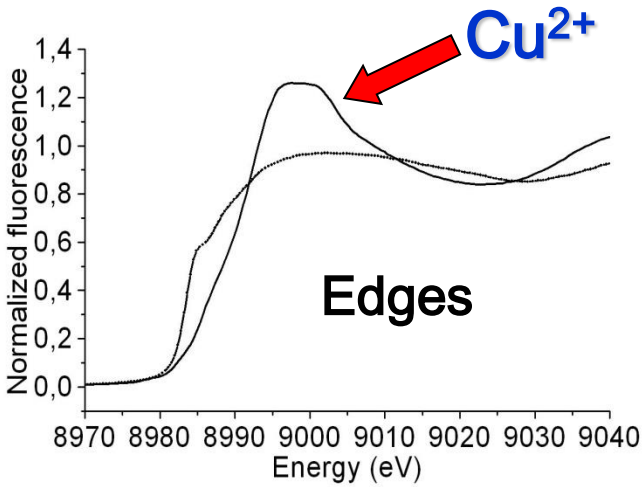

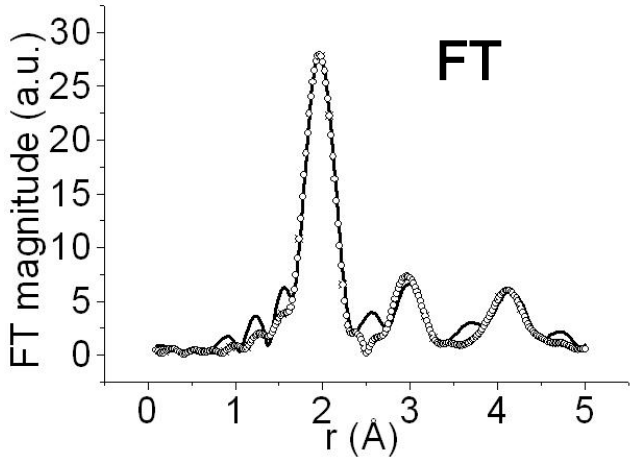

Arnesano, Banci, Bertini, Mangani, Thompsett, *PNAS* 100, 3814 (2003)

Redox-driven metal transfer

The Cu(II) – CopC sample

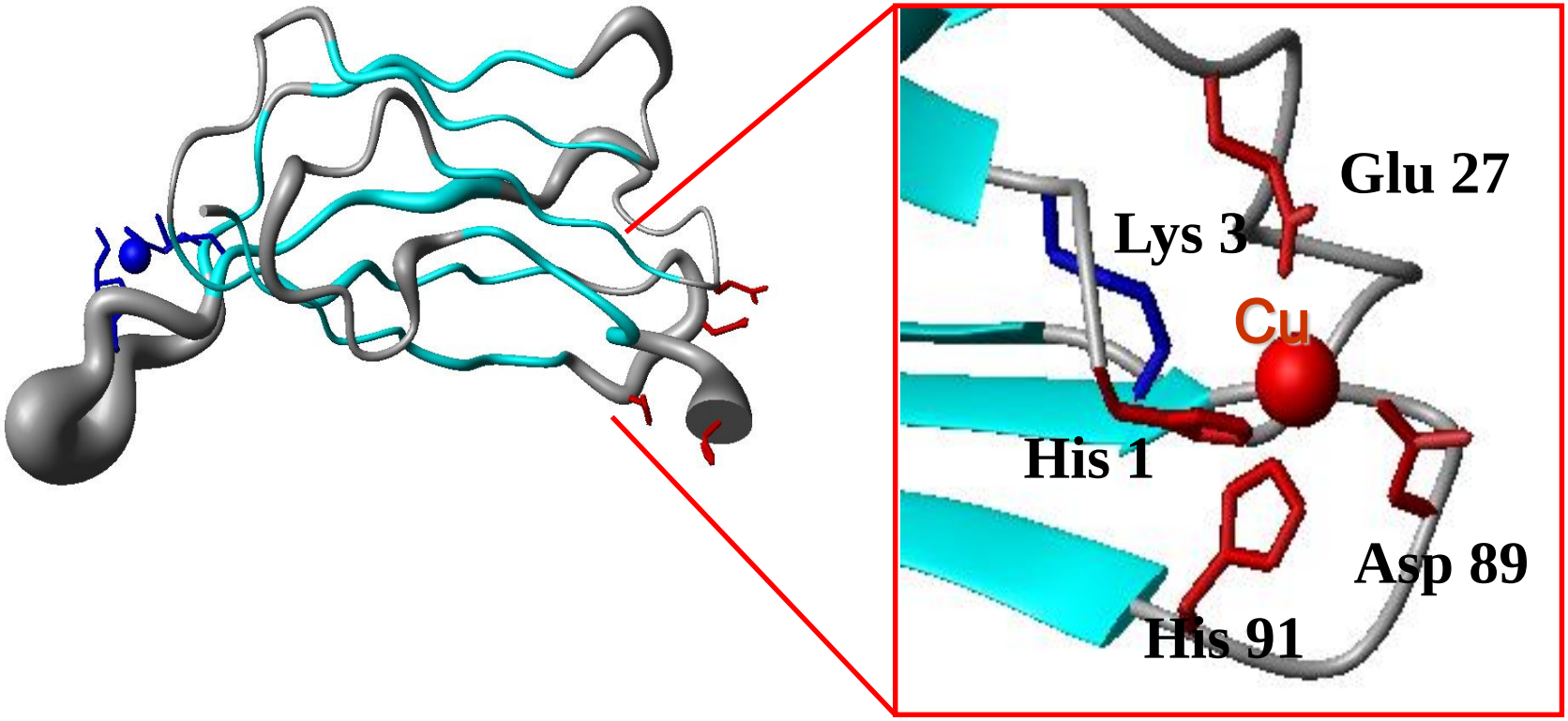

Arnesano, Banci, Bertini, Mangani, Thompsett, *PNAS* 100, 3814 (2003)

Redox-driven metal transfer

The Cu(I) – CopC sample reduced from an aliquot of the Cu(II) sample

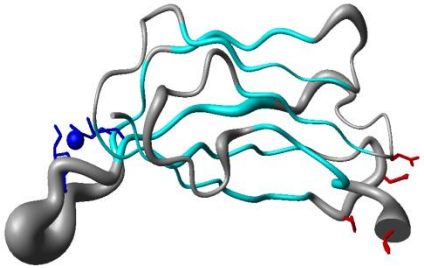

EXAFS results:
1 Cu – His 1.95 Å
3 Cu – S (Met) 2.30 Å

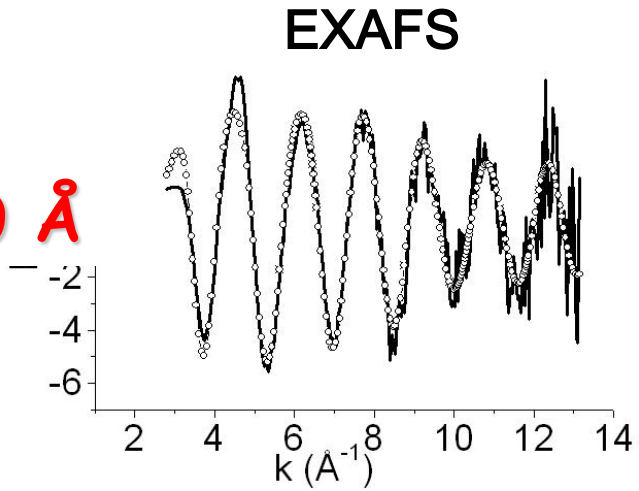

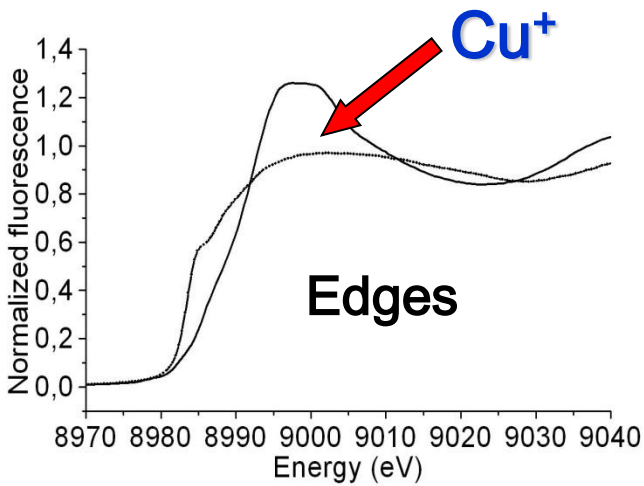

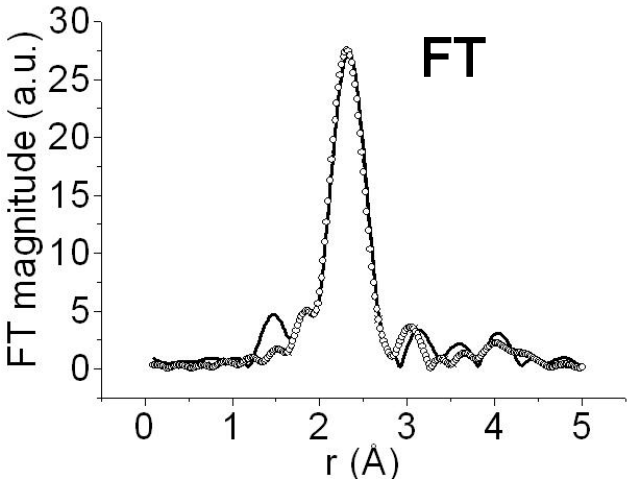

Arnesano, Banci, Bertini, Mangani, Thompsett, *PNAS* 100, 3814 (2003)

Redox-driven metal transfer

The Cu(I) – CopC sample reduced from an aliquot of the Cu(II) sample

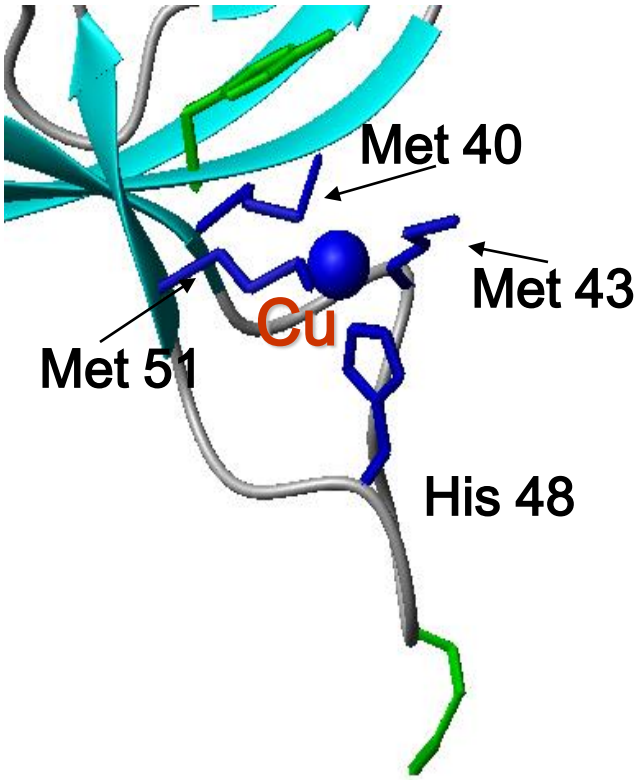

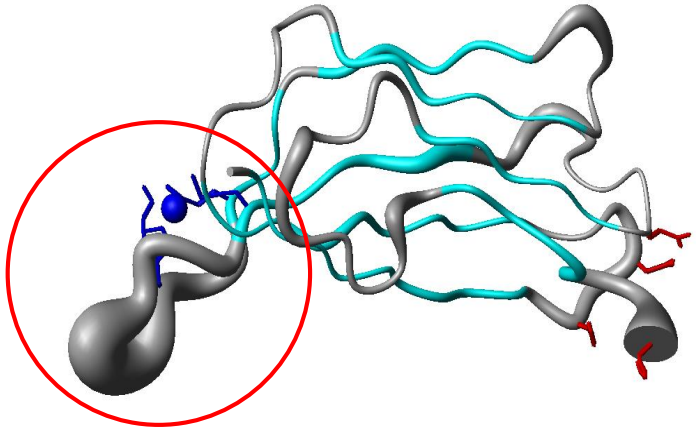

EXAFS results:
1 Cu – His 1.95 Å
3 Cu – Met 2.30 Å

Arnesano, Banci, Bertini, Mangani, Thompsett, *PNAS* 100, 3814 (2003)

Redox-driven metal transfer

NMR + EXAFS constraints

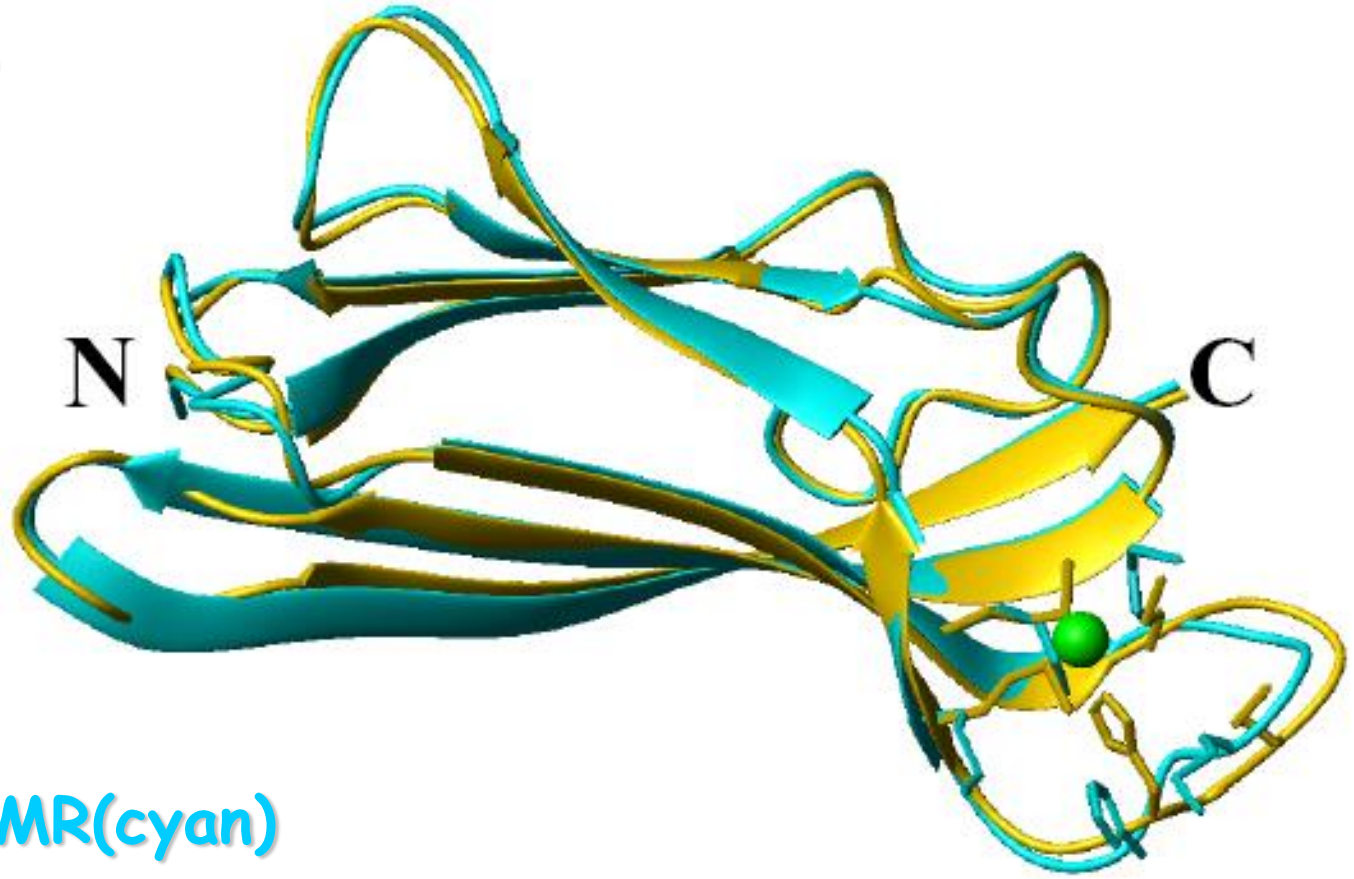

Fit
Cu(I)-CopC NMR(cyan)
Cu(I)-CopC NMR+EXAFS(yellow)

Arnesano, Banci, Bertini, Mangani, Thompsett, *PNAS* 100, 3814 (2003)

Redox-driven metal transfer

Cu migrates from Cu(II) binding site to Cu(I) binding site upon reduction!

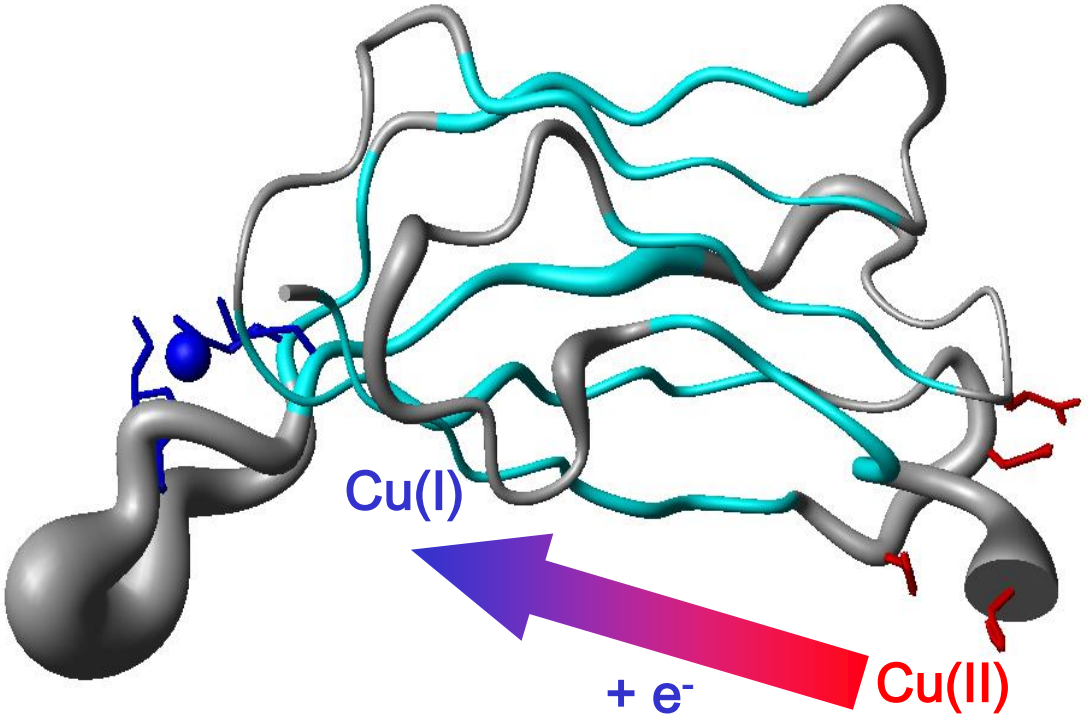

The process is reversible and it can be proposed as a trigger mechanism for copper trafficking

Arnesano, Banci, Bertini, Mangani, Thompsett, *PNAS* 100, 3814 (2003)

XRF+μXANES coupled to optical microscopy of fluorescent-tagged proteins

Normalized XANES spectra at arsenic K-absorption edge in the cytosol, mitochondrial network, nucleus and lysosomes of HepG2 cells exposed to $As(OH)_3$. Light microscopy of a single cell (a); epifluorescence microscopy of the same cell showing in green the mitochondrial network (labelled with rhodamine 123) and in blue the lysosomes (labelled with lysotracker) (b); micro-XRF distribution of potassium (c) and arsenic (d). XANES spectra in the subcellular compartments show that the main arsenic oxidation state is As(III) in all organelles, with a mixture of trivalent and pentavalent arsenic in the nucleus (e).

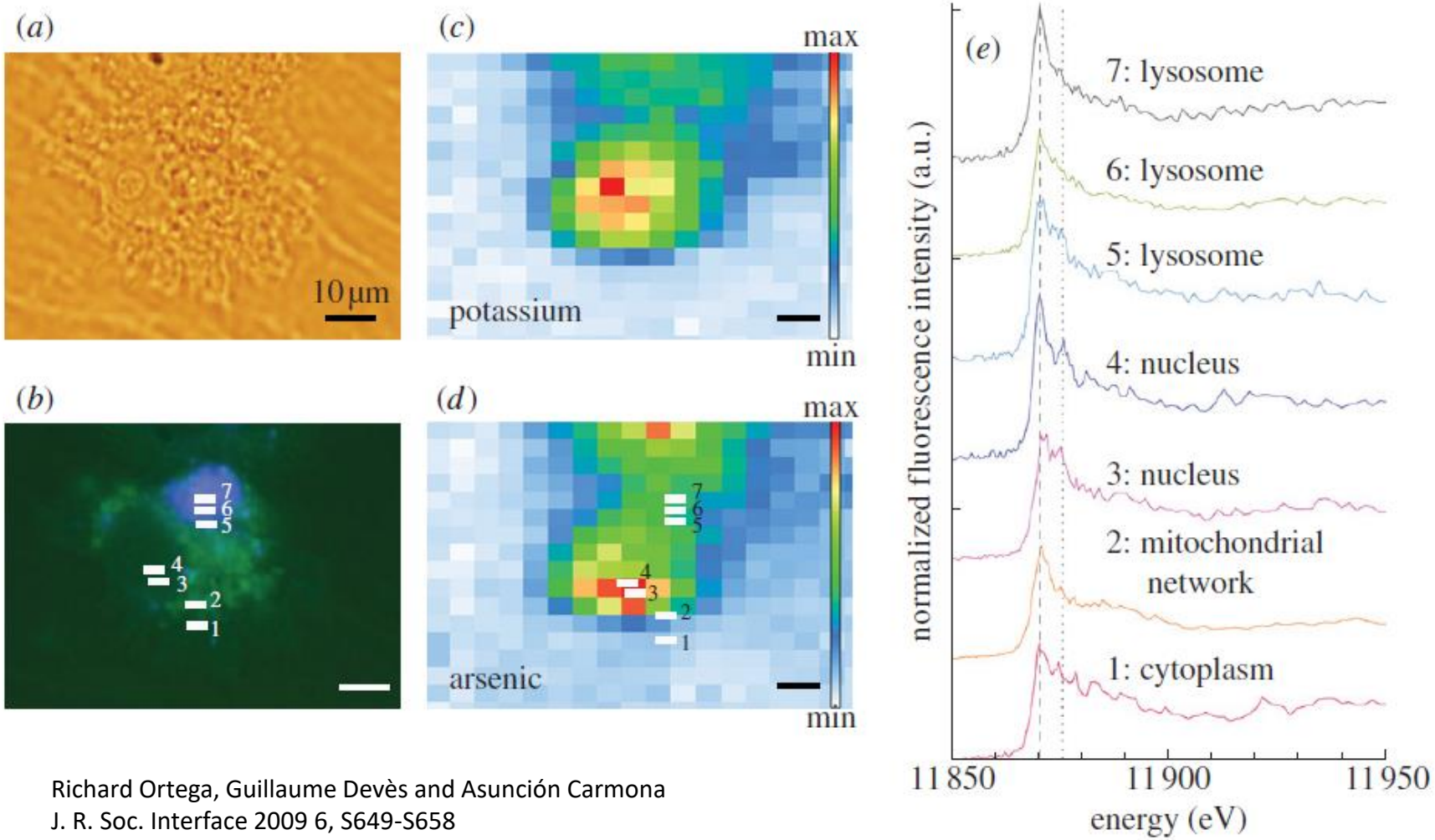

Richard Ortega, Guillaume Devès and Asunción Carmona
J. R. Soc. Interface 2009 6, S649-S658

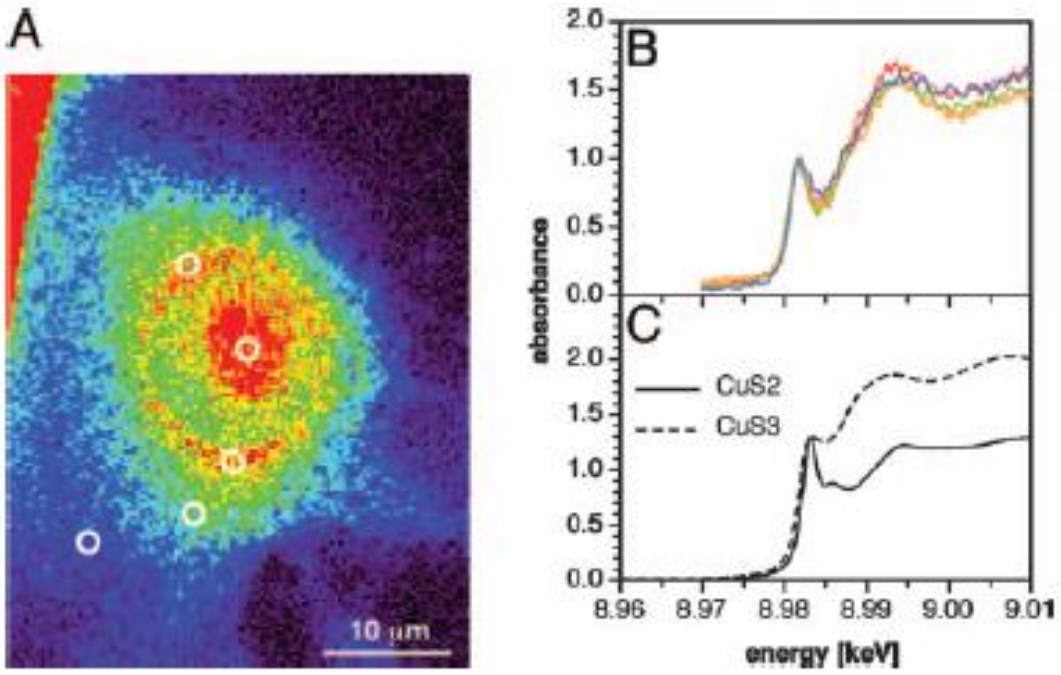

NIH 3T3 fibroblast cell grown in medium supplemented with 150 µM $CuCl_2$.
(A)False-color XRF micrograph showing the copper distribution

(*B*) XANES spectra acquired at various locations (marked with white rings in *A*).

(*C*) XANES reference spectra: CuS2: $[Cu(SC_{10}H_{13})_2][N(C_3H_7)_4]$ and CuS3: $[Cu(SC_6H_5)_3][P(C_6H_5)_4]$

µXRF experiments at the **Advanced Photon Source** of the Argonne National Laboratory.
The instrument at the 2-ID-D beamline: detection limit of 10^{-19} mol·µm^{-2} for Mn, Fe, Cu, or Zn and a spatial resolution of 200 nm.

Yang L. et al. PNAS 102, 11179-11184 (2005)

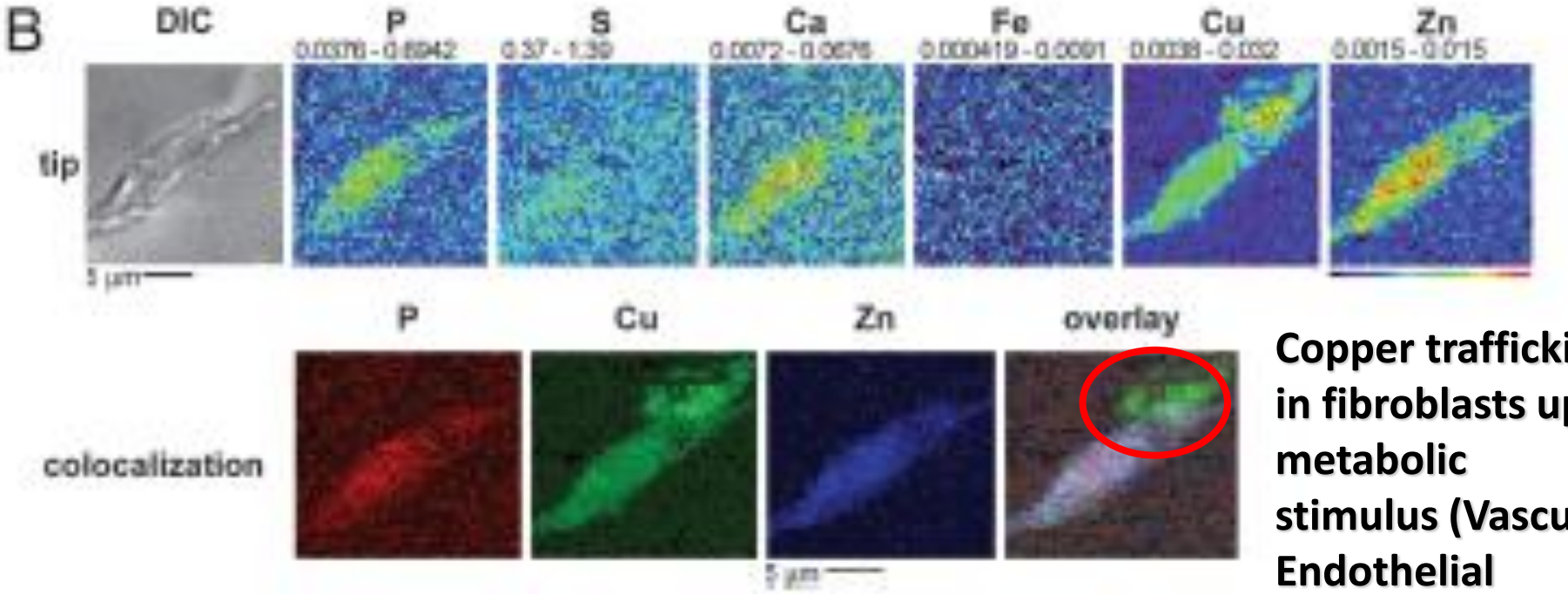

Copper trafficking in fibroblasts upon metabolic stimulus (Vascular Endothelial Growth Factor)

When cells are stimulated with VEGF and bFGF and plated onto the basement membrane surface, **copper translocates** outwards toward the periphery of the cell within 30- 60 min and a substantial amount is excreted.

Finney L. et al. PNAS 104, 2247-2252 (2007)

XAS reference material

International XAS Society:
https://www.ixasportal.net/ixas/
Books and Review Articles:
EXAFS: Basic Principles and Data Analysis, B.K. Teo, Springer, 1986
X-ray Absorption: Principles, Applications, Techniques of EXAFS, SEXAFS, and XANES, in Chemical Analysis 92, D. C. Koningsberger and R. Prins, ed., John Wiley & Sons, 1988.
Basic Principles and Applications of EXAFS, Chapter 10 in Handbook of Synchrotron Radiation, pp 995–1014. E. A. Stern and S. M. Heald, E. E. Koch, ed., North-Holland, 1983.
G. Bunker Introduction to XAFS, Cambridge University Press 2011
Tutorials and other Training Material:
http://gbxafs.iit.edu/training/tutorials.html Grant Bunker's tutorials
http://srs.dl.ac.uk/XRS/courses/ Tutorial from Daresbury Lab, UK
http://bruceravel.github.io/XAS-Education/ Bruce Ravel's XAS Education materials.
Software Resources:
https://bruceravel.github.io/demeter/
http://www.esrf.fr/computing/scientific/exafs/
http://gnxas.unicam.it/pag_gnxas.html
http://leonardo.phys.washington.edu/feff

BioXAS beam lines

- https://www.elettra.trieste.it/elettra-beamlines/xafs.html Elettra general purpose XAS
- http://www.esrf.eu/UsersAndScience/Experiments/CRG/BM08 ESRF Italian XAS beamline
- http://www.esrf.eu/home/UsersAndScience/Experiments/MEx/BM23.html ESRF multi purpose beamline
- http://www.esrf.eu/home/UsersAndScience/Experiments/MEx/ID24.html ESRF Energy dispersive XAS
- http://photon-science.desy.de/facilities/petra_iii/beamlines/p64_advanced_xafs/index_eng.html Petra III
- https://www.diamond.ac.uk/Instruments/Spectroscopy/B18.html Diamond general purpose XAS
- https://www.psi.ch/sls/superxas/superxas Swiss Light Source XAS & XES
- https://bioxas.lightsource.ca/ CLS spectroscopy & imaging